ARL 70-0001
JANUARY 1970

# Aerospace Research Laboratories

## ELECTRIC ARCS IN TURBULENT FLOWS, IV

GERHARD FRIND
BEN LEE DAMSKY
GENERAL ELECTRIC COMPANY
PHILADELPHIA, PENNSYLVANIA

D D C

MAY 12 1970

B

# OFFICE OF AEROSPACE RESEARCH
# United States Air Force

90

**BLANK PAGE**

ARL 70-0001

# ELECTRIC ARCS IN TURBULENT FLOWS, IV

GERHARD FRIND AND BEN LEE DAMSKY

GENERAL ELECTRIC COMPANY
PHILADELPHIA, PENNSYLVANIA

JANUARY 1970

AEROSPACE RESEARCH LABORATORIES
OFFICE OF AEROSPACE RESEARCH
UNITED STATES AIR FORCE
WRIGHT-PATTERSON AIR FORCE BASE, OHIO

# FOREWORD

# ABSTRACT

Heat, mass, and momentum transfer were investigated experimentally in very long, cylindrical axial flow arcs in laminar and turbulent flow conditions. Special attention was given to assure that the end of the arc tube had a section of fully developed flow. In this section the number of significant terms in the energy balance equation is reduced and interpretation of experimental results is simplified. Strong evidence is presented for the existence of turbulence by the fact that all three transfer mechanisms are considerably accelerated in what we consider the "turbulent mode" and also by direct optical study of the arc by a light probe. The onset of turbulence was found with all our methods to occur around 1.5 gram/sec gas flow rate. A considerable number of measurements of heat and momentum transfer are presented in the following operating ranges: Gases - argon and nitrogen; Tube Diameters - 0.5 and 0.7 cm; Tube Length - 50 cm; Mass Flow Rates - 0.1 to 15 gram/sec; Ambient Pressures - 1 to 20 atmosphere; Currents 25 to 200 amperes (some higher).

## LIST OF SYMBOLS

$B$     Boltzmann's Constant

$D$     Tube Diameter

$DP$     Dissociation Energy

$E$     Electrical Gradient

$e$     Average Height of Wall Roughness

$F$     Potential Energy of Energy Level

$g$     Degeneracy of Energy Level

$I$     Spectral Intensity

$IP$     Ionization Energy

$L$     Length of Arc Tube

$m$     Mass of Electron

$N_o$     Density of Radiating Particles in Ground State

$P$     Pressure

$R$     Radius of Tube Containing Arc

$R_e$     Reynolds Number

$r$     Radial Distance from Arc Axis

$S$     Radiation Rate Per Unit Volume

$T$     Absolute Temperature

$v$     Velocity

$W$     Axial Flow Rate

$x,y$     Cartesian Coordinate

$Z$     Partition Function

$\Delta T$     Amplitude of Temperature Fluctuation

## LIST OF SYMBOLS (Cont'd)

$K$      Thermal Conductivity

$K^*$      Effective Thermal Conductivity Produced by Turbulent Mixing

$\lambda$      Wavelength

$\mu$      Kinematic Viscosity

$\varphi$      Excitation Energy

$\rho$      Density

$\sigma$      Electrical Conductivity

$\Omega$      Electrical Resistance

### Subscripts

$D$      With Reference to Tube Diameter

$e$      Electron

$i$      Ion

$J$      Atomic Energy Level Index

$o$      Ground State

## TABLE OF CONTENTS

## LIST OF ILLUSTRATIONS

TITLE

# ELECTRIC ARCS IN TURBULENT FLOWS, IV

## 1.    INTRODUCTION

### 1.1    General Comments

This report is the last in a group of publications (1, 2, 3)* devoted to studying the importance of turbulence for the transport of energy, momentum and mass in coaxial flow arcs. More specifically, work was concentrated on turbulent effects in an area which, in fluid dynamic studies, is usually called the fully developed section of coaxial flows. This, of course, is a very strong restriction on the broad objective of furthering understanding of arc turbulence in toto. Nevertheless, it will be seen from the results described in this paper that persuit of even our limited objective offers formidable problems.

### 1.2    Review of Work from Earlier Reports

To facilitate the task of following the zig-zag course of our investigation, we present in Table 1 a matrix containing what we consider the essential results obtained in all four reports, including this one. The following short discussion of this "matrix" will also familiarize the reader with our earlier work for further reference.

### 1.21    Theoretical Aspects

As for the Theoretical Aspects of this investigation, we discussed in some detail the complexity of the physical processes(1, 2), demonstrated by way of the general energy balance equation. This discussion showed also that the concept of "fully developed conditions" cannot be used in the same way for electrical arcs as for low temperature fluids.

This is so because in hot plasma streams it is difficult to make the "flow" terms in the energy balance equation negligibly small. One must resort to experimental conditions of plasma velocities well under the speed of sound and of limited arc tube diameters (2). Under these strong limitations, fully developed conditions can be expected in the end section of long coaxial arc heaters and an energy balance with a significantly smaller number of terms can be retained (2, 3). This result was essential for our investigation because our first goal was to find, in axial flow arcs, experimental conditions in which the existence of radial turbulent energy

* The numbers in parentheses are references; see page 54.

---

| REPORT | THEORY | EQUIPMENT | VOLTAGE GRADIENT | PLASMA STRUCTURE | TEMPERATURE MEASUREMENTS | PRESSURE GRADIENTS |
|---|---|---|---|---|---|---|
| I | concept of coaxial fully developed flow as goal<br><br>calculations show turbulence is reasonable | cascade discs with terminal pressure tank | low current measurements | measurements of flow velocities at low currents | | |
| II | theory of where achieve fully developed flow<br><br>calculation of energy balance | high voltage power supply | up to 80 amperes in 1 cm tube | photographic studies of 80 ampere arc at several flow rates | | |
| III | | high current power supply | 200 amperes in argon and nitrogen | velocity measurements with image converter camera | temperature distribution determined by $N_2$ band line | 11.2 atm pressure gradients |
| IV | | higher pressure capability | wide variety of pressures and flow rates in argon extended measurements in nitrogen | amplitude and frequencies of light intensities fluctuations at different flow rates and currents | Sodium temperature point | Pressure gradients measured at many flow rates and pressures |

TABLE 1
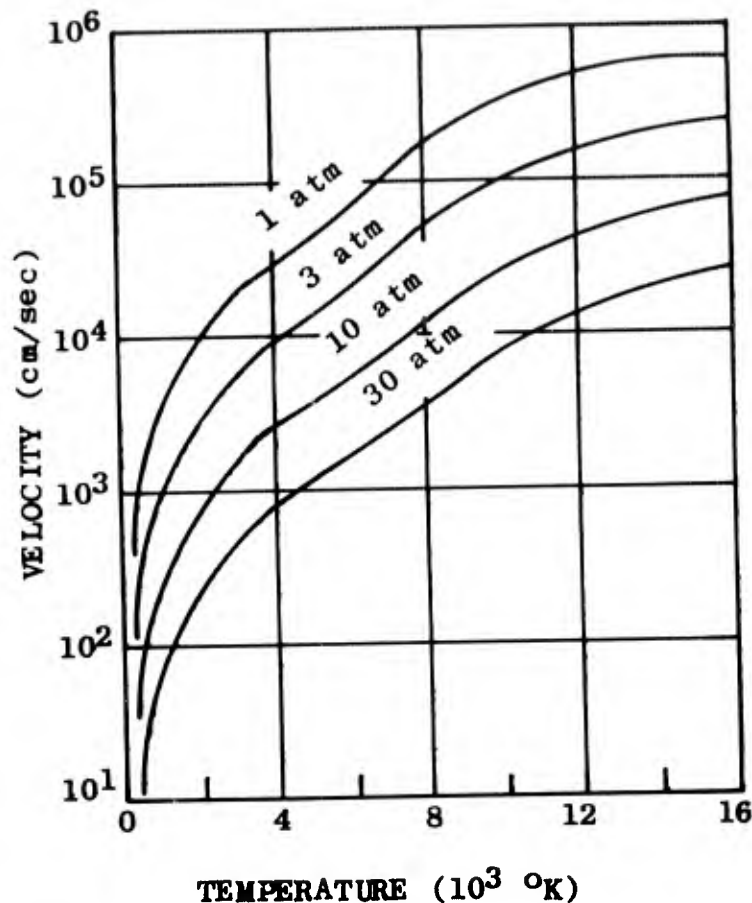
Figure 1—Estimate of Minimum Velocity for Turbulence.

Velocity for which the Reynolds number is
equal to 2000 is plotted against temperature
(assumed homogeneous).

Gas:            Nitrogen
Pressure:      as marked
Tube Diameter:   1 cm

transport could be proven by simple measurements. We felt that
such a proof was too difficult a task if the usually strong flow
terms could not be eliminated and the analysis correspondingly
simplified.

The experiments in all four reports were therefore
planned with the specific condition of fully developed flow in
mind. This entails:

1. Use of velocities well subsonic (below 500 meter/sec)
2. Use of small diameter arc tubes (1.0 cm and less)
3. Concentration of measurements at the end section of a flow
   tube with as high L/D value (length/diameter) as possible
   (we used ratios from 70 to 150).

-3-

Another major aim of earlier theoretical work was the demonstration that turbulence could be reasonably expected under normal operating conditions of arc heaters. Figure 1 reproduces a calculation made in (1) assuming a constant temperature air plasma with pressures between 1 and 30 atm. It is seen that, at the higher pressures, Reynold numbers substantially higher than 2000 can be reached with subsonic velocities even at temperatures between 10,000 and 15,000°K, reasonable values for the core of high current arcs. If we now remember that the electric arc has layers of widely different temperatures, it appears likely that the outer, cooler layers of an arc with their higher density and lower viscosity may show turbulent effects even at quite moderate pressures and flow velocities.

This same calculation may be viewed in another light: using our plasma velocity measurements ((3) section 4.3) as a basis, the velocities of the 10 atmosphere curve in figure 1 were converted into flow rates to give figure 2. The assumptions were: a 10,000°K core temperature for the arc used in (3), and relative velocity and temperature distributions unaffected by changes in the central temperature. Neither assumption is accurate but the curve still serves as an estimate of the requirements for producing turbulence throughout an arc.

1.22    Equipment

Table I gives an idea of the gradual development of our experimental apparatus. The cascade tube of Maecker (4) was used from the beginning, but without the usual water cooling of the copper discs. We felt this omission was a necessary simplification if only for financial reasons. The number of discs in one tube exceeded 500 at times. This large number resulted from the length of tube required for fully developed flow and from the 0.05cm thickness of the individual discs. The discs were made so thin for two reasons; first, voltage gradients as high as 200 volt/cm were found in turbulent arcs, and second, it was expected that a strike-over to the copper walls would occur more easily on account of the violent plasma motions of turbulent conditions.

-4-
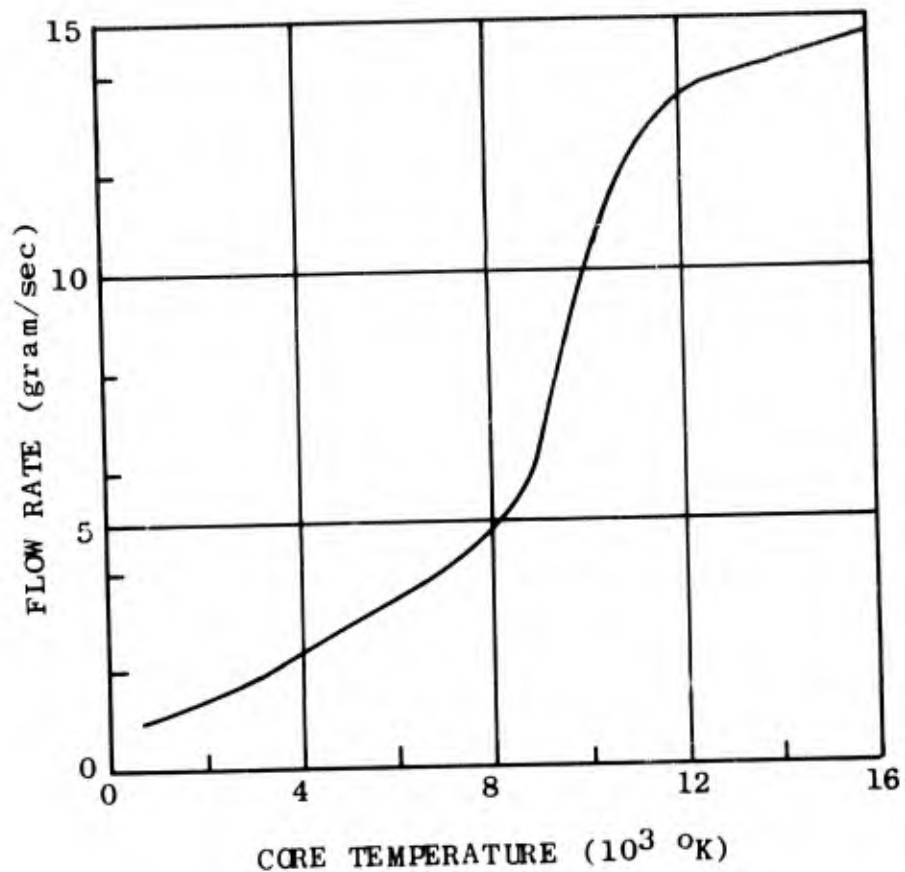
Figure 2-Estimate of Minimum Flow Rate for Turbulence
in 0.7 cm Diameter Tube. The estimate of
figure 1 was adapted using the velocity vs.
flow rate measurements of (3).

Gas:             Argon
Pressure:        10 atm
Tube Diameter:   0.7 cm

There are other advantages in using simple apparatus.
To avoid overheating one has to make relatively short time arc
runs ( ~ 1/2 sec), and so the electrical power source can be
used at a multiple of its steady state capability (1, 2). Also
under the thermal conditions of short arc runs, a segment of
the copper cascade can be replaced with an uncooled quartz tube,
a necessity for studying turbulent structure and flow velocity
by high speed photography.

-5-

Turning to the disadvantages of our short time arc runs, one first notes the necessity for proof that steady state conditions have been reached with regard to time. It was found that the slowest process after starting of the arc was the establishment of steady state flow conditions along the arc heater. Flow was monitored by the pressure drop along the tube (3). We were careful in our experiments to evaluate measurements only with the plasma pressure close to steady state conditions. However, it must be reported that it was difficult to fulfill that condition equally well at all times. Development was slowest for tests combining high flow rate with high current.

1.23    Measurements in the Fully Developed Flow Region

1.231    Heat Flux and Momentum Transfer

Perhaps the most convincing measurements in our group of reports were those of radial heat and momentum transfer in the fully developed section of the long, cylindrical arc tube. This was accomplished (2, 3) by measurements of the axial voltage and pressure gradients. The results of these measurements gave strong support to our conclusion that a laminar state of the arc exists at low flow rates (below about 1.5 gram/sec) while an increasingly turbulent character of the arc obtains at flow rates higher than that number. In our last report (3) the experimental range of voltage gradient measurements was expanded to currents up to 200 amps and to nitrogen in addition to argon; the strong effect of flow rate on pressure gradient was shown at 11.2 atm of argon with 125 amps.

1.232    Plasma Structure

Insight into the plasma structure was gained in all our previous reports by high speed photography. Fig. 21-24 of (2) show convincingly the laminar character of the arcs at low flow rates and the increasingly turbulent character at high flow rates where the arc column is apparently "broken up" into plasma globules of irregular sizes and shapes. Of course, current is flowing steadily and relatively undisturbed even through a strongly temperature modulated plasma.

1.233    Plasma Velocity

Although the measurement of the complete radial velocity distribution V(r) is a long range goal of our investigation, in our last report (3), an approximate measurement of the average plasma speed close to the axis of the tube was accomplished. We followed plasma globules as they proceded along the tube with a high speed camera. Fig. 18 of (3) shows the plasma velocity as function of the mass rate of flow for argon.

-6-

1.234    Plasma Temperature

        In our last report a temperature measurement was made
on both a laminar and a turbulent 50 amp arc in 11.2 atm. of
nitrogen.  The choices of current and gas species were unfor-
tunately not in the "main stream" of our investigation, which
would have called for 125 amps and argon.

        The reason for this inconsequence was our belief that
a turbulent temperature measurement could best be made with the
Milne method (5) which is insensitive against small fluctuations
(6, 7).  Furthermore nitrogen has well known molecular bands
which radiate strongly even below 10,000°K which is the
temperature range of interest.  The atomic lines of Argon, on
the other hand, have peak intensities at much higher tempera-
tures and are difficult to use at 10,000°K.

        The result of the measurement was a surprisingly close
agreement between the laminar and turbulent temperature distri-
butions T(r), see Fig. 28 and Table III in (3).

1.3      Goals of This Investigation

        One of the long range goals of our work on turbulent arcs
is to find empirical relationships between energy, momentum and
mass transfer and nondimensional properties of the temperature
and velocity field.  One more modest goal of this particular
report is to quantify, as far as possible, such relationships as
a function of the mass rate of flow, which in turn is approxi-
mately proportional to some "average" Reynolds number.  This
requires the collection of data at various combinations of test
parameters so correlations of turbulent levels with operating
conditions can be made.  Other goals are to shed more light on
turbulent structure and on the onset of turbulence, and further,
to develop measuring methods suitable for a more precise deter-
mination of such important parameters as plasma temperature and
velocity.  With expanded facilities, the operating parameters
can be extended to higher currents and pressures.  Values chosen
for testing should be as close as possible to typical parameters
used in constricted arc heaters.
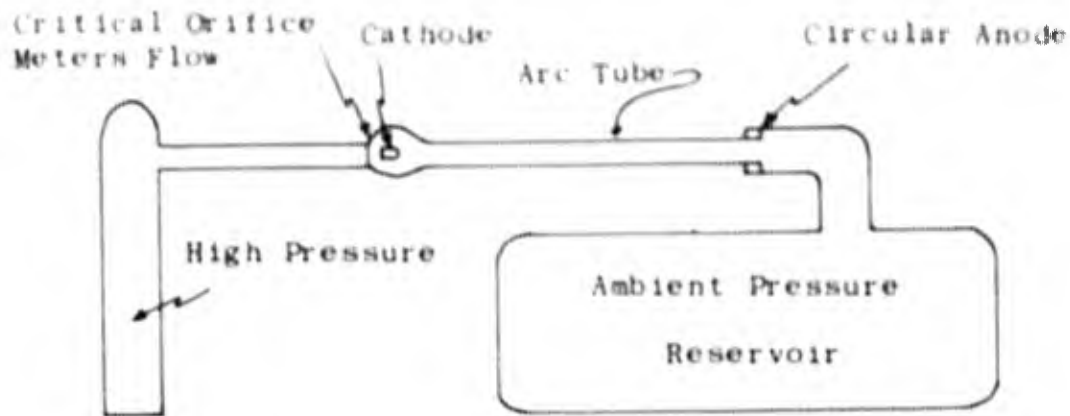
Figure 3-Schematic Diagram of Test Apparatus. The
flow rate is set by the size of the criti-
cal orifice and the value of the upstream
pressure which is three times the ambient
pressure. Arc initiation is accomplished
by exploding a 0.001cm diameter tungsten
fuse wire stretched from anode to cathode.
(See also Fig. 3 and 4 in (3)).

## 2. APPARATUS

The basic experimental arrangement has not changed since
the last report, (3). A schematic diagram of the major equip-
ment is shown in figure 3. We utilize the thermal storage cap-
ability of rectifiers, resistors, and cascade discs to withstand
transient heating and so operated them at levels beyond their
steady state capacity. The uncooled copper discs have been
operated with heat fluxes of $13Kw/cm^2$ for short periods. Transient
operation ( $\leq$ 0.5 sec.) makes it necessary to record data with
Cathode ray oscillographs (CRO). Gas flow is metered by critical
orifices whose upstream pressure is kept at three times the
ambient reservoir pressure. Orifices were calibrated with an
absolute accuracy of $\pm10\%$; relative accuracy is $\pm2\%$. Because
of the extremely high potential gradients produced by turbulent
nitrogen, cascade discs were made of 0.5mm thick copper; for
experiments in argon, 1mm discs were possible. Preparation of
the discs included cleaning in an ultrasonic bath and etching
a 0.02mm deep layer from the surface. This process insured
cleanliness and removed the sharp edges which increase the
chances for "strike over" at the walls. The discs were insulated
by 0.25mm thick teflon washers which were recessed from the arc
to prevent contamination. Before experiments, the discs were
carefully aligned with a steel rod whose diameter matched the
inner diameter of the discs.

-8-

3.          EXPERIMENTS IN THE FULLY DEVELOPED FLOW REGION

3.1         Heat Transfer as Measured by Voltage Gradients

3.11        Choice of Parameters

          One of the long range objectives of our study is to find
an experimental correlation of turbulent heat transfer and non
dimensional quantities of the flow field such as some "average"
Reynolds number.* To accomplish this we need quantitative
experimental data about the radial heat flux, the temperature
distribution, and the velocity distribution. Although we do
not have this data, but have measurements of potential gradient,
flow rate, and average velocity in the arc core, we feel it is
useful to correlate these data. Therefore we attempt in the
following to correlate radial heat flux with axial flow rate
which, in turn, is approximately proportional to the Reynolds
number $Re_D$ of the experiment.

          For these measurements we chose to study the 125 ampere
argon arc, which fills our tube rather well and for which a
large amount of pressure gradient data was also taken. In the
graphs which follow the directly measured quantities, arc vol-
tage gradient, and flow rate are compared. Since the arc
current is held constant at 125 ±4 amperes, the arc power is
proportional to the voltage gradient and since, under the
conditions of our experiments, the flow is fully developed in
the end section of the flow tube, all of the arc power in this
section is transmitted to the wall. The flow rate, on the
other hand, would be strictly proportional to the Reynolds
number only if increasing flow does not alter the temperature
distribution and the relative velocity distribution. Our
preliminary indications are that the temperature does not change
radically with flow at constant current (3) so that flow rate
may be a meaningful measure of relative Reynolds number.

          There are five test variables in the heat transfer
experiments: gas species; tube diameter; mass flow rate;
ambient pressure; and current. In the tests described below
four variables are held fixed and the fifth is varied. This
systematic method helps to isolate and identify quantitatively
the significance of each variable for heat loss. The ranges
of these variables are:

*  An "average" Reynolds number for strongly non homogeneous
   flow conditions, such as found in our experiments, remains to
   be defined. See Eckert's paper (8) for an attempt in this
   direction.

```
gas species:          argon or nitrogen
tube diameter:        0.5 or 0.7 cm
mass flow rate:       0.1-15 gram/sec
ambient pressure:     1-20 atmosphere
current:              25-200 ampere (some higher)
```

The voltage gradient measurements which follow were taken in the terminal portion of our long tubes where fully developed flow conditions exist.

### 3.12      Methods

Potential gradients were measured by attaching resistive dividers ($6 \times 10^6$ $\Omega$ input impedance) to eight cascade discs spaced along the arc tube. A typical current drawn from the plasma region would be $3 \times 10^{-5}$ amperes. Data was recorded as CRO traces.

The potential gradients were almost invariably constant along the tube except in a few cm of the entrance region. As flow rate increased to several grams per second, the potential gradient line of the graph showed a significant voltage at the interception of the axis representing cathode position. This additional voltage resulted from a higher potential gradient in the first few cm of the cascade tube. The excess potential drop increased linearly with flow rate, finally exceeding 100 volts. Since the value of this potential drop corresponds roughly to the power required to heat the incoming gas flow to several thousand degrees Kelvin, we take this as the explaination of the effect and do not include this short segment of the arc constrictor length in the gradient measurements which follow.

A slightly different observation was made of the nitrogen arc below 100 amperes; see (3) for a discussion of this effect.

### 3.13      Results

### 3.131     Variable Flow Rate

### 3.1311    Argon

Figure 4 shows the effect of the flow rate on energy loss in a 15 atmosphere argon arc on a log-log plot. The slope is not constant but continues to increase at the highest flow rates, reaching the value of 0.88 at the end of the graph. This compares closely with the empirical dependance of heat transfer coefficient on Reynolds number found in (9) for low temperature gases, see figure 5. In such homogeneous, low temperature fluids, heat transfer rises rapidly with the onset of turbulence and eventually increases with the 0.80 power of Reynolds number.

-10-
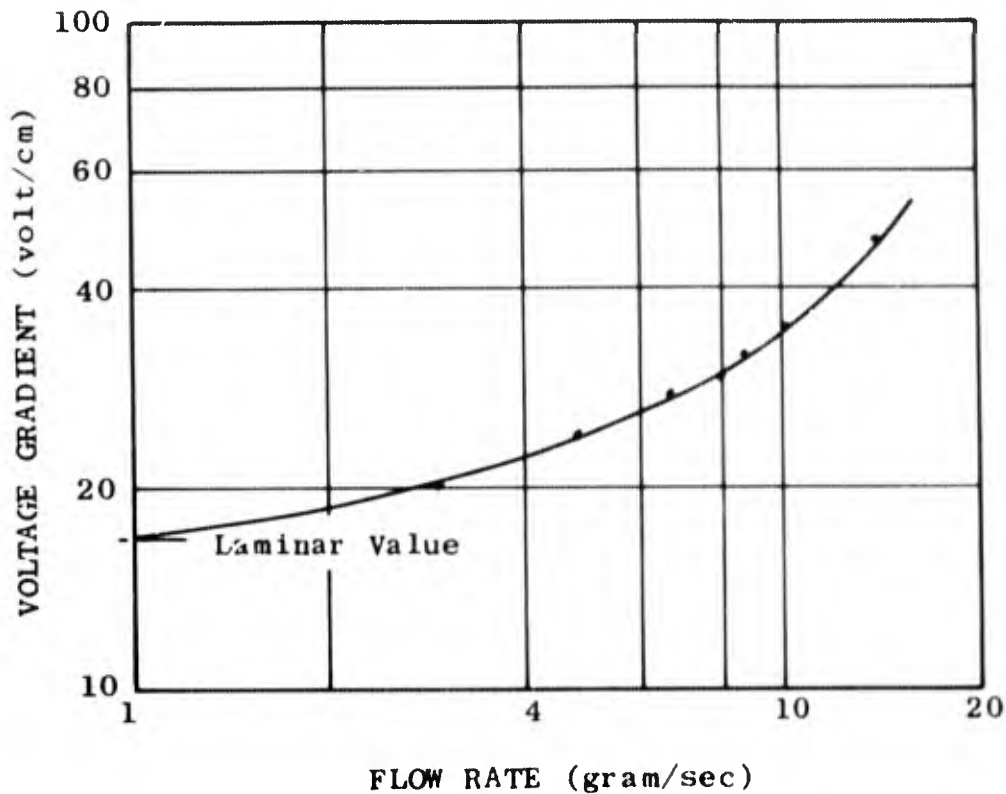
Figure 4-Voltage Gradient vs. Flow Rate at 15 atmospheres
of Argon in a 0.7 cm Tube. The log-log plot
shows an ever increasing slope.

| | |
|---|---|
| Gas: | Argon |
| Pressure: | 15 atm |
| Current: | 124 ±4 amp |
| Tube Diameter: | 0.7 cm |
| Tube Length: | 50 cm |

Whereas our experimental data (figure 4) does not settle into
a linear region on the log-log plot, the proper slope is
approximated closely for the highest flow rates. Let us also
bear in mind that we are plotting radial heat transfer against
flow rate, which is not precisely proportional to Reynolds
number but only approximately so. Tests at still higher flow
rates might have indicated whether the slope of figure 4
would remain constant. However, the large axial pressure grad-
ients involved at these flow rates would make the establishment
of fully developed conditions questionable ((2), pages 7-9 and
see also section 3.2 for measurements of pressure gradients).

-11-
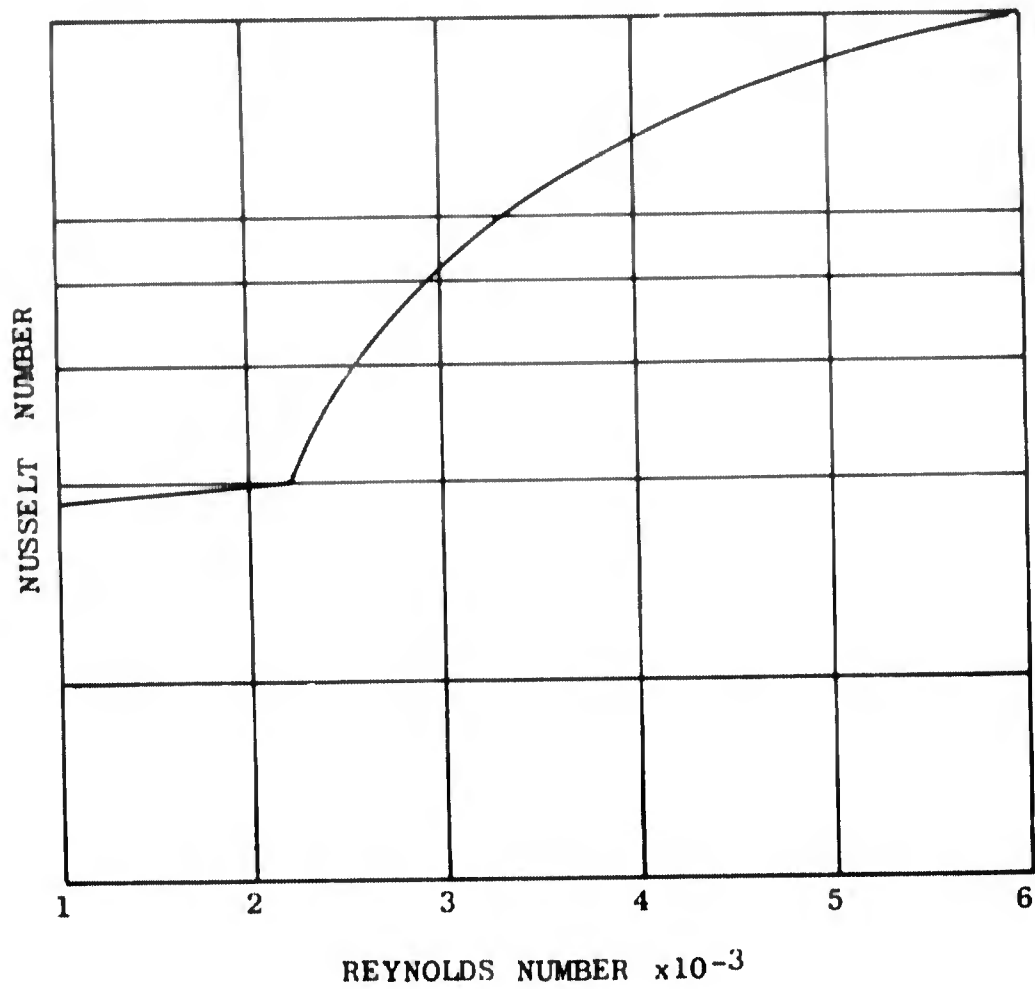
Figure 5-Heat Transfer in a Turbulent Tube (Homogeneous
Fluid)  The data are taken from ( 9 ).

The variation of the slope in figure 4 suggested an
exponential dependance.  This was checked in figure 6 which
shows energy losses from a 6 atmosphere argon arc on a semilog
plot.  Three regions can be seen:

     I     0-1.2 gram/sec
     II   1.2-3.5 gram/sec
     III  3.5 gram/sec and up

-12-
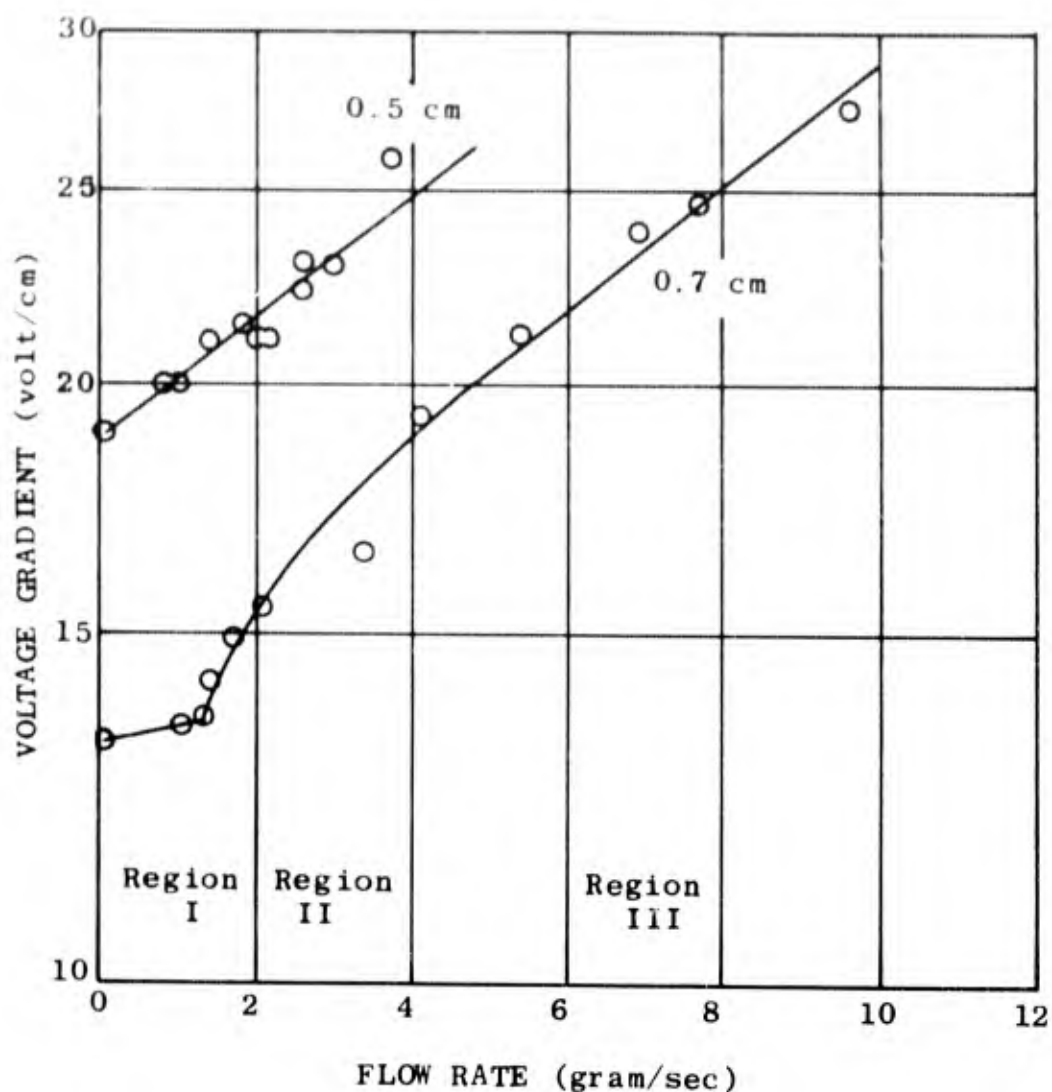
Figure 6-Voltage Gradient vs. Flow Rate at 6 atmospheres
of Argon in 0.5 and 0.7 cm Tubes.

| Gas: | Argon |
|---|---|
| Pressure: | 6 atm |
| Current: | 125 amp $\pm 4$ |
| Tube Diameter: | 0.5 cm and 0.7 cm |
| Tube Length: | 50 cm |

In region I the energy loss is nearly independent of flow rate, as would be expected from laminar flow; in region II there is a sudden increase in energy loss, which could be explained by the onset of turbulence; and in region III the relationship becomes approximately linear on the semilog plot. Notice too that the lowest flow data point lies approximately on the extention of the straight line in region III.
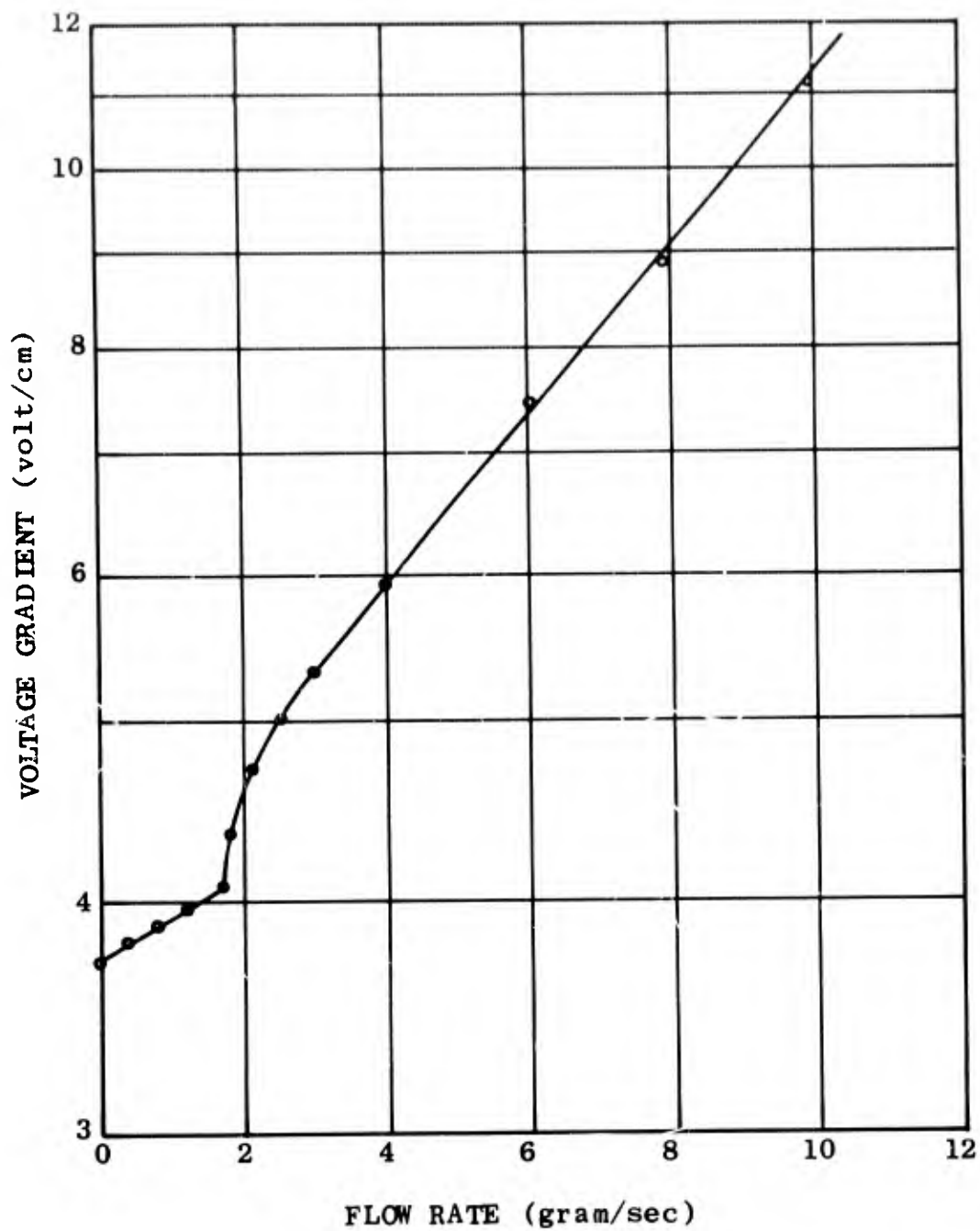
Figure 7-Voltage Gradient vs. Flow Rate at 1 Atmosphere
of Argon in a 1 cm Tube, Data from Runstadler (10)

| Gas: | Argon |
| Pressure: | 1 atm |
| Current: | 50 amp |
| Tube Diameter: | 1 cm |
| Tube Length: | 40 cm |

-14-
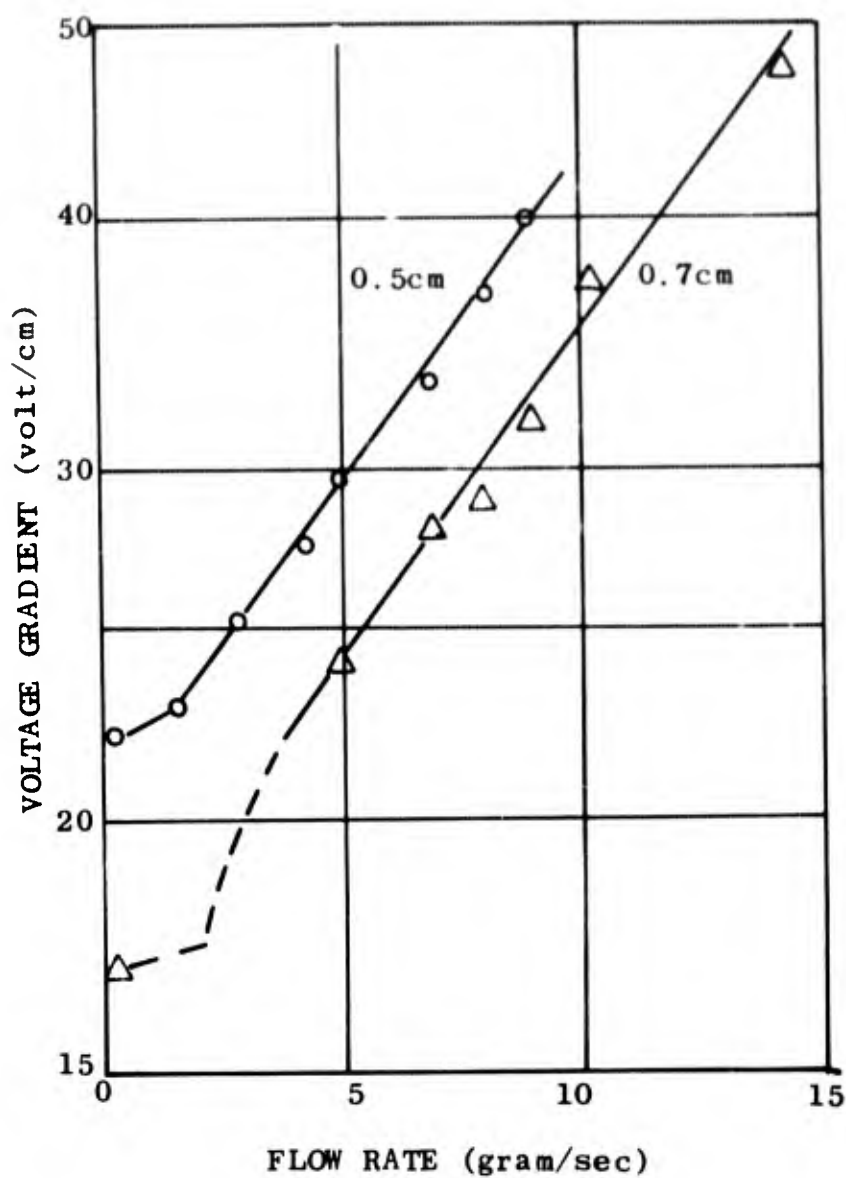
Figure 8-Voltage Gradient vs. Flow Rate at 15
Atmospheres of Argon in 0.5 and 0.7 cm
Tubes

| | |
|---|---|
| Gas: | Argon |
| Pressure: | 15 atm |
| Current: | 125 $\pm$4 amp |
| Tube Diameter: | 0.5 and 0.7 cm |
| Tube Length: | 50 cm |

-15-

These same features can be seen in Runstadler's data on arc voltage measurements (10), figure 7. We replotted Runstadler's results on a semilog scale and there does seem to be an exponentially rising region at higher flow rates. Notice that his conditions are somewhat different (lower current and pressure, and a larger tube diameter), but his result is similar to ours.

It is interesting to see that a smaller arc tube diameter increases energy losses to the walls but maintains the same slope in region III. Figure 8 shows the results of tests in 0.5 and 0.7 cm I. D. tubes at 15 atmospheres of argon. The losses go up about 25% in the 0.5 cm tube but the two lines are parallel within experimental error. This same fact can be seen in figure 6 where the 6 atmosphere results are compared. The power ratio for 6 atmosphere tests are comparable. The power ratio at 6 atmospheres cannot be measured so accurately but is approximately 30%. Notice that the curves again have the same slope and this slope is identical with that found at 11.2 and 15 atmospheres, figure 9. The 20 atmosphere results are shown in figure 10.

If this study of heat transfer is compared with the study of pressure gradients, see section 3.2, it is immediately seen that near 1.5 gram/sec. both the pressure gradient and the energy loss begin to rise rapidly. This correlation again lends weight to our interpretation of this point as the onset of turbulence. Compare also Runstadler's value of 1 gram/sec. (10).

A summary of all the above results in a 0.7 cm I. D. constrictor is contained in figure 11. It has the additional advantage of showing the results on a linear plot as well as the semilog plot used in figure 6 through 10. The striking features of the curves are the strong effect which flow rate has on power loss (an effect which becomes more pronounced at higher flows) and the departure from the lower pressure data which occurs at an ambient pressure of 20 atmospheres. Tests at 1, 3 and 6 atmospheres do not extend to the highest flow rate because such steep pressure gradients would be produced* that the flow terms in the energy balance equation could not be neglected and consequently the potential gradient would not be proportional to radial heat flux.

* See section 3.2 for measurements of pressure gradients.

-16-
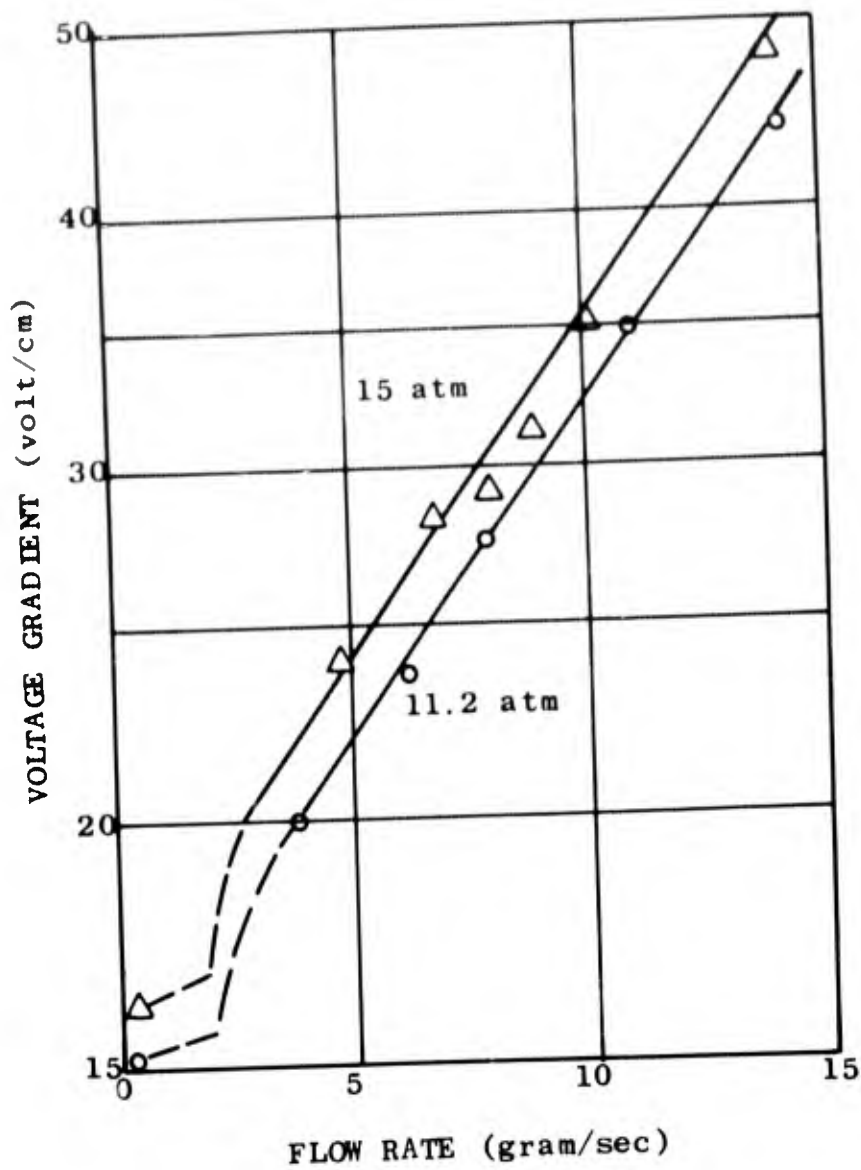
Figure 9-Voltage Gradient vs. Flow Rate
at 11.2 and 15 Atmospheres of
Argon in a 0.7 cm Tube

| | |
|---|---|
| Gas: | Argon |
| Pressure: | 11.2 and 15 atm |
| Current: | 125 $\pm$4 amp |
| Tube Diameter: | 0.7 cm |
| Tube Length: | 50 cm |

-17-
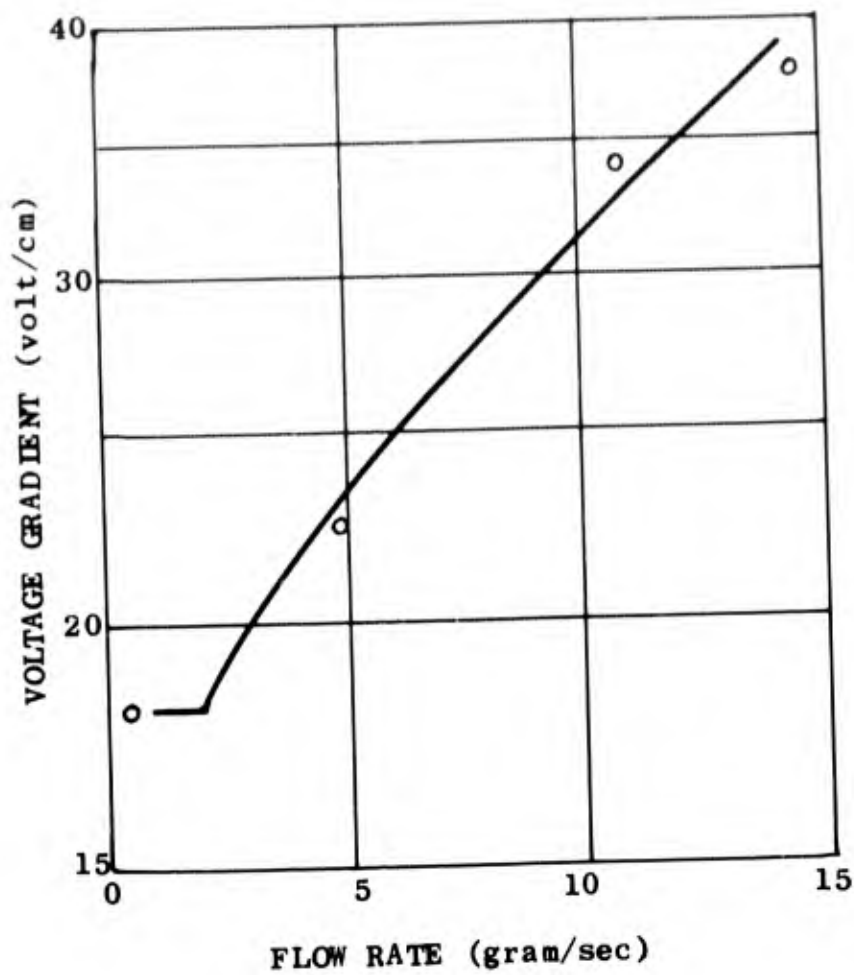
Figure 10-Voltage Gradient vs. Flow Rate
at 20 Atmospheres of Argon in
a 0.7 cm. Tube.

| | |
|---|---|
| Gas: | Argon |
| Pressure: | 20 atm |
| Current: | 125 $\pm$4 amp |
| Tube Diameter: | 0.7 cm |
| Tube Length: | 50 cm |

FLOW RATE (gram/sec)
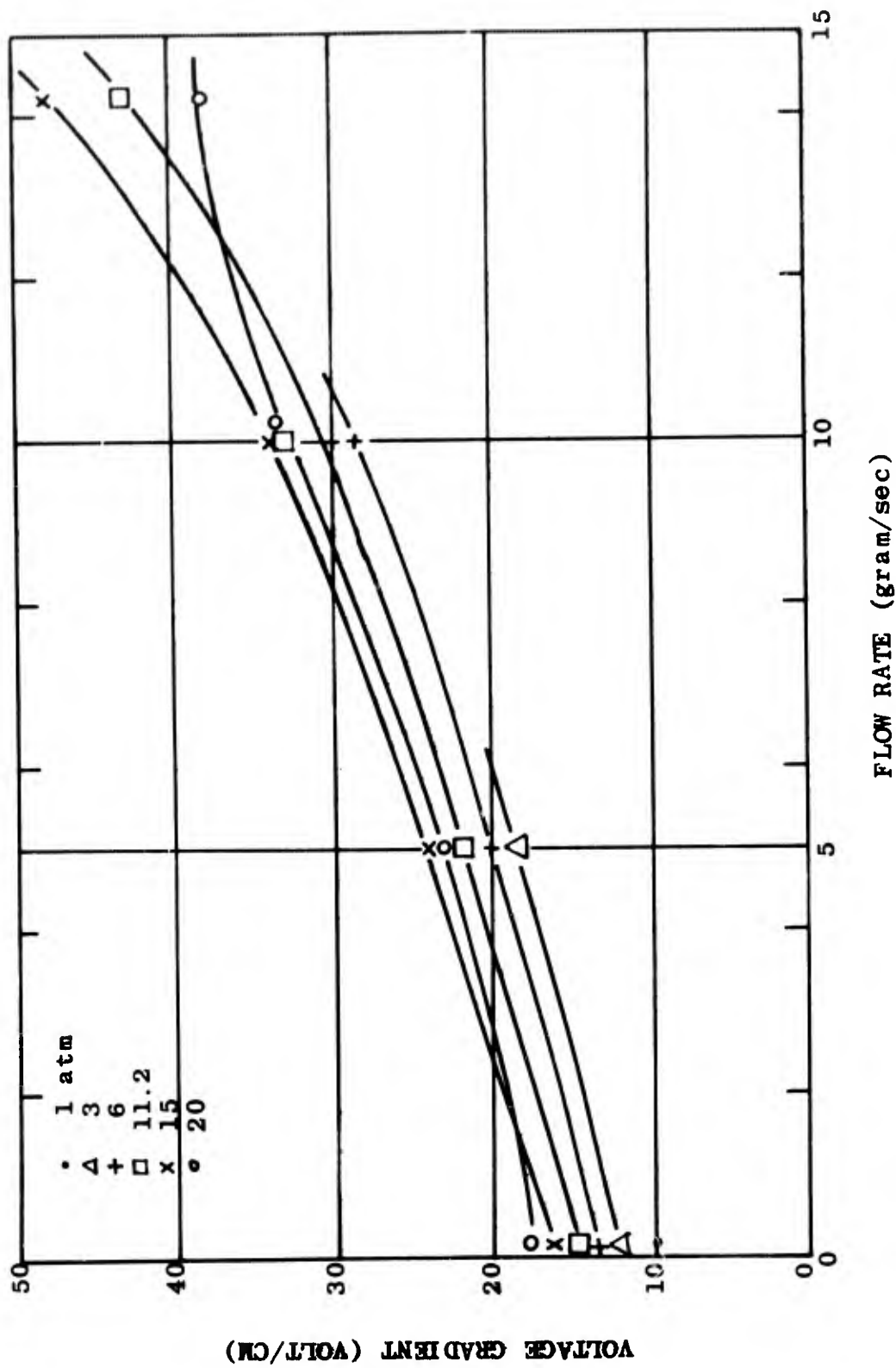
Figure 11—Voltage Gradient vs. Flow Rate in a 0.7 cm Tube, Argon
Pressures from 1 to 20 Atmospheres

Gas:            Argon
Pressure:       1, 3, 6, 11.2, 15, 20 atm
Current:        125 ±4 amp
Tube Diameter:  0.7 cm
Tube Length:    50 cm
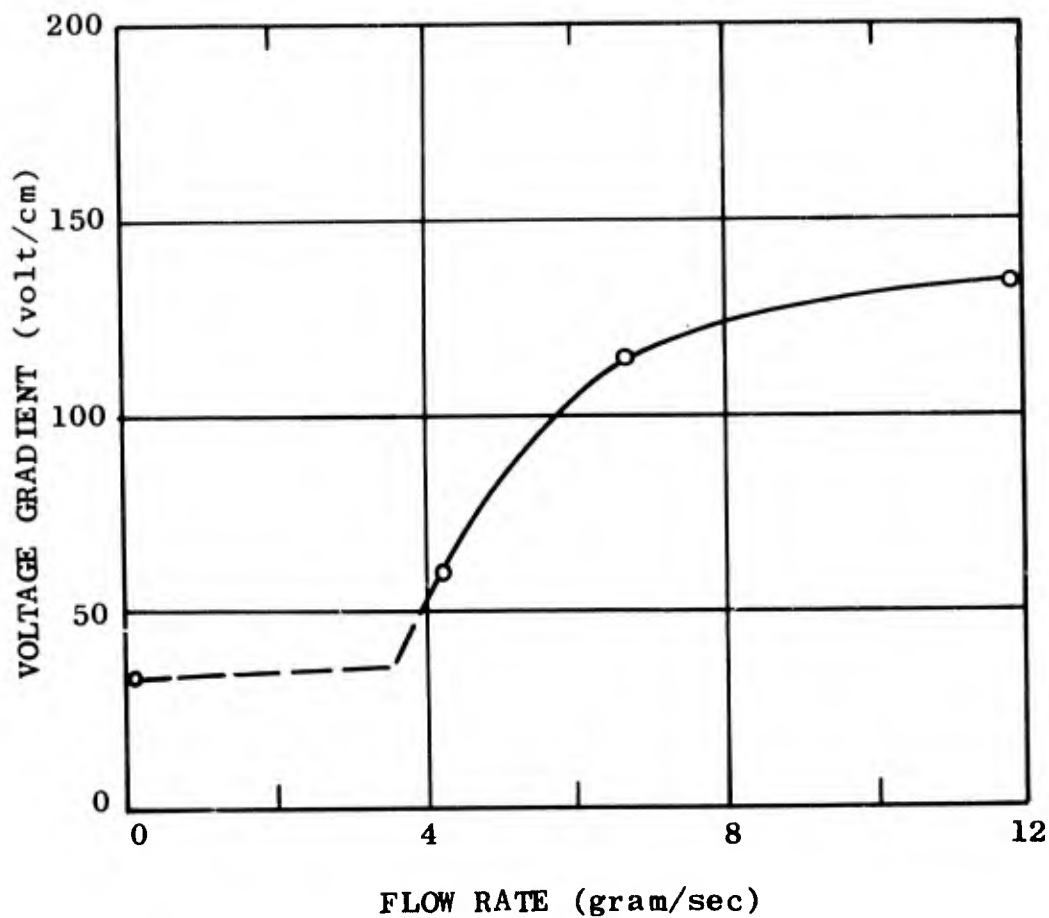
Figure 12-Voltage Gradient vs. Flow Rate at 11.2 Atmospheres
of Nitrogen in a 0.7 cm Tube

| | |
|---|---|
| Gas: | Nitrogen |
| Pressure: | 11.2 atm |
| Current: | 125 $\pm$4 amp |
| Tube Diameter: | 0.7 cm |
| Tube Length: | 50 cm |

3.1312   Nitrogen

A short series of variable flow tests was made in
nitrogen, again at a current level of 125 amperes.  Figure 12
shows that there is a three-fold increase in voltage gradient
for the range of flow rates studied, but the terminal slope
of the graph is low.  Obviously more measurements are
necessary before firm conclusions can be drawn.
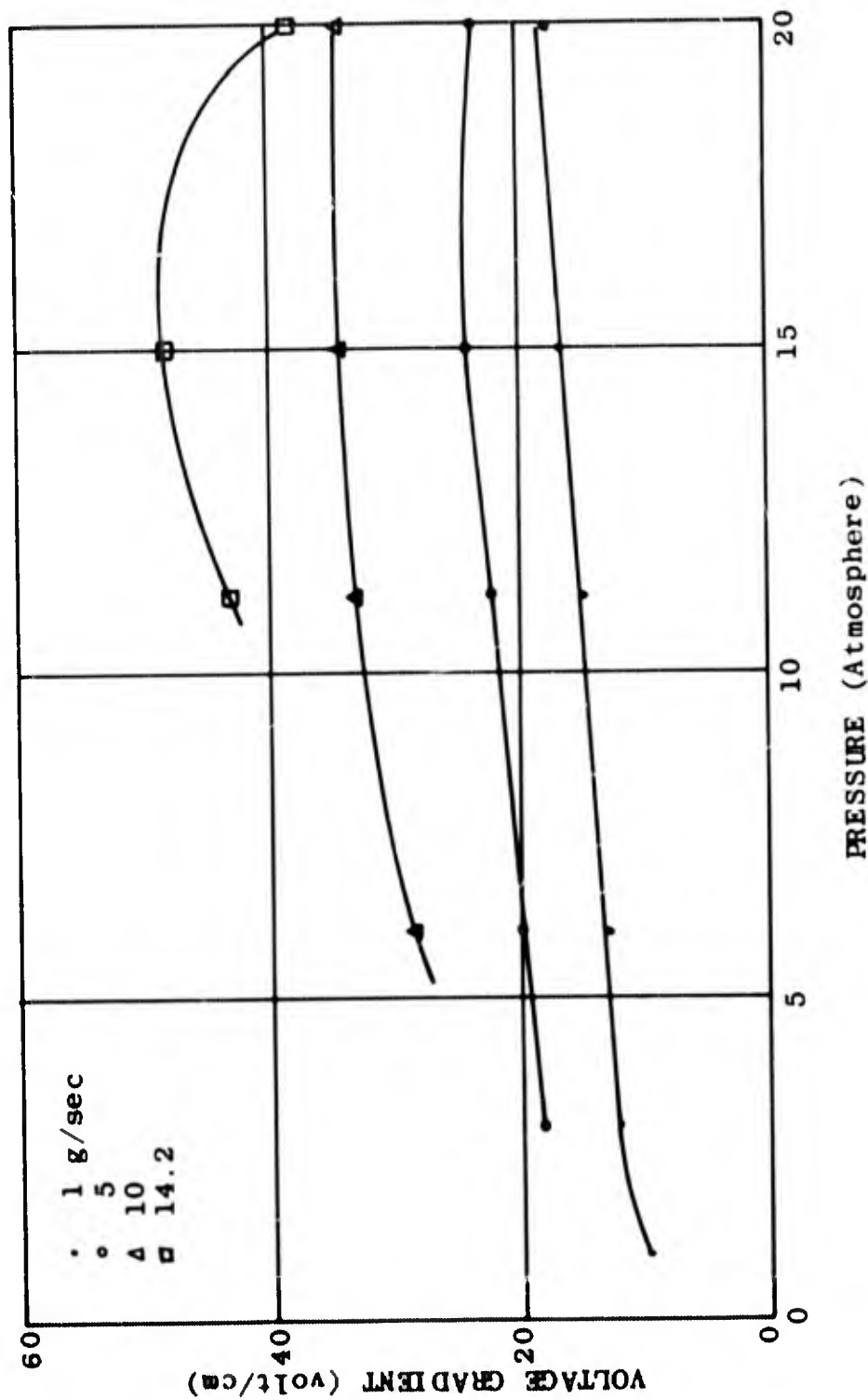
Figure 13-Voltage Gradient vs. Argon Pressure in a 0.7 cm Tube, Flow Rates from 0.1 to 14.2 gram/sec

Gas:              Argon
Current:          125 $\pm$4 amp
Flow Rate:        0.1, 5, 10, 14.2 gram/sec
Tube Diameter:    0.7 cm
Tube Length:      50 cm
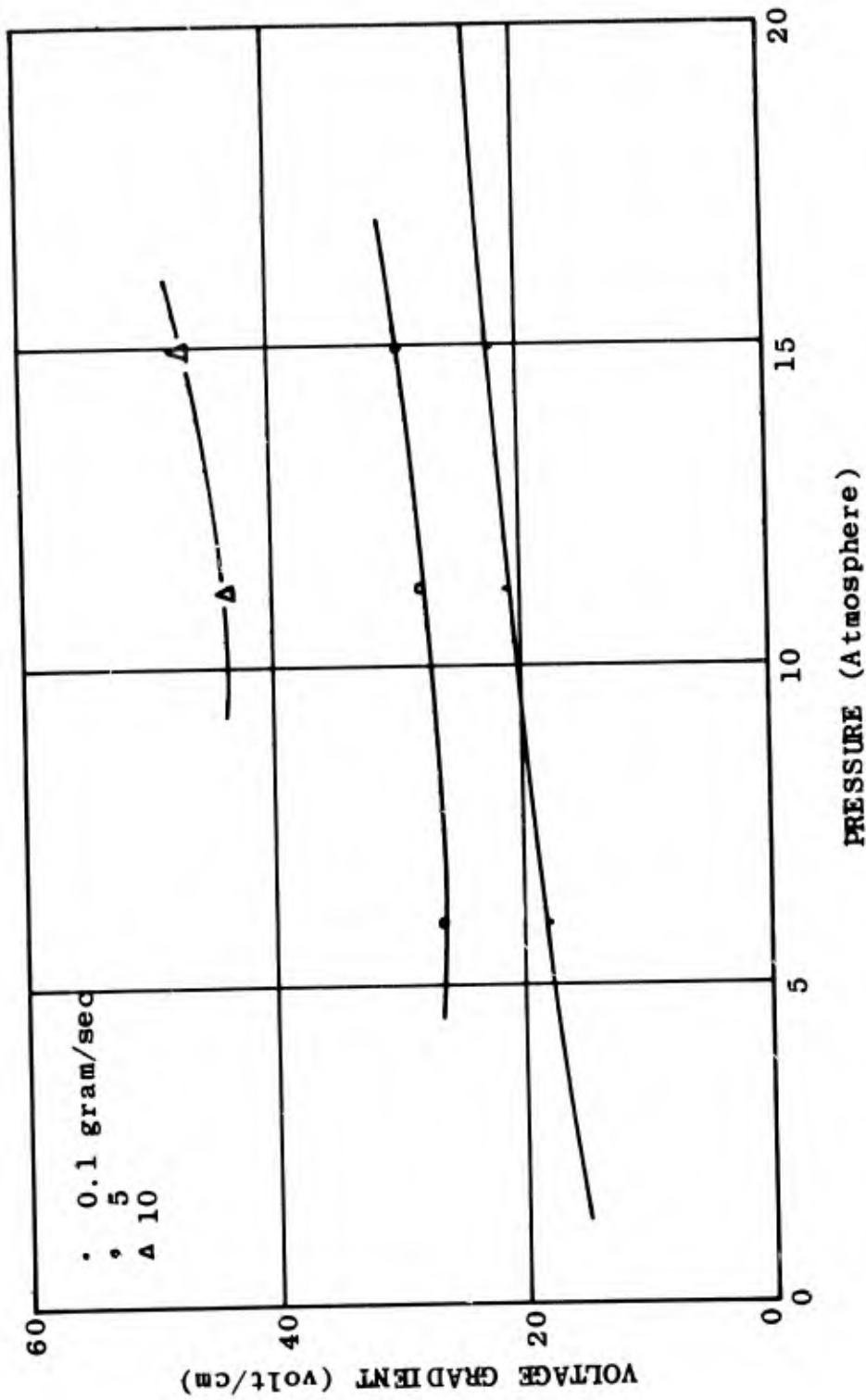
Figure 14–Voltage Gradient vs. Argon Pressure in a 0.5 cm Tube, Flow Rates from 0.1 to 10 gram/sec

Gas:              Argon
Current:          125 $\pm$4 amp
Flow Rate:        0.1, 5, 10 gram/sec
Tube Diameter:    0.5 cm
Tube Length:      50 cm

3.132     Variable Pressure

3.1321    Tube Diameter of 0.7 cm

          The results of figure 11 are replotted in figure 13
to show the influence of pressure more clearly.  Each line
in the graph represents a constant flow rate result with var-
iable ambient pressure.  In addition, to the large flow effect,
there is an interesting increase in the curve for low flow rate
with pressure; since thermal conductivity is approximately
independent of pressure, this rise must be due to increased
radiation losses or to a higher core temperature required to
achieve sufficient ionization.  The behavior at 20 atmospheres
is anomalous, especially at the highest flow rate.

3.1322    Tube Diameter of 0.5 cm

          Figure 14 is a repeat of the previous one with a smaller
tube diameter.  The laminar or low flow test series shows a
higher power loss than the previous graph while the dependence
of heat flux on flow rate is also greater.  The same flow rate
produces a greater increase in voltage gradient too.  We feel
this to be due to the smaller flow area which results in about
twice the plasma velocity and thus in an increased Reynolds number
for a given flow rate.

3.133     Variable Current

3.1331    Argon

          All previous results described in section 3.1 have been
for 125 ampere arcs.  It is important to determine that the
effects seen at that current level exist at higher currents
too.  In the graphs which follow, ambient pressure is fixed and
current varied; different data lines indicate different flow
rates.

          Figure 15 shows the results for 11.2 atmosphere argon
in a 0.7 cm I. D. tube.  Because a number of flow rates were
studied a fairly complete picture emerges.  The laminar curve
shows a slow but steady increase in voltage gradient with
current, as expected; the data taken with high flow rates show
an initial decrease before beginning to rise again at higher
currents.  The initial decrease is quite probably the result
of higher plasma temperatures which increase viscosity and
diminish turbulence.  There is no sign, however, that turbulent
effects will disappear at any current reasonably extrapolated
from this graph.

-23-
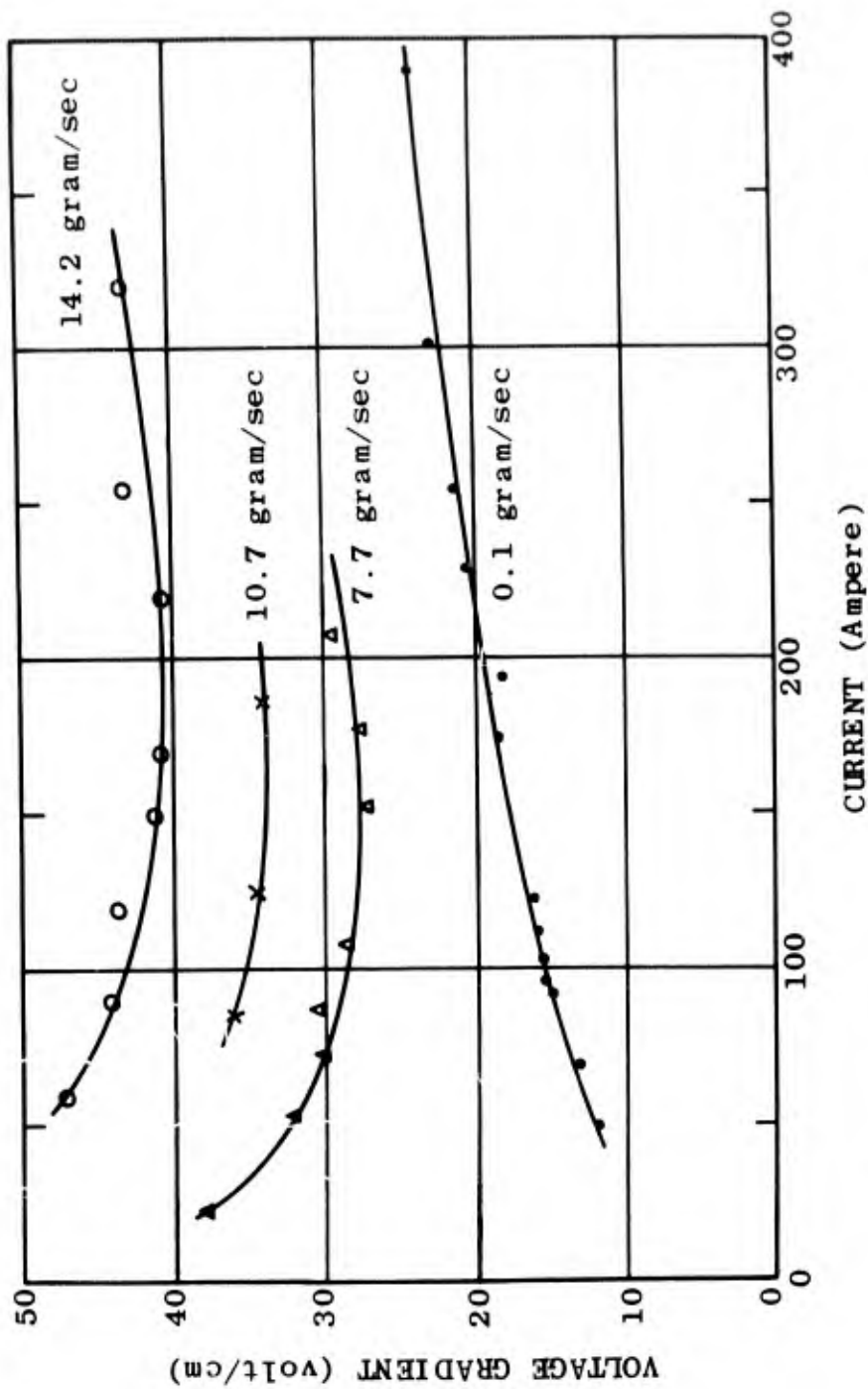
Figure 15-Characteristics of 11.2 Atmosphere Argon Arcs in a 0.7 cm Tube, Flow Rates from 0.1 to 14.2 gram/sec

Gas:              Argon
Pressure:         11.2 atm
Flow Rate:        0.1, 7.7, 10.7, 14.2 gram/sec
Tube Diameter:    0.7 cm
Tube Length:      50 cm
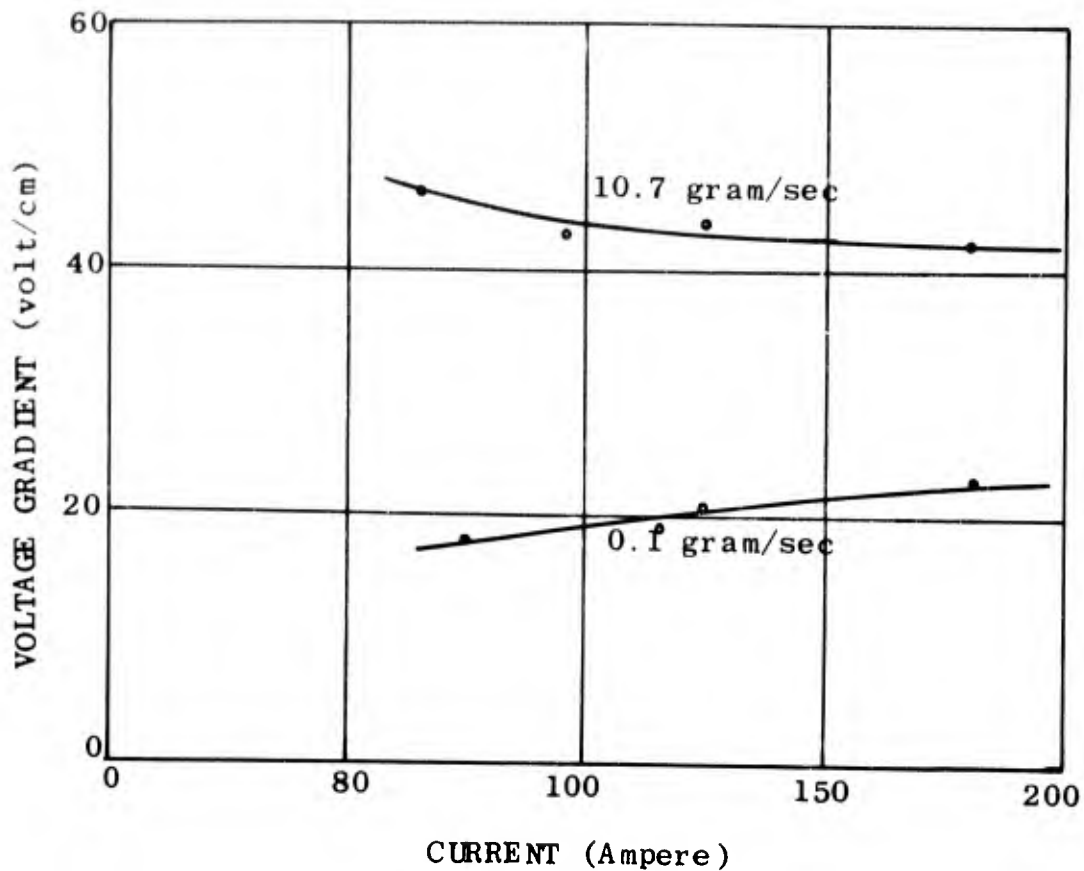
Figure 16-Characteristics of 11.2 Atmosphere Argon
Arcs in a 0.5 cm Tube, Flow Rates of 0.1
and 10.7 gram/sec

| Gas: | Argon |
|---|---|
| Pressure: | 11.2 atm |
| Flow Rate: | 0.1, 10.7 gram/sec |
| Tube Diameter: | 0.7 cm |
| Tube Length: | 50 cm |

Figure 16, when compared with figure 15, shows again
that the same flow rate in a smaller tube produces a higher
power loss. This follows the pattern of "classical" turbulence
in homogeneous fluids.

The work is extended to 15 and 20 atmospheres ambient
respectively in figures 17 and 18. The independence of voltage
gradient on current at 20 atmospheres is especially noteworthy.
It shows no sign of declining at the highest current tested.

-25-
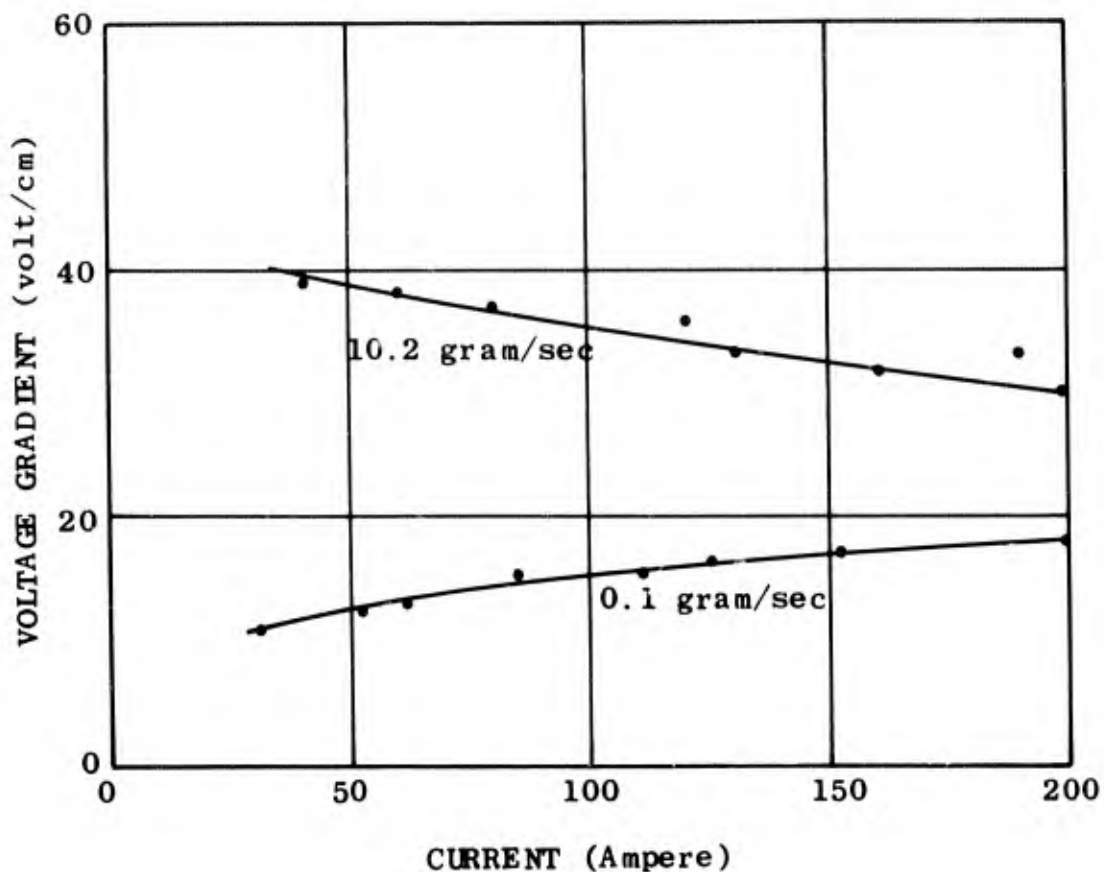
Figure 17-Characteristics of 15 Atmosphere Argon
Arcs in a 0.7 cm tube, Flow Rates of
0.1 and 10.2 gram/sec

| | |
|---|---|
| Gas: | Argon |
| Pressure: | 15 atm |
| Flow Rate: | 0.1, 10.2 gram/sec |
| Tube Diameter: | 0.7 cm |
| Tube Length: | 50 cm |

## 3.1332    Nitrogen

With the substitution of nitrogen for argon, figure 19
is comparable to figure 15.  Four flow rates were tested over
a wide range of currents.  The laminar curve is only slightly
dependent on current; the high flow rate curves decline markedly
even above 50 amperes.  The decrease in the separation of the
turbulent and laminar curves at high currents is more pronounced
than in argon.  Notice however that the curve for the 12 gram/sec
flow rate shows still more than a three fold increase over the
0.1 gram/sec value for heat transfer at the highest currents
tested.
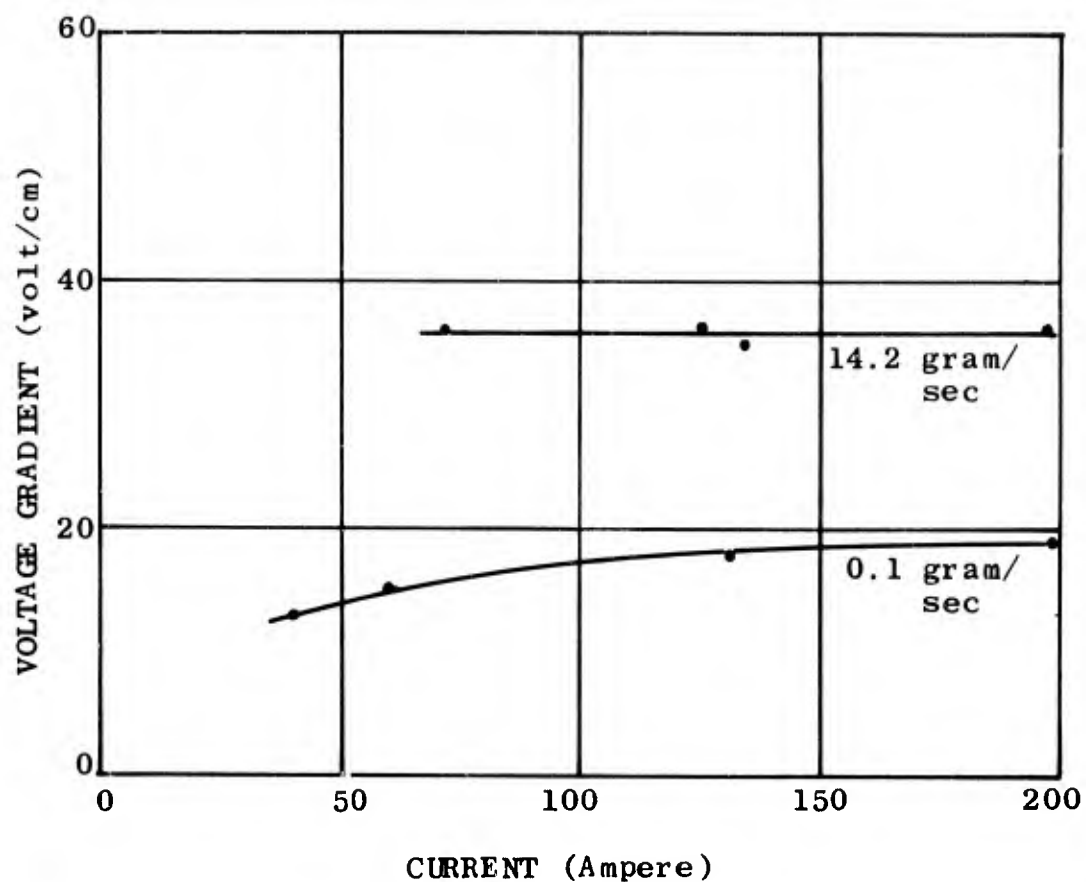
Figure 18–Characteristics of 20 Atmosphere Argon
Arcs in a 0.7 cm Tube. Flow Rates of
0.1 and 14.2 gram/sec

| | |
|---|---|
| Gas: | Argon |
| Pressure: | 15 atm |
| Flow Rate: | 0.1, 14.2 gram/sec |
| Tube Diameter: | 0.7 cm |
| Tube Length: | 50 cm |

3.134    Variable Tube Diameter

It is possible to gain an approximate idea of the in-
fluence of tube diameter on turbulent effects within the ranges
of current and flow rate covered in this report. In the present
investigation, tube diameters of 0.5 and 0.7 cm were used but
the 1 cm tube has been studied for an earlier report (2). The

-27-
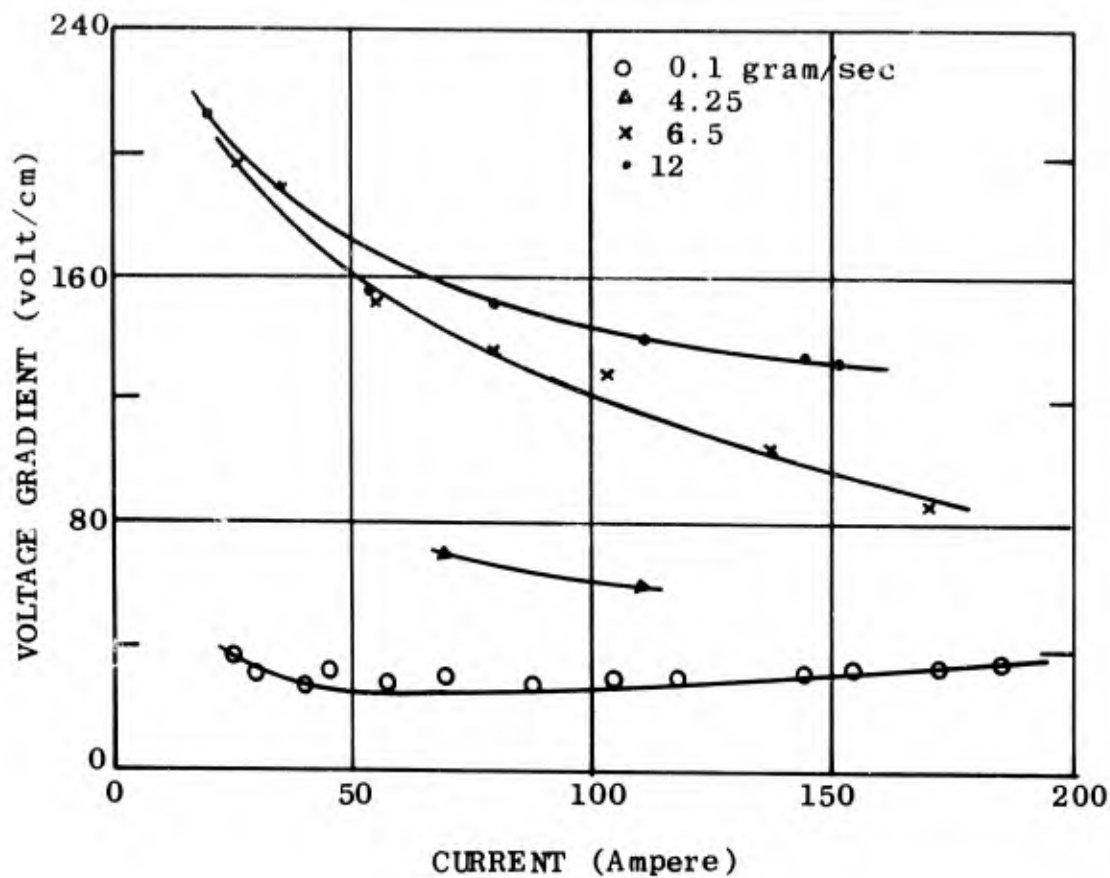
Figure 19–Characteristics of 11.2 Atmosphere
        Nitrogen Arcs in a 0.7 cm Tube, Flow
        Rates from 0.1 to 12 gram/sec

| | |
|---|---|
| Gas: | Nitrogen |
| Pressure: | 11.2 atm |
| Flow Rate: | 0.1, 4.25, 6.5, 12 gram/sec |
| Tube Diameter: | 0.7 cm |
| Tube Length: | 50 cm |

graph of figure 20 was put together by extrapolating the 1.0 cm
diameter results (2) from 80 to 100 amperes.  The results then
do not represent direct measurements, but they should be accurate
enough for a view of the major effect.  Judging from figure 20,
a tube 2 cm in diameter would show an appreciable increase in
potential gradient only with a flow rate significantly above
15 gram/sec. while a tube 0.5 cm in diameter shows such an
effect with a few gram/sec.

-28-
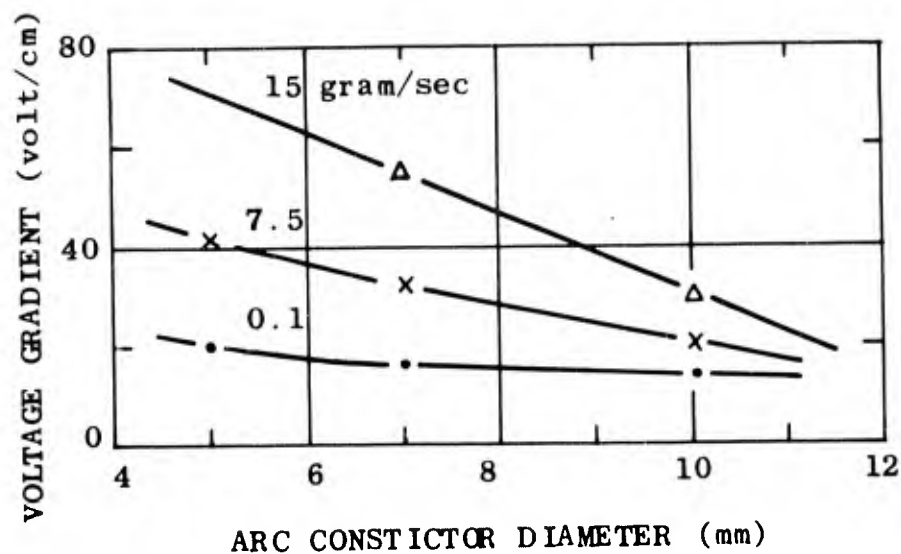
Figure 20-Voltage Gradient vs. Tube Diameter
at 10 atmospheres of Argon, Flow
Rates from 0.1 to 15 gram/sec

| Gas: | Argon |
|---|---|
| Flow Rate: | 0.1, 7.5, 15 gram/sec |
| Pressure: | 10 atm |
| Current: | 100 amp |
| Tube Length: | 50 and 75 cm |

## 3.2     Momentum Transfer as Measured by Pressure Gradients

## 3.21     Empirical Low Temperature Results

Earlier investigations of pressure drops along tubes
with turbulent flows have resulted in experimentally known
relationships for homogeneous fluids of moderate temperature.
Although a comprehensive theory has not been developed we will
summarize the important results below.

-29-

Taking the definition of friction factor, and rearranging the empirical relationships quoted in Rohsenow and Choi (11) we find that:

1) $\quad \dfrac{\Delta P}{\Delta L} \propto [Re]$ $\qquad$ in laminar flow

and

2) $\quad \dfrac{\Delta P}{\Delta L} \propto \dfrac{\mu^2}{\rho} [Re]^{1.8}$ $\qquad$ in turbulent flow

(D held constant)

but,

3) $\quad \dfrac{\Delta P}{\Delta L} \propto \dfrac{\mu^2}{\rho} [Re]^2$ $\qquad$ in far turbulent flow

(D held constant)

where $P$ = pressure
$\quad\quad\;\; L$ = length of tube
$\quad\quad\;\; \mu$ = viscosity
$\quad\quad\;\; \rho$ = density
and $\quad D$ = tube diameter

The point of transition from 2) to 3) depends on the surface roughness ratio e/D for the tube wall which is quite high in our case. (This "rough" wall, e/D = 0.036, is the result of the 0.25 mm thick, recessed teflon spacers which isolate the individual copper discs of the cascade tube). The graph of (11) indicates that, in our tube, equation 3) should hold for $Re_D \geq 30,000$. It must be emphasized that the equations quoted above and the result for wall roughness are empirical-they satisfy data from experiments conducted on homogeneous fluids near room temperature.

## 3.22    Methods

In an earlier report (3) we presented the results of pressure gradient measurements on 125 ampere arcs at 11.2 atmospheres. The sensor response, the measuring technique, and the accuracy of this system were discussed there. Briefly, a quartz pressure-charge transducer is mounted at the end of a thin, electrically insulating tube which runs through a copper disc to the arc channel. The dead volume before the transducer is minimized so the response time of the system is held to a few milliseconds. Because of this limit we miss the high frequency fluctuations but are able to read the average pressure well. Measurements were made at 5 points along the tube

-30-

FLOW RATE (gram/sec)
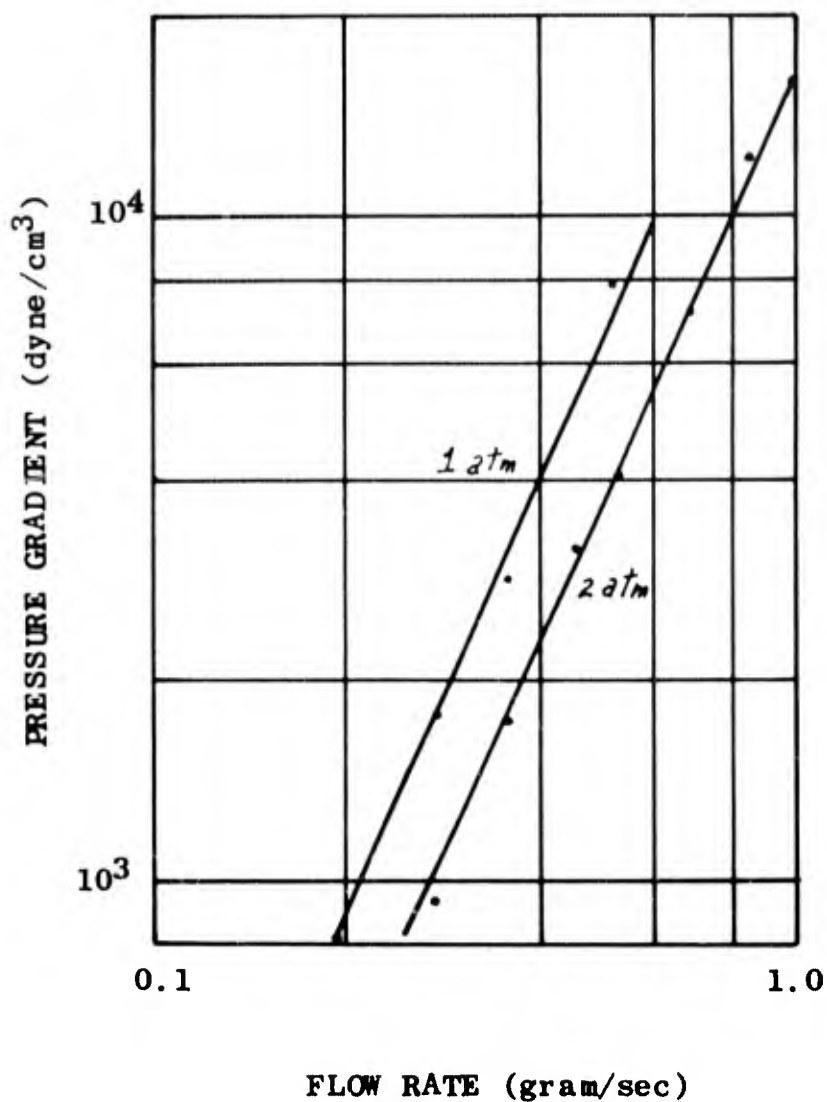
Figure 21-Pressure Gradient vs.
Flow Rate, Comparing 1
and 2 Atmospheres of
Argon without Arc

| Gas· | Argon |
|---|---|
| Pressure: | 1, 2 atm |
| Current: | None |
| Tube Diameter: | 0.7 cm |
| Tube Length: | 50 cm |

simultaneously to establish the gradient. Preference was
given to the fully developed flow region but no strong
departures from linearity were seen in any segment of the
tube. The current value of 125 amperes was chosen because
the pressure gradient and plasma velocity were found to be
largely independent of current in that area; it was also a
convenient value for our apparatus.

-31-

From a log-log plot of our data we found a constant
1.8 power dependence of pressure gradient on flow rate, an
indication that the flows were in the turbulent area, equation
2). While it would be desirable to extend these 11.2 atmos-
phere measurements to lower flow rates so the laminar region
could be explored, the sensitivity of our instrumentation sets
a limit. Consequently the ambient arc pressure was lowered to
permit measurement of the pressure gradient at lower flow rates
for which the flow is laminar. Equation 2) shows that the pres-
sure gradient goes as 1/o for a constant Reynolds number or,
since:

$$4) \quad Re_D = \frac{4W}{\pi D \mu}$$

for constant flow rate, diameter, and viscosity (W, D, and μ
respectively).

This variation of pressure gradient with ambient pres-
sure can be seen in figure 21. The data was taken in our cas-
cade tube with no arc burning. For a fixed flow rate, the two
atmosphere case shows about half the pressure drop of the one
atmosphere case.

3.23    Measurements in Hot Flow

A series of measurements with the arc burning is shown
in figure 22, which is a log-log plot of pressure gradients
against flow rates at ambient pressures of 1, 2, 3, and 11.2
atmospheres. The gas was argon in all cases; the arc current
varied from 112 to 129 amperes. Since it was established in
(3) that pressure gradients changed only slowly with currents
above 100 amperes, the small current variation is negligible.

The major result from figure 22 is the expected trans-
ition from a laminar to turbulent dependence of pressure
gradient on flow rate. Specifically the slope of the curve
changes abruptly from 1.0 to approximately 1.8 which is the
behavior predicted by equations 1) and 2). This transition
occurs in the neighborhood of 1.5 gram/second, a point which
agrees well with the one atmosphere experiments of Runstadler
(10). His curve of friction factors, however, shows only
marginal evidence of turbulence; by increasing pressure above
one atmosphere we have shown both the laminar and the clearly
turbulent branches of the curve.

-32-
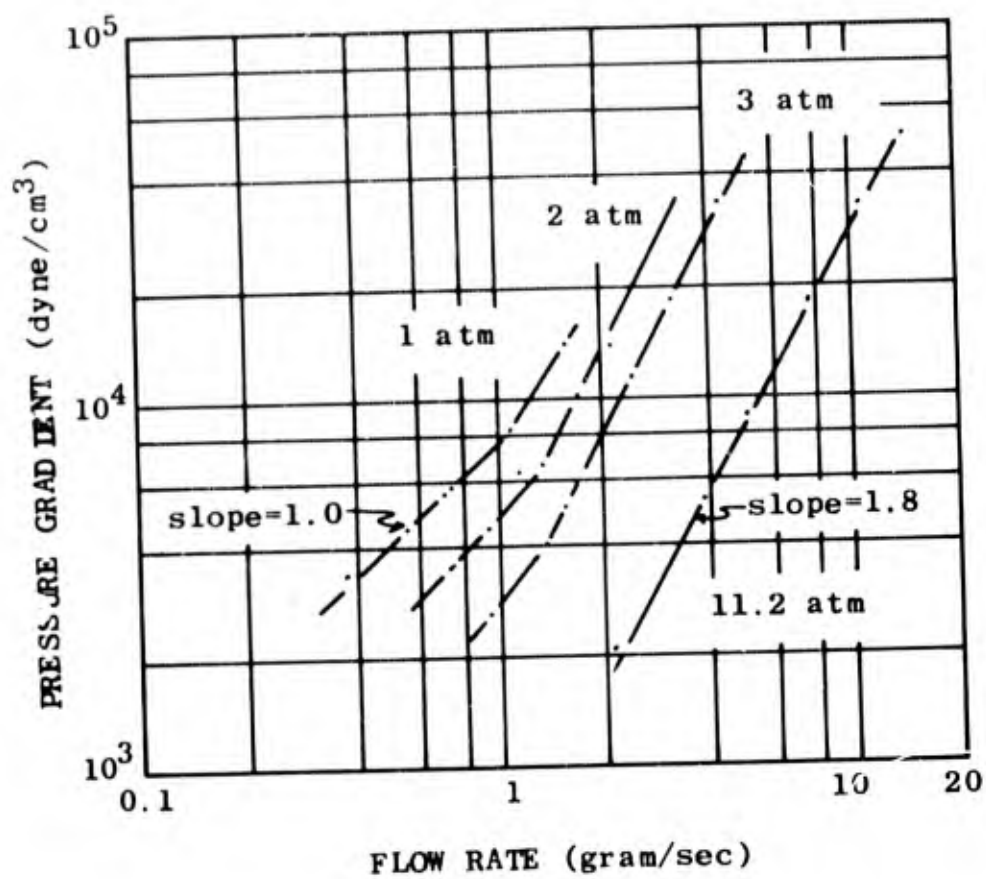
Figure 22-Pressure Gradient vs. Flow Rate, Argon
Pressure from 1 to 11.2 Atmospheres

| Gas: | Argon |
|------|-------|
| Pressure: | 1, 2, 4, 11.2 atm |
| Current: | 125, +4, --13 amp |
| Tube Diameter: | 0.7 cm |
| Tube Length: | 50 cm |
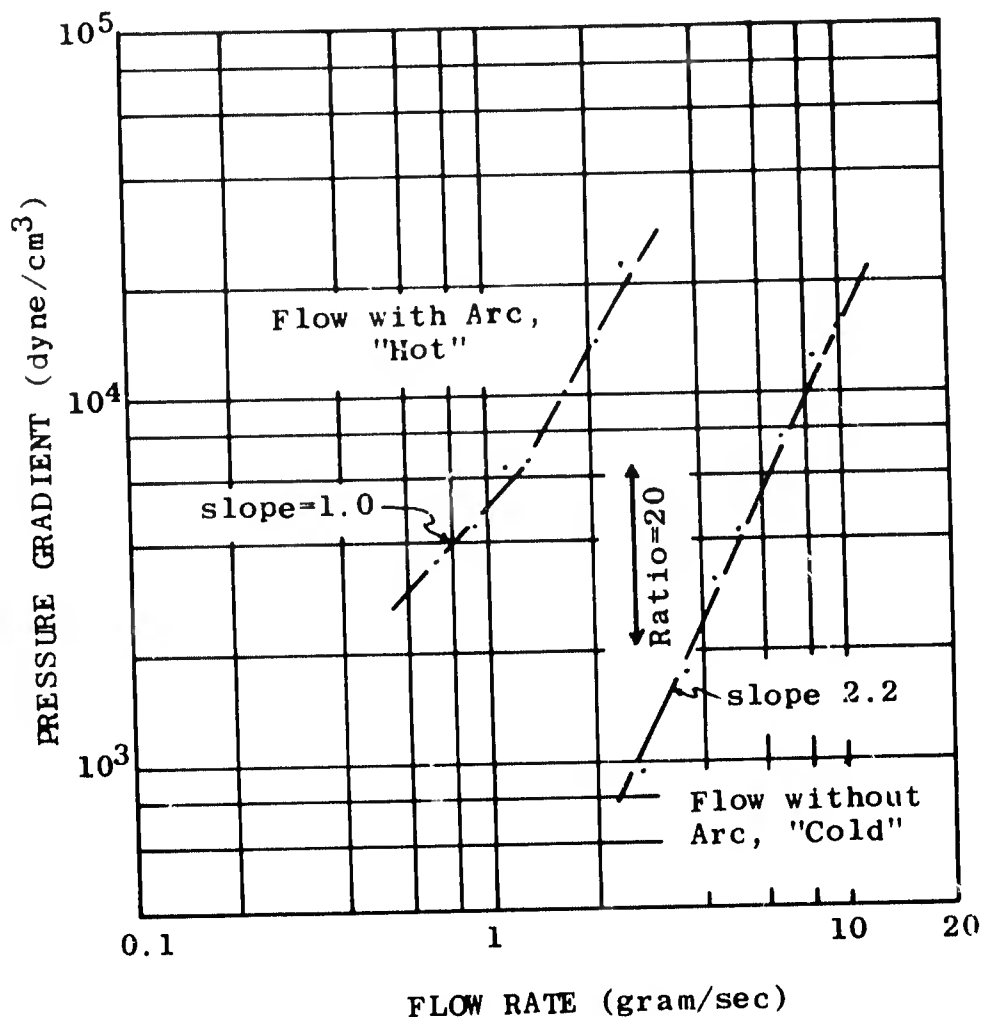
Figure 23-Pressure Gradient vs. Flow Rate,
2 Atmosphere Argon with and with-
out an arc.

| Gas: | Argon |
| Pressure: | 2 atm |
| Current: | 125 amp, none |
| Tube Diameter: | 0.7 cm |
| Tube Length: | 50 cm |

The large effect which the presence of the arc has on the pressure gradient in the tube is evident from figure 23. At 3 gram/sec flow rate, the only area of overlap for the two curves, the ratio of the two pressure drops was found to be 20:1. But this measurement is at constant flow rate, not constant Re. It has been argued (10) that the proper choice of Re to describe the flow through an arc is the room temperature value. The graph above shows that, insofar as the pressure gradient is concerned, this selection is incorrect. The Re for this tube at 1.5 gram/sec is 13,000 if computed from room temperature fluid properties. The corresponding number for a 12,000°K model is 800. If one uses a more sophisticated choice of reference temperature, the average enthalpy value suggested by Eckert (9), the Re at 1.5 gram/sec is 1,400.

-34-
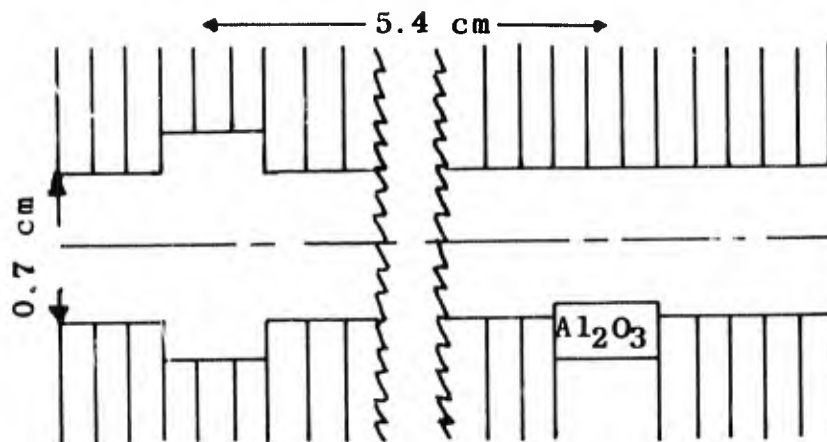
Figure 24-Diagram of Doping Method Used for
Mass Transport Study. Gas flow
is from right to left.

3.3        Mass Transfer as Measured by Radial Diffusion of Atoms

3.31       Method

One of the distinguishing attributes of turbulent flow
is the existence of macroscopic flow perpendicular to the direc-
tion of major flow.   It was therefore of great interest for our
investigation to make some direct tests on turbulent mass trans-
fer in addition to the experiments on heat and momentum transfer.
Our stygmatic Ebert spectrograph enables us to study such motion
and we have utilized that ability.  The diffusion of a dopant
species in the arc can be compared when flow rates are high and
low, thus giving an idea of the rate at which turbulent mixing
procedes compared with the rate of unassisted molecular diffusion.

In this study, dopant material was deliberately intro-
duced, not symmetrically from the electrode, but from one side
of the tube so that its diffusion toward an even concentration
over the tube crossection could be observed.  This was done
by placing a crystal of $Al_2O_3$ at the edge of the arc and
allowing it to ablate.  Spectral observation was made through
a window located 5.4 cm downstream from the point of introduc-
tion, (figure 24).  Two "near resonance" Al I lines, $\lambda$ = 3944 Å
and 3961.5 Å, are prominent enough for use even at low partial
pressures.
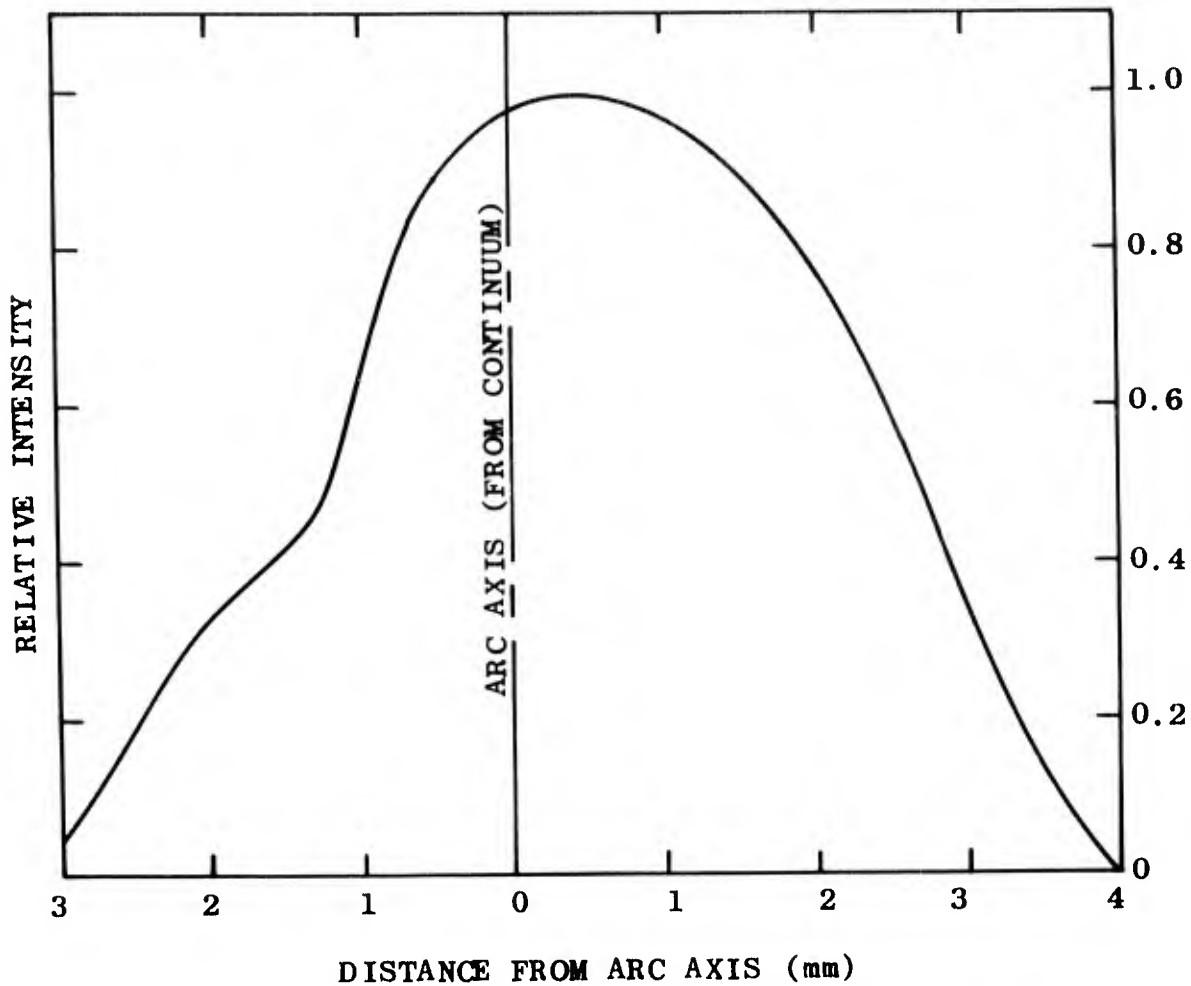
Figure 25-Line Intensity (Al I $\lambda$ = 3961.5 Å)
    Observed 5.4 cm Downstream from Introduction
    Point; Flow Rate 0.3 gram/sec.  The Aluminum
    was introduced from the right side as seen
    here.

| | |
|---|---|
| Gas: | Argon |
| Pressure: | 11.2 atm |
| Current: | 50 ampere |
| Flow Rate: | 0.3 gram/sec |
| Tube Diameter: | 0.7 cm |
| Dopant Introduction Point: | 41 cm from cathode |
| Window: | 46.4 cm from cathode |
| Tube Length: | 50 cm |
| Test #: | 458 |
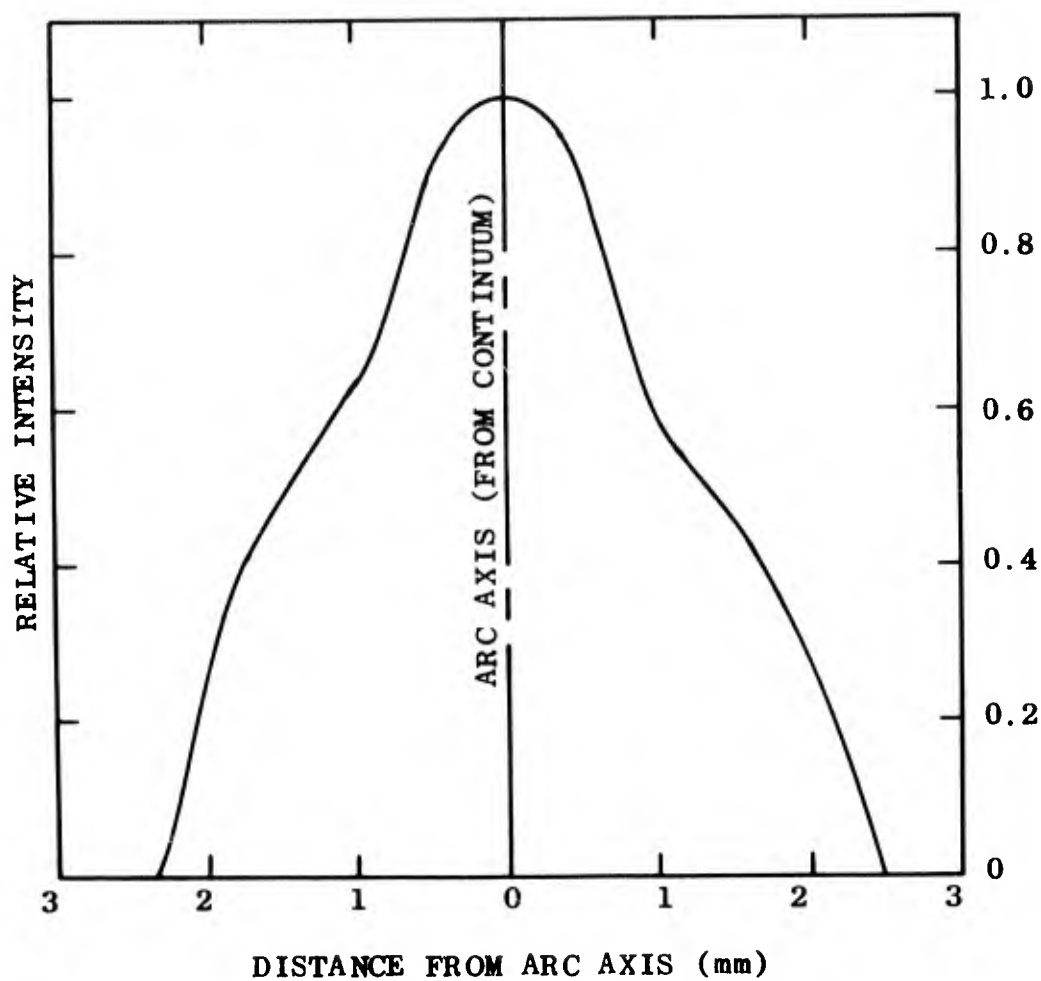
Figure 26-Line Intensity (Al I $\lambda$ = 3961.5 Å)
Observed 5.4 cm Downstream from Intro-
duction Point, Flow Rate 5 gram/sec.
The aluminum was introduced from the
right side as seen here.

| | |
|---|---|
| Gas: | Argon |
| Pressure: | 11.2 atm |
| Current: | 50 amp |
| Flow Rate: | 5 gram/sec |
| Tube Diameter: | 0.7 cm |
| Dopant Introduction Point: | 41 cm from cathode |
| Window: | 46.4 cm from cathode |
| Tube Length: | 50 cm |
| Test #: | 459 |

-37-

## 3.32 Results

Figures 25 and 26 show the intensities of the 3961.5 Å line in argon arcs of 50 amperes and 11.2 atm. with flow rates of 0.3 gram/sec. and 5 gram/sec. respectively.

These intensities are observed side-on and therefore represent values integrated through the varying depth of the arc, (I(x) values). The data are presented in the way because the graph of figure 25 is obviously strongly asymmetric and an Abel inversion cannot be performed without a much more sophisticated measurement as done by Olsen (12).

The arc axes marked on figures 25 and 26 were determined from the centers of the continuous radiation distribution which, significantly, was quite symmetric in both cases. In the high flow rate example, the maximum of the Al line intensity coincides with the maximum of the continuous radiation, as expected for a symmetrical distribution. But, for the laminar flow case, the line intensity distribution is stronly asymmetric, indicative of the asymmetric concentration of aluminum atoms.

In interpreting figs. 25 and 26 we feel that, in the laminar case, the time lapse between introduction of the sluminum and examination of the spectrum was obviously too short to achieve a symmetric distribution of the dopant species through the arc by molecular diffusion alone.

## 3.33 Discussion

In evaluating our observations of the last section, it is important to know whether the temperature distribution in these experiments was axially symmetric. If this were not so, small changes in temperatures might account for the observed line asymmetry rather than differences in the density of the aluminum atoms.

The arguments for accepting an unaltered temperature distribution and unaltered electrical and thermal conditions in the arc are:

1. The continuous radiation (which would also be quite sensitive to small changes in temperature) was symmetric.
2. Only a small percentage of the arc plasma is aluminum. Partial pressure of aluminum was estimated to be 50 dynes/cm$^2$ from an absolute measurement of the $\lambda = 3944$ Å line whose transition probability is known.
3. The arc voltage gradient remained unchanged when compared with tests containing no aluminum.

RATIO OF INTENSITY AT LEFT AND RIGHT SIDES OF AXIS

DISTANCE FROM ARC AXIS (mm)
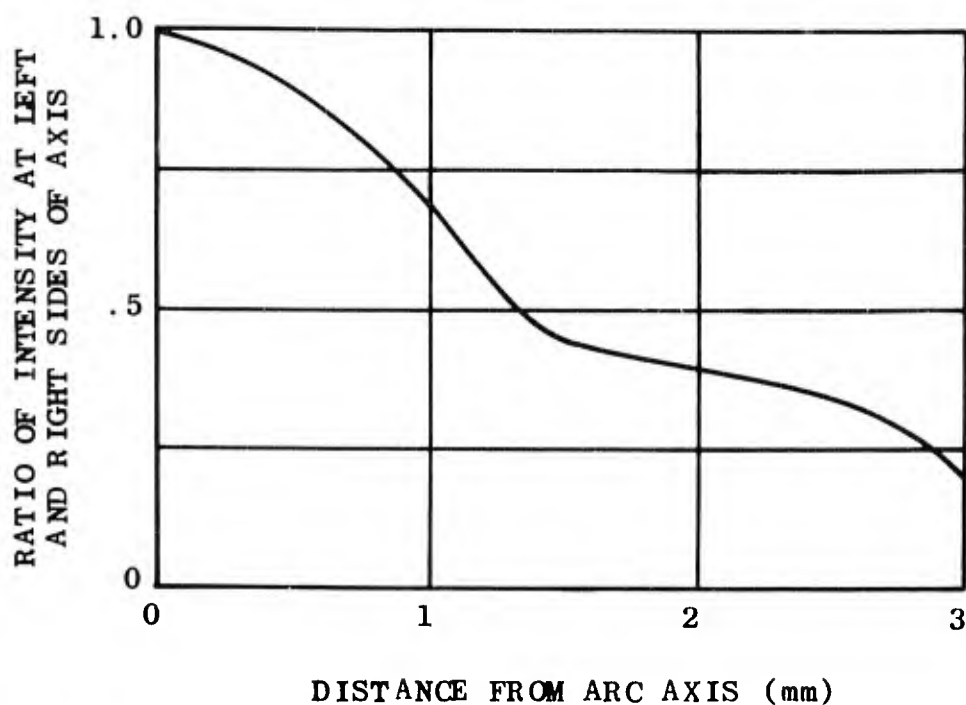
Figure 27–Ratio of Intensities at Two Sides
of Arc Axis, Based on Figure 25.
The aluminum distribution is clearly
asymmetric.   0.3 gram/sec flow rate

To show the distribution of aluminum more clearly, we
plot in figure 27 and 28 the intensity ratios at successive
distances from the arc axis.   The 5 gram/sec. test is essentially
symmetric, Fig. 28 while the 0.3 gram/sec. test shows an ever
increasing disparity as the edges of the plasma are approached,
fig. 27.

It would, of course, be valuable if diffusion veloci-
ties could be derived from our experiments.   However, an exact
measure of diffusion velocities was not accomplished.   Still,
there are firm conclusions which can be drawn.

Figures 25 and 26 show clearly that diffusion is much
more uniform at the higher flow rate, but a consideration of
the axial flow velocities makes the comparison even more start-
ling.   If we take from our earlier plasma velocity measurements
(3) average axial velocities of 9 meter/sec. and 150 meter/sec.
for the two tests, the two respective diffusion times between
introduction of dopant and measurement become 6 msec. and 360
μsec. which differ by a factor of 15.   Since the aluminum
distribution is much more uniform in the high flow case, we
can conclude that turbulence has increased the rate of diffusion
of aluminum in argon at least a factor of 15.

-39-

DISTANCE FROM ARC AXIS (mm)
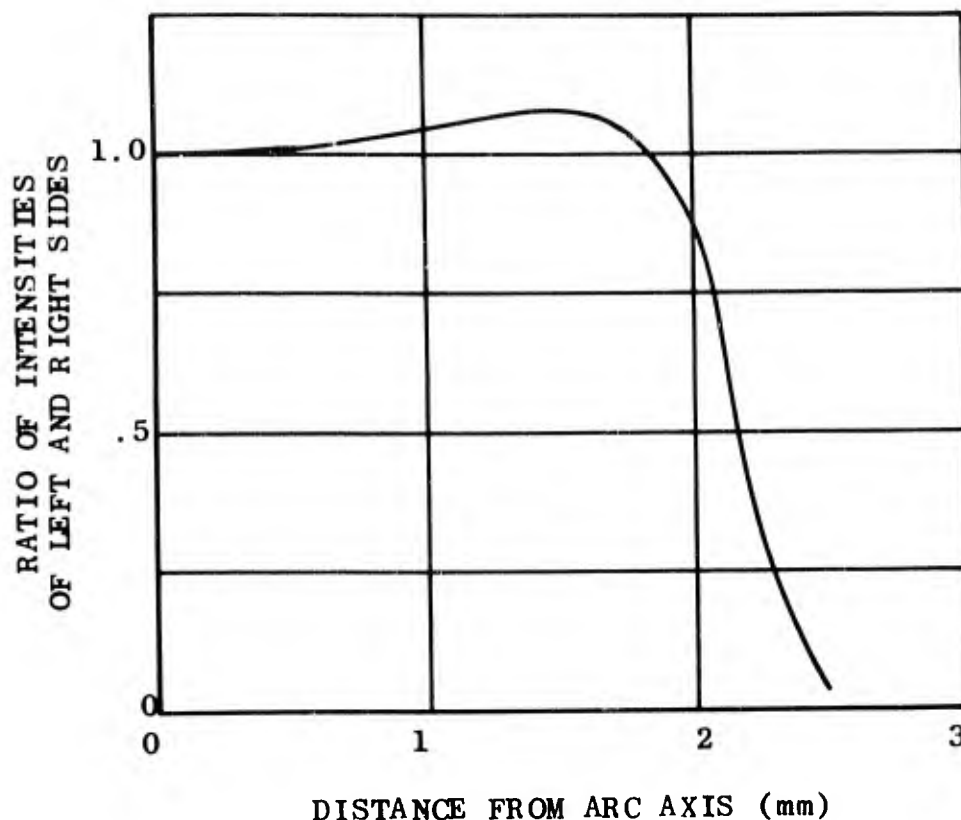
Figure 28—Ratio of Intensities at Two
Sides of Arc Axis, Based on
Figure 26.  The aluminum
distribution is symmetric
except at the very edges.
5.0 gram/sec flow rate

## 3.4        Fluctuations of Light Intensity

## 3.41       Method

Our earlier insight into the local three dimensional
structure of turbulent arcs was mainly based on direct high
speed photography of arcs (2, 3).  Whereas the movies pro-
vided a striking confirmation of the non laminar character of
high flow rate arcs, a quantitative measure of light fluctua-
tions cannot be conveniently taken from such records.

Besides being a measure of plasma turbulence, a determin-
ation of the amplitude and frequency distribution of the light
fluctuations is also important for a judgement of the accuracy
of temperature measurements.  As reported earlier (3), the critical
problem for turbulent temperature measurements is that light
intensity is linear with temperature only in restricted temperature
ranges.  If the limits of this linear range are exceeded, a
mistake is introduced when the intensity average is accepted as
a measure of the temperature average.

-40-

To measure light fluctuations a magnified image (x8) of the arc was projected on a photo-diode.[*]

The light window was 45 cm downstream from the cathode in a 50 cm tube of 0.7 cm diameter. An f2.5 lens with 7.5 cm diameter was used for this purpose. Pertinent specifications of the photo-diode were:

| | |
|---|---|
| Sensitivity: | 0.5 amp/watt at 9,000Å |
| Quantum Efficiency: | 70% |
| Rise Time: | $5 \times 10^{-8}$ or better |
| Linear Range: | 7 decades |
| Spectral Sensitivity Range: | 3dB points at 3,500Å and 11,300Å |
| Active Area: | 5.1 $mm^2$ |

The rise time includes a probe and the CRO: it was checked using a fast solid state laser with 9,000 Å output. Because of the magnification, the diode can resolve approximately 0.25 mm in the arc. The response of the diode, however, represents an integrated value running side on through the arc. The sensor was placed in the center of the arc image and so integrated light from a diameter which included the arc core.

In the tests of the following section, the CRO trace displaying the photo-diode response was delayed about 200 msec after arc ignition to allow time to establish steady state conditions. The trace then sweeps the screen rapidly providing a short sample (typically 500 μsec) of the fluctuations. Although repeat tests were made to establish reproducibility they proved to be redundent and are not shown here.

| | |
|---|---|
| Gas: | Argon |
| Pressure: | 11.2 atm |
| Current: | 53 amp |
| Flow Rate: | 3.75 gram/sec |
| Tube Diameter: | 0.7 cm |
| Window: | 45 cm from cathode |
| Tube Length: | 50 cm |
| Test #: | 468 |

Zero Intensity

1 msec

Figure 29-Light Fluctuations of a 50 Ampere Argon Arc with 3.75 gram/sec Flow Rate, Slow Sweep

* The photo-diode was a SGD-100 silicon diffused model of Edgerton, Grier, and Germershausen, Boston, Mass.

## 3.42    Results

For a view of the slow fluctuations the oscilliscope was
set to cover a 5 msec period with figure 29 as a result.   The
light comes from a 50 ampere argon arc in a 0.7 cm I. D. constric-
tor.   The ambient pressure was 11.2 atm. and the flow rate 3.75
gram/sec.

From this figure one can see that, in the fully developed
region of a high flow rate arc, there is a impressive level of
fluctuations.   The general nature of the trace is irregular with
a mixture of frequencies.   No signs of "snaking" of the arc
column, which would create slow, regular swings in the average
intensity are visible even at this low current.
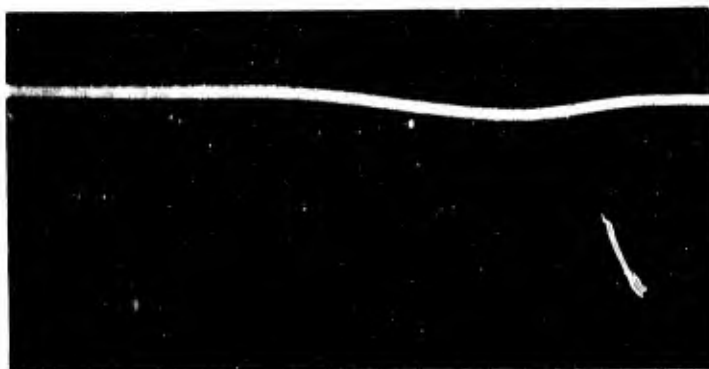


| | |
|---|---|
| Gas: | Argon |
| Pressure: | 11.2 atm |
| Current: | 54 amp |
| Flow Rate: | 0.3 gram/sec |
| Tube Diameter: | 0.7 cm |
| Window: | 45 cm from cathode |
| Tube Length: | 50 cm |
| Test #: | 476 |

Zero Intensity

100μsec

Figure 30-Light Fluctuations of a 50 Ampere Argon Arc with 0.3
gram/sec Flow Rate, Fast Sweep
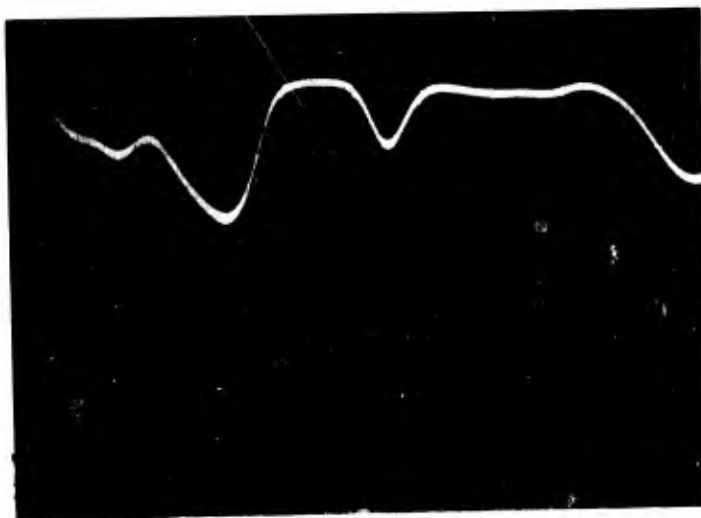


| | |
|---|---|
| Gas: | Argon |
| Pressure: | 11.2 atm |
| Current: | 53 amp |
| Flow Rate: | 1.1 gram/sec |
| Tube Diameter: | 0.7 cm |
| Window: | 45 cm from cathode |
| Tube Length: | 50 cm |
| Test #: | 475 |

Zero Intensity

100μsec

Figure 31-Light Fluctuations of a 50 Ampere Argon Arc with 1.1
gram/sec Flow Rate, Fast Sweep
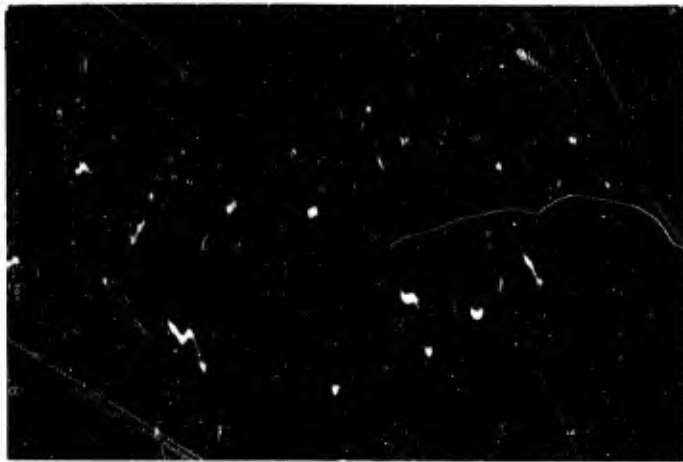
| Gas: | Argon |
|---|---|
| Pressure: | 11.2 atm |
| Current: | 53 amp |
| Flow Rate: | 3.75 gram/sec |
| Tube Diameter: | 0.7 cm |
| Window: | 45 cm from cathode |
| Tube Length: | 50 cm |
| Test #: | 471 |

Zero Intensity

100µsec

Figure 32-Light Fluctuations of a 50 Ampere Argon Arc with 3.75 gram/sec Flow Rate, Fast Sweep



| Gas: | Argon |
|---|---|
| Pressure: | 11.2 atm |
| Current: | 53 amp |
| Flow Rate: | 10.8 gram/sec |
| Tube Diameter: | 0.7 cm |
| Window: | 45 cm from cathode |
| Tube Length: | 50 cm |
| Test #: | 474 |

Zero Intensity

100µsec

Figure 33-Light Fluctuations of a 50 Ampere Argon Arc with 10.8 gram/sec Flow Rate, Fast Sweep

Gas:                Argon
Pressure:           11.2 atm
Current:            53 amp
Flow Rate:          15.5 gram/sec
Tube Diameter:      0.7 cm
Window:             45 cm from cathode
Tube Length:        50 cm
Test #:             473

Zero Intensity

100μsec

Figure 34-Light Fluctuations of a 50 Ampere Argon Arc with 15.5
        gram/sec Flow Rate, Fast Sweep

For a correlation of figure 29 with our other measure-
ments recall that the pressure gradient is on the turbulent
branch of the curve (figure 22) and the heat transfer has nearly
doubled over its laminar value (figure 15).

The series of figures 30 through 34 show this same
arc with increasing flow rates; the time scale is fixed at
50μsec/division. At 0.3 gram/sec there are few fluctuations
and they are slow and of low amplitude. At 1.1 gram/sec the
fluctuations are faster and of appreciable amplitude. With
3.75 gram/sec the integrated light intensity almost disappears
at times. At 10.8 and 15.5 gram/sec this trend continues: the
light modulations increase both in amplitude and frequency.

The extreme intensity variations seen in figures 29
through 34 occur in a 50 ampere arc; a higher current arc which
better fills the tube shows modulations with less amplitude at
the same flow rate. In a 125 ampere arc with 7.7 gram/sec flow
rate the RMS fluctuation amplitude is only about 20% of the DC
average value. Compare figure 35 with figure 33 and notice
that although the amplitude is supressed, the frequency ranges
are comparable.

Another record of light intensity fluctuations over a
longer duration is shown in figure 36. The slow sweep rate,
100 msec/division, shows the output of the photo-diode during
the entire length of a test. Conditions are: 125 ampere argon
arc with 3.75 gram/sec flow. There seems to be little change
in intensity or fluctuation as the arc continues to burn.

-44-
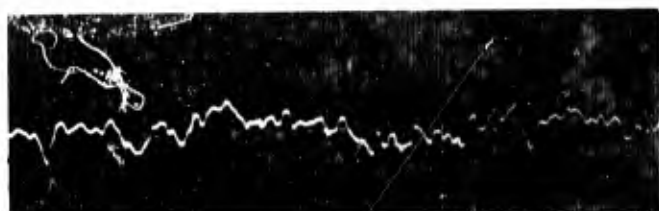
| Gas: | Argon |
| Pressure: | 11.2 atm |
| Current: | 125 amp |
| Flow Rate: | 7.7 gram/sec |
| Tube Diameter: | 0.7 cm |
| Tube Length: | 50 cm |
| Test #: | 457 |
| Window: | 45 cm from cathode |

← Zero Intensity

100μsec

Figure 35-Light Fluctuations of a 125 Ampere Argon Arc with
7.7 gram/sec Flow Rate, Fast Sweep
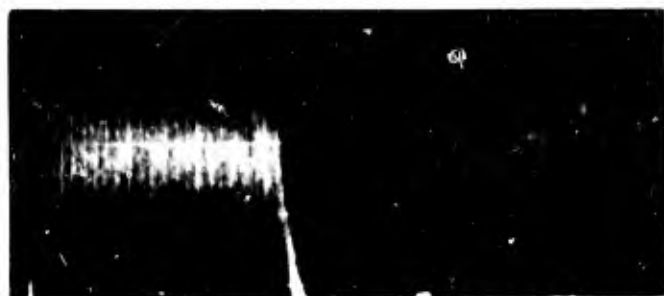


| Gas: | Argon |
| Pressure: | 11.2 atm |
| Current: | 128 amp |
| Flow Rate: | 3.75 gram/sec |
| Tube Diameter: | 0.7 cm |
| Window: | 45 cm from cathode |
| Tube Length: | 50 cm |
| Test #: | 453 |

← Zero Intensity

200msec

Figure 36-Light Fluctuations of a 125 Ampere Argon Arc with
3.75 gram/sec Flow Rate, Slow Sweep

3.5        Temperature Measurements

3.51       Methods

3.511      Milne Lorentz Method

        In an earlier report (3) measurements of the radial
temperature distribution of both laminar and turbulent 11.2 atm
50 amp nitrogen arcs, burning in a 0.7 cm tube had been reported.
These measurements were made by applying the Milne method
to the molecular band $\lambda$ =3371 Å of nitrogen. However only
the temperature of parts close to the arc axis could be measured
and it was highly desireable to get more points at the lower
temperatures of the outer mantle of the discharge.

        Such a low temperature measurement has been performed
earlier ( 13 ) by using the Milne peaking method on trace
additives, specifically on sodium which has prominent resonance
lines.

-45-

Although distortions of temperature measurements made
with trace additives due to demixing by diffusion cannot be
ignored, there were nevertheless several reasons for considering
this measuring method.  No argon or nitrogen line is suitable for
any except the highest temperatures which require much higher
currents.  It can be argued that violent mixing of the turbulent
arcs we wish to study should overwhelm the demixing caused by
diffusion.  In support of this, the image converter photographs
of (3) indicate an eddy velocity of roughly 20 meter/sec which
probably exceeds the diffusion velocity of sodium in nitrogen.
Finally, if additives prove sufficiently accurate, a series of
them could be used to give the radial position of lower temperature
isotherms and thus provide a complete temperature distribution
for arcs.  For these reasons an application of the Milne peaking
method on lines of trace elements was thought to be useful.

### 3.512    Calculation of Line Intensities for Milne-Lorentz Method

In this section the theoretical dependency of the Milne
maximum of the sodium D lines on plasma temperature is determined.
For this purpose the equilibrium atomic and molecular species
concentrations for a nitrogen-copper-sodium system must be found
at the temperatures of interest, and the temperature dependence
of a sodium spectral line calculated on this basis.

The temperature variation of spectral line intensity
is described by:

$$5) \qquad I_j \propto \frac{N_0}{Z_0} \, exp \left[ -\frac{F_j}{BT} \right]$$

In this equation both $N_0$ and $Z_0$ are also temperature dependent
so equation 5) must be supported further.

Before we persue our calculation, it may be remarked
that it is the variation of these two factors, $N_0$ and $Z_0$, which
decreases the line intensity at high temperatures to produce the
"Milne maximum".

Provided the atomic energy levels are known, $Z_0(T)$ can
be calculated from the definition of the partition function:

$$6) \qquad Z_0(T) \equiv \sum_j g_j \, exp \left[ -\frac{F_j}{BT} \right]$$

The temperature dependence of $N_0$ is embodied in the
Saha equation which describes the ionization of an atomic
species:

$$7) \qquad \frac{P_i P_A}{P_0} = \frac{2(2\pi m)^{3/2}}{h^3} \frac{Z_i}{Z_0} \, exp \left[ -\frac{IP}{BT} \right]$$

If only one atomic species is involved, then electrical

neutrality insures that

$$8) \qquad P_e = P_i$$

and 7) can be solved in a straight forward manner.

The system we must consider, however, consists of the dominant gas, nitrogen or argon, the additive, sodium for instance, and a trace of copper.

As a result of this multicomponent gas composition equation 8) is no longer accurate. Electrons are contributed by the dominant gas and the copper vapor as well as the sodium so the situation is described by:

$$9) \qquad P_{e \ (total)} = P_e \ (additive) + P_e \ (dominant \ gas) + P_e \ (copper)$$

The additive is chosen to have a considerably lower ionization temperature than the dominant gas so a "Milne" temperature point on the outside of the arc can be found. Near the radius of the Milne maximum there will be insignificant ionization of nitrogen or argon but copper has an ionization potential of 7.72 eV which is near enough to the 5.14 eV value of sodium to produce an appreciable ionization level. This additional source of electrons will be even more important if the arc contains more copper contamination than trace dopant and many water cooled copper cascades do produce a high partial pressure of copper. If the Saha equation 7) must be extended to higher temperatures, the influence of the dominant gas will be felt. Although the ionization potential of this gas may be 14 eV or higher, the density of the dominant gas is so much greater than the dopant that the former may be the major electron source. As a result of these additional gases, equation 7) must be applied to all electron sources and the set of equations solved simultaneously (see appendix). Our computer program includes an iternative solution to the parallel Saha equations, starting from an initial estimate to the total electron density. The situation is also complicated by the necessity to compute the dissociation of molecular nitrogen into atomic nitrogen because the two forms have different ionization potentials and thus contribute electrons in unequal degrees.

The appendix contains a simple block diagram of the computer program and some results for sodium additives in nitrogen at 5, 11.2 and 20 atmospheres. The mole fractions of each constituent are printed along with the spectral intensity of the sodium D lines. A low level of copper contamination was used because our short duration arc is relatively copper free. The results show that spectral intensity

-47-

does not continue to fall at temperatures above that of the Milne maximum but may level off or even increase.

If a non-resonance spectral line is chosen instead of the D lines, the temperature of the Milne maximum is shifted to a higher value by the change in the exponential factor of equation 5). Although the other factors in 5) remain as before, Pe grows rapidly with temperature and so will be much higher at the Milne temperature of a non resonance line. A higher electron pressure Pe can however broaden the Milne maximum or even eliminate it altogether. This can be seen by writing the Saha equation as:

$$10) \qquad \left(\frac{P_i}{P_o}\right) P_e = S(T)$$

where S(T) is a function only of temperature. If we consider the two cases of single and multiple electron sources we see that Pe = Pi in the former but the latter it may be that $P_e \gg P_i \; (sodium)$ and the ionization will be strongly supressed. The ionization of the dopant atom is, as we recall, the process responsible for forming the Milne maximum so if ionization is supressed, there will be no Milne maximum.

From this discussion it is clear that the Milne maximum will be more pronounced if

1. The Milne temperature is low and/or
2. The partial pressures of unwanted contaminants (e.g. copper) are low

Item 1. calls for a dopant with low ionization energy and a spectral line with low excitation energy. Item 2 calls for pure gas, clean cool walls, and well chosen electrode materials.

3.52    Apparatus

Sodium was introduced into the arc by doping a carbon cathode with NaCl and relying on the arc to ablate the material. So only a gross control over the doping level is achieved, but it proved fairly simple to produce suitable sodium D lines.

A magnified image of the arc was projected on the slit of a 3.4 meter Ebert Spectrograph producing a stygmatic spectrum on the photographic plate. Exposure time was 40 msec.

The response of the plate to different exposures was calibrated by using the anode crater of carbon arc as a constant intensity source and a variable aperture in the spectrograph to cover the range of exposure levels (14). The spectral plate was evaluated by reading local emulsion densities within the arc exposure with a microphotometer and comparing these readings with readings taken within the calibrated exposure of the carbon crater. The resulting values, which are integrated intensities viewed side-on, must undergo an Abel inversion before the radial light intensity $I(r)$ is known. From the theoretical temperature dependence of spectral line intensity (see section 3.512) the intensities can then be converted to temperatures.

3.53      Results

Two 50 ampere 11.2 atm nitrogen arcs were seeded as described above and the radial position of the Na $\lambda$ =5896 Å line intensity maximum determined. Although the flow rate was 0.1 gram/sec in one case and 5.0 gram/sec in the other, the radial positions of the maxima were identical within our accuracy. From the known transition probability of the 5896 Å line, the partial pressure of sodium was estimated to be about 50 dyne/cm$^2$. At this density the peak spectral intensity was calculated to be $3500^{\circ}$K, so this value is marked in figure 37.

For comparison, in this Fig. also the results of the temperature distribution measurements made with a nitrogen band line (3) on laminar and turbulent 50 ampere arcs are shown.

3.54      Discussion

As was shown in some detail (3), a temperature measurement in a turbulent arc using the Milne method is less accurate as large intensity fluctuations are present. Our measurements of the intensity fluctuations in a 0.7 cm I. D. 50 ampere turbulent nitrogen arc showed a very considerable level of fluctuations (section 3.4). This fact then limits the accuracy of these temperature measurements. Since the light fluctuations were found to be much smaller at currents of 125 amperes, a turbulent temperature measurement at that current level seems to be the next logical step.

-49-
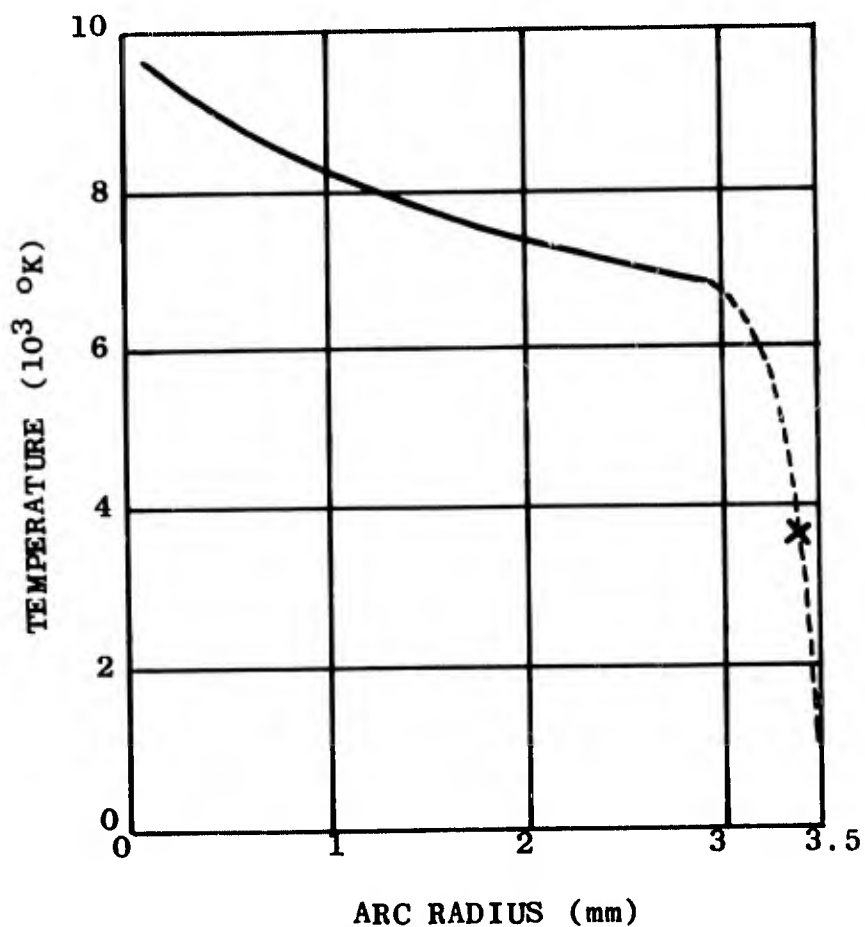
Figure 37-Radial Temperature Distribution
of a 50 Ampere Nitrogen Arc.  The
line shows the result from a nitro-
gen molecular line; the "x" indicates
the result of our sodium line measure-
ment.

| | |
|---|---|
| Gas: | Nitrogen |
| Current: | 50 ±2 amp |
| Pressure: | 11.2 atm |
| Flow Rate: | 0.1 and 5 gram/sec |
| Tube Diameter: | 0.7 cm |
| Window Position: | 44 cm from cathode |
| Tube Length: | 50 cm |
| Shot #: | 437 and 444 |

# 4.   CONCLUSIONS

The conclusions which follow result from experiments in the fully developed flow sections of long arc constrictors. From our experiments it is evident that turbulent effects exist in the developing region too, but it is difficult to separate the contributions of all the energy terms there, especially those of the flow terms.

## 4.1   Existence of Turbulence

The strongest evidence we have presented in the previous sections to establish the existence of turbulence is the effect that increasing the flow rate has on heat transfer. It is interesting to note that our plasma temperature measurements tend to amplify this evidence. It was found (3) that the laminar and the turbulent temperature distributions of a 50 amp nitrogen arc were quite close. This implied that neither increased radiation nor greater ordinary thermal conduction can be responsible for the strongly increased radial heat flux in the turbulent case. Since our measurements are made in the fully developed flow section, the only remaining energy transport term to which the greatly increased losses can be assigned is turbulent thermal conduction.

Other effects we have seen which indicate turbulence include the behavior of axial pressure gradients at high flow rates, a significant enhancement of mass transport at only 5 gram/sec flow rate, and the three dimensional structure of the arc observed directly with high speed photography and indirectly with a localized light sensor. These individual effects become even more convincing when viewed together. Furthermore, the dependence of turbulent effects on experimental parameters (pressure, flow rate, tube diameter) follows a pattern similar to that of turbulence seen at low temperatures.

## 4.2   Onset of Turbulence

The effects which establish the existence of turbulence agree closely as to the minimum conditions which show turbulent effects. For our 0.7 cm I. D. tube, we found the increase in heat transfer and the change in pressure gradient dependence both began between 1 and 2 gram/sec. The fluctuations in light intensity also begin in this area (see figures 31 and 32).

-51-

4.3       Dependence of Turbulent Level on Parameters of Experiment

In addition to establishing turbulence, our aim is to
provide useful data as to the level of the effect under differ-
ing operating conditions.  In this way useful information for
design specifications of plasma apparatus such as arc heaters
is generated and values can be extrapolated even beyond the
limits of our measurements.

The effects on heat flux of current, pressure, flow
rate, and tube diameter were all studied.  Pressure gradients
were compared at different currents, pressures and flow rates.
Light fluctuations were seen at different currents and flow
rates.  These measurements should form the foundation for de-
sign studies or more theoretical extensions of the present work.

4.4       Measuring Techniques

In the process of making measurements several signifi-
cant measuring techniques were developed.  We saw that naturally
occuring plasma structures could be utilized for measuring the
plasma velocity near axis.  The only requirements are high
speed photographic equipment and a window in the copper cascade
which does not disturb the arc yet exposes a sufficient length
of the arc to view.

The sodium D lines were used as a measure of the radial
position of the temperature corresponding to their maximum
intensity.  A close examination of the equations governing ion-
ization and dissociation equilibria shows that the high electron
density at the arc core may inhibit further ionization of dopant
atoms and so alter the temperature dependence of their spectral
line intensities.  This complicating effect can be avoided by
choosing dopant lines with expected maxima at temperatures so
low that they lie well out from the arc axis.

Fluctuations of total visible light were so large for
a 50 ampere 10 atmosphere argon arc at flow rates above 3 gram/sec
in a 0.7 cm I. D. tube, that averaging errors must be significant.
The same study showed that, if the current increased to 125
amperes, the arc was suitably stable for a measurement at flow
rates below 10 gram/sec and possibly higher.

A method for observing mass transport was devised.  The
intense heat flux from the arc can be used to ablate low thermal
conductivity materials placed at the side of the constrictor tube.
Spectral observations made with stygmatic equipment focused at
a downstream point can show the gradual diffusion of the ablated
material through the arc.

-52-

# 5.  SUGGESTIONS FOR FUTURE WORK

## 5.1    Measure Radiation Term

Our present measurement of the total radial heat flux in the fully developed section includes the radiation term with the conduction term.  Direct measurement of the radiation term at several flow rates, currents and pressures will allow separation of their contributions.

## 5.2    Correlate Re with $T(r)$ and $v(r)$

Before an attempt can be made to correllate heat flux with some average Reynolds number, measuring methods for radial turbulent temperature and velocity distributions will have to be improved or new ones devised.

## 5.3    Investigate Turbulent Structure

An insight concerning the actual motion of plasma in an axial flow arc might be gained from photography at framing rates high enough to follow short term motions within a tube segment ($10^6$ frames per sec).  An alternate way to get a continuous view of plasma motions would be a streak camera.

## 5.4    Extend Parameters of Arc Operation

Because of the interest in use of high current devices, it would be desireable to extend the turbulence studies to higher currents, pressures, flow rates and tube diameters.  Two obstacles are the necessity for long water cooled tubes and a power supply of about 10 megawatt.

## REFERENCES

1. Frind, G: Electric Arcs in Turbulent Flows, Aerospace Research Laboratory Report, ARL 64-148 (1964).

2. Frind, G: Electric Arcs in Turbulent Flows II, Aerospace Research Laboratory Report, ARL 66-0073 (1966).

3. Frind, G. and Damsky, B. L: Electric Arcs in Turbulent Flows III, Aerospace Research Laboratory Report, ARL 68-0067 (1968).

4a. Maecker, H: Brennkammer fuer Hochstromboegen in Verschiedenen Gasen, (in German), Z. f. Naturf., 11a, 32-34 (1956).

   b. Messung und Auswertung von Bogen Characteristiken (Ar, $N_2$) (in German), Z. f. Physik, 158, 392-404 (1960).

   c. Eine Kaskadenbogenkammer fuer sehr hohe Leistung (in German), Z. f. Ang. Physik, 15, 440-441 (1963).

5a. Fowler, R. H. and Milne, E. A: The Intensity of Absorption Lines in Stellar Spectra, and the Temperatures and Pressures of the Reversing Layers of Stars.
    Mon. Not. Rey. Astr. Soc. 83, 403-424 (1923)
    Mon. Not. Roy. Astr. Soc. 84, 499-515 (1924)

   b. Larentz, R. W: A Method for the Measurement of Temperature in Optically Thin Arc Columns, (in German), Z. f. Physik,
    129, 327-342 (1951)
    129, 343-364 (1951)

6. Burhorn et al: Temperaturmessungen an Wasserstabilisierten Hochleistungsboegen, (in German), Z. f. Physik, 131, 28-40 (1951).

7. Lochte-Holtgreven, W: Production and Measurement of High Temperatures, Rep. on Progress in Physics Vol. XXI, (1958), (See pages 346ff, especially fig. 22).

8. Eckert, E. R. G. and Drake, R. M: Heat and Mass Transfer, McGraw Hill, New York (1959), (See pages 269ff, second ed.).

9. Eckert, E. R. G. and Drake, R. M: Heat and Mass Transfer, McGraw Hill, New York, (1959).

10. Runstadler, P. W: Laminar and Turbulent Flow of an Argon Arc Plasma, Tech. Rep. No. 22 of Eng. and Applied Physics, Harvard (1965).

11. Rohsenow, W. M. and Choi, H. Y: Heat Mass and Momentum Transfer, Prentice-Hall, Englewood Cliffs, N. J. (1963).

12. Olsen, H. N. et al: Investigation of the Interaction of and External Magnetic Field with an Electric Arc, Aerospace Research Laboratory Report, ARL 66-0016 (1966).

13. Maecker, H: Electron Density and Temperature in the Column of the High Current Carbon Arc. Z. f. Phys., 136, 119-136, 1953.

14. Null, M. R. and Lozier, W. W: Carbon Arc as a Radiation Standard, J Opt. Soc. Am., 52, 1156-1162, (1962).

15. Moore, C. E: Atomic Energy Levels, Circular #467 of NBS, (1949), Supt. of Documents, Gov't Printing Office, Washington 25, D. C.

16. Fast, J. D: The Dissociation of Nitrogen in the Welding Arc, Philips Research Reports 2, 382, (1947).

17. Logan, J. G. Jr.: The Calculation of the Thermodynamic Properties of Air at High Temperatures, Cornell Aeronautical Lab Report #AD - 1052 - A - 1, (1956).

18. Hilsenrath, J. and Klein, M: Table of Thermodynamic Properties and Chemical Composition of Nitrogen, Arnold Eng. Dev. Center, Rep TR - 66 - 65, (1966).

The program to compute the equilibrium concentrations
of atomic and molecular species had to include the following
processes:

1. $N_2 \rightleftharpoons N + N$
2. $N_2 \rightleftharpoons N_2^+ + e$
3. $N \rightleftharpoons N^+ + e$
4. $Cu \rightleftharpoons Cu^+ + e$
5. $Na \rightleftharpoons Na^+ + e$

The extent to which the dissociation or ionization
procedes is described by a Saha equation (see equation 7) in
text).

Process 1) is necessary to the others because it deter-
mines the concentration of N; the other processes are coupled
through their common production of electrons. The sixth
equation which allows the five Saha equations for the other
five processes to be solved is:

6) $P_{e\,(total)} = P_{e\,(N_2)} + P_{e\,(N)} + P_{e\,(Cu)} + P_{e\,(Na)}$

Where the parenthetical subscript indicates the source of the
electrons.

To solve these 6 simultaneous equations an interative
method was used. After solving the Saha equation for process
1), the ionization of each of the various species is computed
assuming no other species contributes electrons. The degree
of ionization thus calculated is too high since extra electrons
supress the ionization process. The total electron pressure
is added up, see 6), giving an estimate of total electron
pressure. These estimates are alternately too low and too
high so, to speed the convergence, the Saha equations are solved
again using the average of the two previous electron pressures.
When additional repetitions of this cycle do not change the
values, the computation is complete.

A Block diagram of the program is shown below:

Inputs: **Total pressure, Cu partial pressure, Na partial pressure**

Calculate dissociation of $N_2 \rightleftharpoons N + N$

Average two previous $P_e$ values (estimates)

Solve Saha equation of $N_2$

Solve Saha for N

Solve Saha for Cu

Solve Saha for Na

$$P_e = P_{e(N_2)} + P_{e(N)} + P_{e(Cu)} - P_{e(Na)}$$

Compare $P_e$ with previous $P_e$

Calculate Na Radiation Intensity (equation 5) in test)

Print Answers

Move to Different Temperature

END
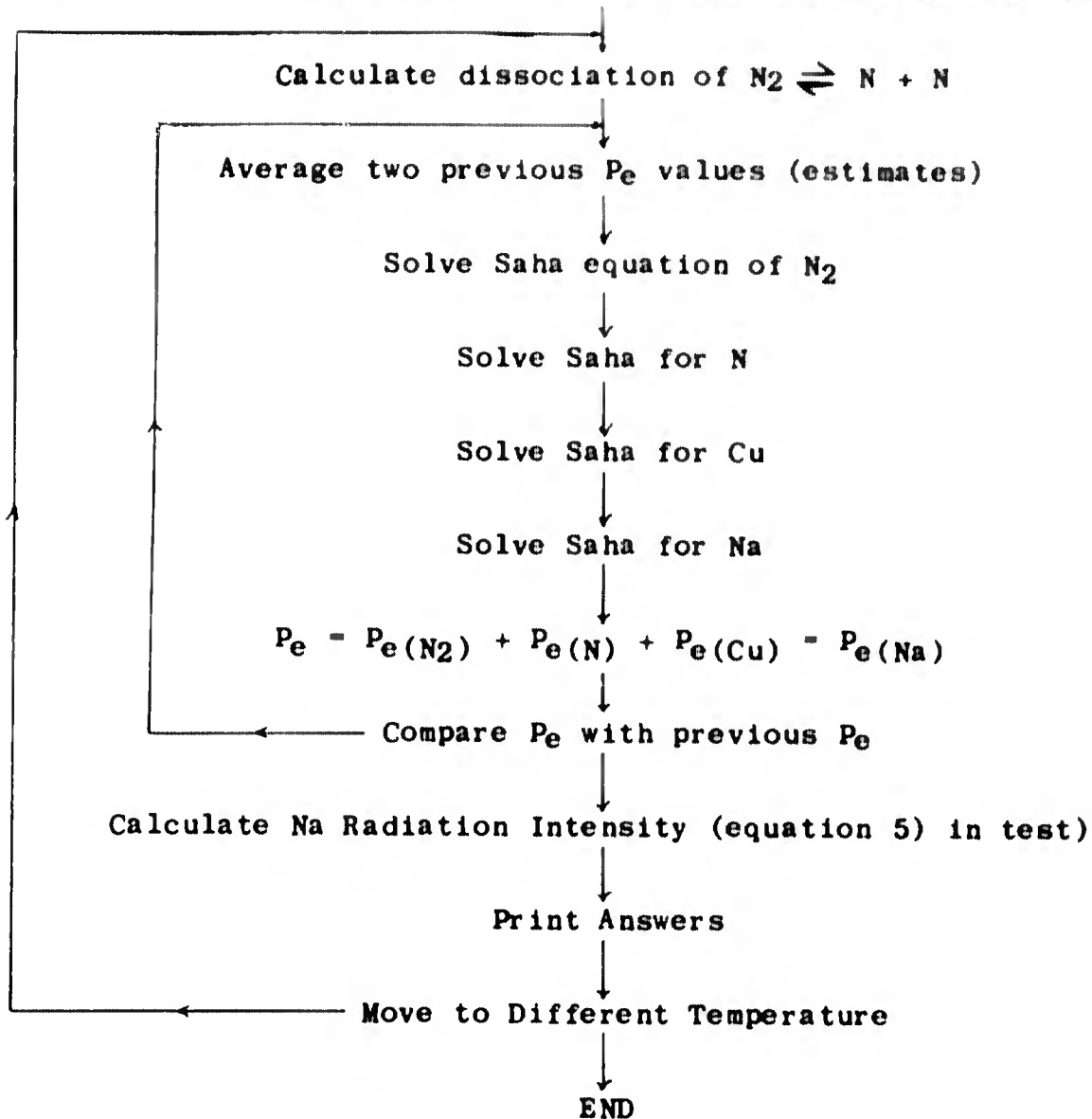
Atomic and ionic partition functions were calculated summing only the first eight energy levels (or groups of closely spaced energy levels). Energies, degeneracies, and ionization potentials were taken from (15). The partition function of the nitrogen molecule was calculated using the methods of (16). Values of the molecular constants for the nitrogen molecular ion ere taken from (17).

To test the completed program, it was run with negligible traces of copper and sodium in nitrogen and the computed species concentrations compared with the tabulations in (18). Agreement was better than 1%.

-57-

Some representative computations from the computer program are shown on the following pages. The printing format for each temperature "unit" is diagramed as follows:

| Temp | Cu Atom | Na Atom | $N_2$ Molecule | $N_2$ Molec-Ion | electron |
|------|---------|---------|----------------|-----------------|----------|
| Temp | Cu Ion  | Na Ion  | N Atom         | N Ion           | Spec Intens |
|      |         |         |                |                 | 5896 Å |

These twelve items together describe the equilibrium state for the temperature and pressures listed. The temperature is listed at the left in $^{\circ}$K. It is constant for two lines after which there is a skip before the temperature is increased. The temperature range covered is 2,000 to 10,000$^{\circ}$K in steps of 200$^{\circ}$K. The atomic and molecular species pressures are listed next, normalized against the total pressure. The total spectral intensity of a sodium D line is listed at the lower right in arbitrary units.

There are six compositions for which the equilibria are calculated. In order they are:

    I.    10 Atm $N_2$; 1 x $10^{-10}$ dyne/cm$^2$ Cu; 1 x $10^{-10}$ d/cm$^2$ Na

   II.   11.2 Atm $N_2$; 500 dyne/cm$^2$ Cu; 50 dyne/cm$^2$ Na

 III.   11.2 Atm $N_2$; 500 dyne/cm$^2$ Cu; 150 dyne/cm$^2$ Na

  IV.   11.2 Atm $N_2$; 500 dyne/cm$^2$ Cu; 500 dyne/cm$^2$ Na

   V.   5 Atm $N_2$; 500 dyne/cm$^2$ Cu; 50 dyne/cm$^2$ Na

  VI.   20 Atm $N_2$; 500 dyne/cm$^2$ Cu; 50 dyne/cm$^2$ Na

Each condition occupies 3 pages.

# CHEMICAL COMPOSITION OF IMPURE NITROGEN

CONDITION: 1.0000E-10 DYNES CU; 1.0000E-10 DYNES NA
1.0130E+07 TOTAL PRESSURE

| TEMP | CU ATOM | NA ATOM | N2 MOLEC | N2 MOL-ION | ELECTRONS |
|------|---------|---------|----------|------------|-----------|
| TEMP | CU ION | NA ION | N ATOM | N ION | SPEC INTEN |
| (DEG K) | (FRACTION OF TOTAL PRESSURE) | | | | (RELATIVE) |
| 2.00E+03 | 9.18E-18 | 5.12E-23 | 1.00E+00 | 2.59E-21 | 5.29E-18 |
| 2.00E+03 | 3.48E-19 | 4.94E-18 | 2.79E-10 | 2.97E-28 | 2.57E-21 |
| 2.20E+03 | 3.03E-18 | 6.57E-24 | 1.00E+00 | 4.90E-18 | 1.33E-17 |
| 2.20E+03 | 3.42E-18 | 4.94E-18 | 3.86E-09 | 4.48E-24 | 1.00E-21 |
| 2.40E+03 | 2.00E-18 | 1.15E-23 | 1.00E+00 | 2.72E-16 | 2.81E-16 |
| 2.40E+03 | 3.94E-18 | 4.94E-18 | 3.45E-08 | 1.41E-21 | 4.42E-21 |
| 2.60E+03 | 1.87E-18 | 2.71E-23 | 1.00E+00 | 5.57E-15 | 5.57E-15 |
| 2.60E+03 | 4.00E-18 | 4.94E-18 | 2.21E-07 | 1.25E-19 | 2.28E-20 |
| 2.80E+03 | 1.77E-18 | 5.70E-23 | 1.00E+00 | 7.36E-14 | 7.36E-14 |
| 2.80E+03 | 4.05E-18 | 4.94E-18 | 1.09E-06 | 5.79E-18 | 9.37E-20 |
| 3.00E+03 | 1.69E-18 | 1.08E-22 | 1.00E+00 | 6.94E-13 | 6.94E-13 |
| 3.00E+03 | 4.09E-18 | 4.94E-18 | 4.33E-06 | 1.62E-16 | 3.18E-19 |
| 3.20E+03 | 1.62E-18 | 1.88E-22 | 1.00E+00 | 4.97E-12 | 4.98E-12 |
| 3.20E+03 | 4.12E-18 | 4.94E-18 | 1.45E-05 | 3.01E-15 | 9.22E-19 |
| 3.40E+03 | 1.56E-18 | 3.07E-22 | 1.00E+00 | 2.85E-11 | 2.85E-11 |
| 3.40E+03 | 4.16E-18 | 4.94E-18 | 4.23E-05 | 3.97E-14 | 2.35E-18 |
| 3.60E+03 | 1.51E-18 | 4.72E-22 | 1.00E+00 | 1.35E-10 | 1.35E-10 |
| 3.60E+03 | 4.18E-18 | 4.94E-18 | 1.10E-04 | 3.95E-13 | 5.40E-18 |
| 3.80E+03 | 1.46E-18 | 6.94E-22 | 1.00E+00 | 5.43E-10 | 5.46E-10 |
| 3.80E+03 | 4.20E-18 | 4.94E-18 | 2.57E-04 | 3.09E-12 | 1.13E-17 |
| 4.00E+03 | 1.42E-18 | 9.81E-22 | 9.99E-01 | 1.91E-09 | 1.93E-09 |
| 4.00E+03 | 4.22E-18 | 4.94E-18 | 5.53E-04 | 1.98E-11 | 2.21E-17 |
| 4.20E+03 | 1.39E-18 | 1.34E-21 | 9.99E-01 | 5.99E-09 | 6.10E-09 |
| 4.20E+03 | 4.24E-18 | 4.94E-18 | 1.11E-03 | 1.06E-10 | 4.04E-17 |
| 4.40E+03 | 1.37E-18 | 1.78E-21 | 9.98E-01 | 1.69E-08 | 1.74E-08 |
| 4.40E+03 | 4.25E-18 | 4.93E-18 | 2.09E-03 | 4.88E-10 | 7.01E-17 |
| 4.60E+03 | 1.35E-18 | 2.32E-21 | 9.96E-01 | 4.37E-08 | 4.57E-08 |
| 4.60E+03 | 4.26E-18 | 4.93E-18 | 3.72E-03 | 1.96E-09 | 1.16E-16 |

-59-

# CHEMICAL COMPOSITION OF IMPURE NITROGEN

CONDITION: 1.0000E-10 DYNES CU; 1.0000E-10 DYNES NA
1.0130E+07 TOTAL PRESSURE

| TEMP | CU ATOM | NA ATOM | N2 MOLEC | N2 MOL-ION | ELECTRONS |
|------|---------|---------|----------|------------|-----------|
| TEMP | CU ION | NA ION | N ATOM | N ION | SPEC INTEN |
| (DEG K) | (FRACTION | OF TOTAL | PRESSURE) | | (RELATIVE) |
| 4.80E+03 | 1.33E-18 | 2.96E-21 | 9.94E-01 | 1.04E-07 | 1.11E-07 |
| 4.80E+03 | 4.27E-18 | 4.93E-18 | 6.33E-03 | 7.03E-09 | 1.85E-16 |
| 5.00E+03 | 1.32E-18 | 3.72E-21 | 9.90E-01 | 2.31E-07 | 2.54E-07 |
| 5.00E+03 | 4.27E-18 | 4.93E-18 | 1.03E-02 | 2.27E-08 | 2.84E-16 |
| 5.20E+03 | 1.32E-18 | 4.61E-21 | 9.84E-01 | 4.81E-07 | 5.48E-07 |
| 5.20E+03 | 4.28E-18 | 4.93E-18 | 1.62E-02 | 6.66E-08 | 4.25E-16 |
| 5.40E+03 | 1.32E-18 | 5.64E-21 | 9.75E-01 | 9.44E-07 | 1.12E-06 |
| 5.40E+03 | 4.28E-18 | 4.93E-18 | 2.45E-02 | 1.80E-07 | 6.20E-16 |
| 5.60E+03 | 1.32E-18 | 6.85E-21 | 9.64E-01 | 1.75E-06 | 2.20E-06 |
| 5.60E+03 | 4.28E-18 | 4.93E-18 | 3.60E-02 | 4.51E-07 | 8.84E-16 |
| 5.80E+03 | 1.33E-18 | 8.24E-21 | 9.49E-01 | 3.10E-06 | 4.15E-06 |
| 5.80E+03 | 4.27E-18 | 4.93E-18 | 5.15E-02 | 1.05E-06 | 1.24E-15 |
| 6.00E+03 | 1.34E-18 | 9.85E-21 | 9.28E-01 | 5.23E-06 | 7.54E-06 |
| 6.00E+03 | 4.27E-18 | 4.93E-18 | 7.17E-02 | 2.31E-06 | 1.70E-15 |
| 6.20E+03 | 1.35E-18 | 1.17E-20 | 9.03E-01 | 8.45E-06 | 1.33E-05 |
| 6.20E+03 | 4.26E-18 | 4.93E-18 | 9.74E-02 | 4.80E-06 | 2.30E-15 |
| 6.40E+03 | 1.37E-18 | 1.38E-20 | 8.71E-01 | 1.31E-05 | 2.26E-05 |
| 6.40E+03 | 4.25E-18 | 4.93E-18 | 1.29E-01 | 9.46E-06 | 3.07E-15 |
| 6.60E+03 | 1.38E-18 | 1.62E-20 | 8.32E-01 | 1.96E-05 | 3.74E-05 |
| 6.60E+03 | 4.25E-18 | 4.93E-18 | 1.68E-01 | 1.78E-05 | 4.05E-15 |
| 6.80E+03 | 1.39E-18 | 1.89E-20 | 7.87E-01 | 2.82E-05 | 6.02E-05 |
| 6.80E+03 | 4.24E-18 | 4.93E-18 | 2.13E-01 | 3.20E-05 | 5.26E-15 |
| 7.00E+03 | 1.40E-18 | 2.18E-20 | 7.34E-01 | 3.92E-05 | 9.45E-05 |
| 7.00E+03 | 4.24E-18 | 4.92E-18 | 2.65E-01 | 5.53E-05 | 6.74E-15 |
| 7.20E+03 | 1.41E-18 | 2.51E-20 | 6.76E-01 | 5.27E-05 | 1.45E-04 |
| 7.20E+03 | 4.23E-18 | 4.92E-18 | 3.24E-01 | 9.20E-05 | 8.55E-15 |
| 7.40E+03 | 1.41E-18 | 2.87E-20 | 6.13E-01 | 6.85E-05 | 2.16E-04 |
| 7.40E+03 | 4.23E-18 | 4.92E-18 | 3.87E-01 | 1.48E-04 | 1.07E-14 |

# CHEMICAL COMPOSITION OF IMPURE NITROGEN

CONDITION: 1.0000E-10 DYNES CU; 1.0000E-10 DYNES NA
1.0130E+07 TOTAL PRESSURE

| TEMP<br>TEMP<br>(DEG K) | CU ATOM<br>CU ION | NA ATOM<br>NA ION<br>(FRACTION OF TO | N2 MOLEC<br>N ATOM<br>TAL PRESSURE) | N2 MOL-ION<br>N ION | E'ECTRONS<br>SPEC INTEN<br>(RELATIVE) |
|---|---|---|---|---|---|
| 7.60E+03 | 1.41E-18 | 3.26E-20 | 5.46E-01 | 8.62E-05 | 3.16E-04 |
| 7.60E+03 | 4.23E-18 | 4.92E-18 | 4.53E-01 | 2.30E-04 | 1.33E-14 |
| 7.80E+03 | 1.40E-18 | 3.67E-20 | 4.78E-01 | 1.05E-04 | 4.52E-04 |
| 7.80E+03 | 4.24E-18 | 4.92E-18 | 5.21E-01 | 3.47E-04 | 1.62E-14 |
| 8.00E+03 | 1.39E-18 | 4.11E-20 | 4.11E-01 | 1.25E-04 | 6.34E-04 |
| 8.00E+03 | 4.24E-18 | 4.92E-18 | 5.88E-01 | 5.09E-04 | 1.96E-14 |
| 8.20E+03 | 1.37E-18 | 4.57E-20 | 3.47E-01 | 1.44E-04 | 8.71E-04 |
| 8.20E+03 | 4.25E-18 | 4.91E-18 | 6.52E-01 | 7.27E-04 | 2.35E-14 |
| 8.40E+03 | 1.34E-18 | 5.05E-20 | 2.88E-01 | 1.61E-04 | 1.17E-03 |
| 8.40E+03 | 4.26E-18 | 4.91E-18 | 7.10E-01 | 1.01E-03 | 2.79E-14 |
| 8.60E+03 | 1.31E-18 | 5.54E-20 | 2.35E-01 | 1.76E-04 | 1.56E-03 |
| 8.60E+03 | 4.28E-18 | 4.91E-18 | 7.62E-01 | 1.38E-03 | 3.28E-14 |
| 8.80E+03 | 1.28E-18 | 6.06E-20 | 1.90E-01 | 1.88E-04 | 2.03E-03 |
| 8.80E+03 | 4.29E-18 | 4.91E-18 | 8.06E-01 | 1.84E-03 | 3.82E-14 |
| 9.00E+03 | 1.25E-18 | 6.59E-20 | 1.52E-01 | 1.98E-04 | 2.61E-03 |
| 9.00E+03 | 4.31E-18 | 4.90E-18 | 8.43E-01 | 2.42E-03 | 4.42E-14 |
| 9.20E+03 | 1.21E-18 | 7.14E-20 | 1.20E-01 | 2.05E-04 | 3.32E-03 |
| 9.20E+03 | 4.33E-18 | 4.90E-18 | 8.73E-01 | 3.11E-03 | 5.08E-14 |
| 9.40E+03 | 1.17E-18 | 7.70E-20 | 9.50E-02 | 2.10E-04 | 4.16E-03 |
| 9.40E+03 | 4.35E-18 | 4.90E-18 | 8.97E-01 | 3.95E-03 | 5.80E-14 |
| 9.60E+03 | 1.13E-18 | 8.29E-20 | 7.49E-02 | 2.13E-04 | 5.16E-03 |
| 9.60E+03 | 4.37E-18 | 4.89E-18 | 9.15E-01 | 4.95E-03 | 6.59E-14 |
| 9.80E+03 | 1.10E-18 | 8.91E-20 | 5.91E-02 | 2.14E-04 | 6.34E-03 |
| 9.80E+03 | 4.39E-18 | 4.89E-18 | 9.28E-01 | 6.13E-03 | 7.46E-14 |
| 1.00E+04 | 1.06E-18 | 9.54E-20 | 4.67E-02 | 2.13E-04 | 7.72E-03 |
| 1.00E+04 | 4.41E-18 | 4.89E-18 | 9.38E-01 | 7.50E-03 | 8.40E-14 |

-61-

# CHEMICAL COMPOSITION OF IMPURE NITROGEN

CONDITION: 5.0000E+02 DYNES CU; 5.0000E+01 DYNES NA
1.1350E+07 TOTAL PRESSURE

| TEMP TEMP (DEG K) | CU ATOM CU ION | NA ATOM NA ION | N2 MOLEC N ATOM | N2 MOL-ION N ION | ELECTRONS SPEC INTEN |
|---|---|---|---|---|---|
| | | (FRACTION OF TOTAL PRESSURE) | | | (RELATIVE) |
| 2.00E+03 | 4.41E-05 | 4.40E-06 | 1.00E+00 | 8.65E-30 | 1.42E-09 |
| 2.00E+03 | 5.58E-15 | 1.42E-09 | 2.63E-10 | 9.35E-37 | 2.47E-04 |
| 2.20E+03 | 4.41E-05 | 4.39E-06 | 1.00E+00 | 9.28E-27 | 6.25E-09 |
| 2.20E+03 | 9.43E-14 | 6.25E-09 | 3.64E-09 | 8.02E-33 | 7.50E-04 |
| 2.40E+03 | 4.41E-05 | 4.36E-06 | 1.00E+00 | 3.16E-24 | 2.17E-08 |
| 2.40E+03 | 1.00E-12 | 2.17E-08 | 3.26E-08 | 1.54E-29 | 1.88E-03 |
| 2.60E+03 | 4.41E-05 | 4.28E-06 | 1.00E+00 | 4.45E-22 | 6.23E-08 |
| 2.60E+03 | 7.54E-12 | 6.23E-08 | 2.09E-07 | 9.42E-27 | 4.03E-03 |
| 2.80E+03 | 4.41E-05 | 4.10E-06 | 1.00E+00 | 3.16E-20 | 1.53E-07 |
| 2.80E+03 | 4.32E-11 | 1.53E-07 | 1.03E-06 | 2.35E-24 | 7.56E-03 |
| 3.00E+03 | 4.41E-05 | 3.75E-06 | 1.00E+00 | 1.32E-18 | 3.26E-07 |
| 3.00E+03 | 2.02E-10 | 3.26E-07 | 4.09E-06 | 2.91E-22 | 1.24E-02 |
| 3.20E+03 | 4.41E-05 | 3.19E-06 | 1.00E+00 | 3.63E-17 | 6.10E-07 |
| 3.20E+03 | 8.16E-10 | 6.09E-07 | 1.37E-05 | 2.07E-20 | 1.75E-02 |
| 3.40E+03 | 4.40E-05 | 2.42E-06 | 1.00E+00 | 7.26E-16 | 9.96E-07 |
| 3.40E+03 | 2.99E-09 | 9.93E-07 | 4.00E-05 | 9.57E-19 | 2.08E-02 |
| 3.60E+03 | 4.40E-05 | 1.59E-06 | 1.00E+00 | 1.14E-14 | 1.42E-06 |
| 3.60E+03 | 1.04E-08 | 1.41E-06 | 1.03E-04 | 3.17E-17 | 2.03E-02 |
| 3.80E+03 | 4.40E-05 | 9.02E-07 | 1.00E+00 | 1.48E-13 | 1.79E-06 |
| 3.80E+03 | 3.45E-08 | 1.75E-06 | 2.43E-04 | 7.98E-16 | 1.65E-02 |
| 4.00E+03 | 4.38E-05 | 4.70E-07 | 9.99E-01 | 1.59E-12 | 2.08E-06 |
| 4.00E+03 | 1.08E-07 | 1.97E-06 | 5.23E-04 | 1.55E-14 | 1.19E-02 |
| 4.20E+03 | 4.34E-05 | 2.47E-07 | 9.99E-01 | 1.37E-11 | 2.38E-06 |
| 4.20E+03 | 3.02E-07 | 2.08E-06 | 1.05E-03 | 2.29E-13 | 8.35E-03 |
| 4.40E+03 | 4.26E-05 | 1.41E-07 | 9.98E-01 | 9.23E-11 | 2.85E-06 |
| 4.40E+03 | 7.23E-07 | 2.13E-06 | 1.97E-03 | 2.51E-12 | 6.23E-03 |
| 4.60E+03 | 4.11E-05 | 9.02E-08 | 9.96E-01 | 4.92E-10 | 3.62E-06 |
| 4.60E+03 | 1.47E-06 | 2.16E-06 | 3.52E-03 | 2.09E-11 | 5.05E-03 |

# CHEMICAL COMPOSITION OF IMPURE NITROGEN

CONDITION: 5.0000E+02 DYNES CU; 5.0000E+01 DYNES NA
1.1350E+07 TOTAL PRESSURE

| TEMP TEMP (DEG K) | CU ATOM CU ION | NA ATOM NA ION | N2 MOLEC N ATOM | N2 MOL-ION N ION | ELECTRONS SPEC INTEN |
|---|---|---|---|---|---|
| | | (FRACTION OF TOTAL PRESSURE) | | | (RELATIVE) |
| 4.80E+03 | 3.89E-05 | 6.26E-08 | 9.94E-01 | 2.17E-09 | 4.77E-06 |
| 4.80E+03 | 2.60E-06 | 2.17E-06 | 5.98E-03 | 1.38E-10 | 4.37E-03 |
| 5.00E+03 | 3.58E-05 | 4.59E-08 | 9.90E-01 | 8.29E-09 | 6.33E-06 |
| 5.00E+03 | 4.14E-06 | 2.18E-06 | 9.74E-03 | 7.68E-10 | 3.93E-03 |
| 5.20E+03 | 3.19E-05 | 3.47E-08 | 9.85E-01 | 2.83E-08 | 8.31E-06 |
| 5.20E+03 | 6.09E-06 | 2.19E-06 | 1.53E-02 | 3.71E-09 | 3.58E-03 |
| 5.40E+03 | 2.73E-05 | 2.66E-08 | 9.77E-01 | 8.90E-08 | 1.07E-05 |
| 5.40E+03 | 8.36E-06 | 2.19E-06 | 2.32E-02 | 1.60E-08 | 3.27E-03 |
| 5.60E+03 | 2.25E-05 | 2.06E-08 | 9.66E-01 | 2.60E-07 | 1.33E-05 |
| 5.60E+03 | 1.08E-05 | 2.19E-06 | 3.41E-02 | 6.31E-08 | 2.97E-03 |
| 5.80E+03 | 1.79E-05 | 1.61E-08 | 9.51E-01 | 7.09E-07 | 1.62E-05 |
| 5.80E+03 | 1.31E-05 | 2.19E-06 | 4.87E-02 | 2.27E-07 | 2.70E-03 |
| 6.00E+03 | 1.39E-05 | 1.29E-08 | 9.32E-01 | 1.79E-06 | 1.98E-05 |
| 6.00E+03 | 1.51E-05 | 2.20E-06 | 6.78E-02 | 7.45E-07 | 2.50E-03 |
| 6.20E+03 | 1.10E-05 | 1.10E-08 | 9.08E-01 | 4.03E-06 | 2.49E-05 |
| 6.20E+03 | 1.65E-05 | 2.20E-06 | 9.22E-02 | 2.16E-06 | 2.42E-03 |
| 6.40E+03 | 9.20E-06 | 1.01E-08 | 8.77E-01 | 8.04E-06 | 3.31E-05 |
| 6.40E+03 | 1.74E-05 | 2.20E-06 | 1.23E-01 | 5.46E-06 | 2.52E-03 |
| 6.60E+03 | 8.13E-06 | 1.01E-08 | 8.41E-01 | 1.42E-05 | 4.65E-05 |
| 6.60E+03 | 1.80E-05 | 2.20E-06 | 1.59E-01 | 1.21E-05 | 2.82E-03 |
| 6.80E+03 | 7.53E-06 | 1.06E-08 | 7.97E-01 | 2.27E-05 | 6.74E-05 |
| 6.80E+03 | 1.83E-05 | 2.20E-06 | 2.03E-01 | 2.42E-05 | 3.30E-03 |
| 7.00E+03 | 7.18E-06 | 1.15E-08 | 7.47E-01 | 3.39E-05 | 9.92E-05 |
| 7.00E+03 | 1.84E-05 | 2.20E-06 | 2.53E-01 | 4.47E-05 | 3.97E-03 |
| 7.20E+03 | 6.97E-06 | 1.27E-08 | 6.91E-01 | 4.76E-05 | 1.46E-04 |
| 7.20E+03 | 1.85E-05 | 2.20E-06 | 3.09E-01 | 7.77E-05 | 4.83E-03 |
| 7.40E+03 | 6.84E-06 | 1.41E-08 | 6.29E-01 | 6.38E-05 | 2.13E-04 |
| 7.40E+03 | 1.86E-05 | 2.20E-06 | 3.70E-01 | 1.28E-04 | 5.90E-03 |

CHEMICAL COMPOSITION OF IMPURE NITROGEN

CONDITION: 5.0000E+02 DYNES CU; 5.0000E+01 DYNES NA
1.1350E+07 TOTAL PRESSURE

| TEMP<br>TEMP<br>(DEG K) | CU ATOM<br>CU ION<br>(FRACTION | NA ATOM<br>NA ION<br>OF TOTAL | N2 MOLEC<br>N ATOM<br>PRESSURE) | N2 MOL-ION<br>N ION | ELECTRONS<br>SPEC INTEN<br>(RELATIVE) |
|---|---|---|---|---|---|
| 7.60E+03 | 6.74E-06 | 1.58E-08 | 5.64E-01 | 8.20E-05 | 3.06E-04 |
| 7.60E+03 | 1.87E-05 | 2.19E-06 | 4.35E-01 | 2.03E-04 | 7.19E-03 |
| 7.80E+03 | 6.64E-06 | 1.76E-08 | 4.97E-01 | 1.02E-04 | 4.34E-04 |
| 7.80E+03 | 1.87E-05 | 2.19E-06 | 5.02E-01 | 3.11E-04 | 8.71E-03 |
| 8.00E+03 | 6.54E-06 | 1.96E-08 | 4.30E-01 | 1.22E-04 | 6.04E-04 |
| 8.00E+03 | 1.88E-05 | 2.19E-06 | 5.69E-01 | 4.61E-04 | 1.05E-02 |
| 8.20E+03 | 6.43E-06 | 2.17E-08 | 3.66E-01 | 1.42E-04 | 8.27E-04 |
| 8.20E+03 | 1.88E-05 | 2.19E-06 | 6.33E-01 | 6.63E-04 | 1.25E-02 |
| 8.40E+03 | 6.31E-06 | 2.39E-08 | 3.06E-01 | 1.61E-04 | 1.11E-03 |
| 8.40E+03 | 1.89E-05 | 2.19E-06 | 6.92E-01 | 9.30E-04 | 1.48E-02 |
| 8.60E+03 | 6.17E-06 | 2.62E-08 | 2.52E-01 | 1.78E-04 | 1.47E-03 |
| 8.60E+03 | 1.89E-05 | 2.19E-06 | 7.45E-01 | 1.27E-03 | 1.74E-02 |
| 8.80E+03 | 6.01E-06 | 2.86E-08 | 2.05E-01 | 1.92E-04 | 1.92E-03 |
| 8.80E+03 | 1.90E-05 | 2.19E-06 | 7.91E-01 | 1.71E-03 | 2.02E-02 |
| 9.00E+03 | 5.85E-06 | 3.11E-08 | 1.65E-01 | 2.03E-04 | 2.47E-03 |
| 9.00E+03 | 1.91E-05 | 2.19E-06 | 8.30E-01 | 2.25E-03 | 2.34E-02 |
| 9.20E+03 | 5.68E-06 | 3.37E-08 | 1.31E-01 | 2.12E-04 | 3.14E-03 |
| 9.20E+03 | 1.92E-05 | 2.19E-06 | 8.62E-01 | 2.90E-03 | 2.69E-02 |
| 9.40E+03 | 5.50E-06 | 3.64E-08 | 1.04E-01 | 2.18E-04 | 3.93E-03 |
| 9.40E+03 | 1.93E-05 | 2.18E-06 | 8.88E-01 | 3.69E-03 | 3.07E-02 |
| 9.60E+03 | 5.33E-06 | 3.92E-08 | 8.26E-02 | 2.21E-04 | 4.88E-03 |
| 9.60E+03 | 1.94E-05 | 2.18E-06 | 9.08E-01 | 4.64E-03 | 3.49E-02 |
| 9.80E+03 | 5.15E-06 | 4.21E-08 | 6.53E-02 | 2.23E-04 | 5.99E-03 |
| 9.80E+03 | 1.94E-05 | 2.18E-06 | 9.23E-01 | 5.75E-03 | 3.95E-02 |
| 1.00E+04 | 4.98E-06 | 4.51E-08 | 5.18E-02 | 2.23E-04 | 7.30E-03 |
| 1.00E+04 | 1.95E-05 | 2.18E-06 | 9.34E-01 | 7.05E-03 | 4.45E-02 |

## CHEMICAL COMPOSITION OF IMPURE NITROGEN

CONDITION: 5.0000E+02 DYNES CU, 1.5000E+02 DYNES NA
1.1350E+07 TOTAL PRESSURE

| TEMP<br>TEMP<br>(DEG K) | CU ATOM<br>CU ION | NA ATOM<br>NA ION<br>(FRACTION OF | N2 MOLEC<br>N ATOM<br>TOTAL PRESSURE) | N2 MOL-ION<br>N ION | ELECTRONS<br>SPEC INTEN<br>(RELATIVE) |
|---|---|---|---|---|---|
| 2.00E+03<br>2.00E+03 | 4.41E-05<br>3.22E-15 | 1.32E-05<br>2.45E-09 | 1.00E+00<br>2.63E-10 | 4.99E-30<br>5.40E-37 | 2.45E-09<br>7.43E-04 |
| 2.20E+03<br>2.20E+03 | 4.41E-05<br>5.44E-14 | 1.32E-05<br>1.08E-08 | 1.00E+00<br>3.64E-09 | 5.35E-27<br>4.63E-33 | 1.08E-08<br>2.25E-03 |
| 2.40E+03<br>2.40E+03 | 4.41E-05<br>5.79E-13 | 1.31E-05<br>3.77E-08 | 1.00E+00<br>3.26E-08 | 1.82E-24<br>8.89E-30 | 3.77E-08<br>5.66E-03 |
| 2.60E+03<br>2.60E+03 | 4.41E-05<br>4.33E-12 | 1.30E-05<br>1.09E-07 | 1.00E+00<br>2.09E-07 | 2.55E-22<br>5.41E-27 | 1.09E-07<br>1.22E-02 |
| 2.80E+03<br>2.80E+03 | 4.41E-05<br>2.46E-11 | 1.27E-05<br>2.69E-07 | 1.00E+00<br>1.03E-06 | 1.80E-20<br>1.34E-24 | 2.69E-07<br>2.34E-02 |
| 3.00E+03<br>3.00E+03 | 4.41E-05<br>1.13E-10 | 1.20E-05<br>5.84E-07 | 1.00E+00<br>4.09E-06 | 7.36E-19<br>1.62E-22 | 5.84E-07<br>3.97E-02 |
| 3.20E+03<br>3.20E+03 | 4.41E-05<br>4.40E-10 | 1.10E-05<br>1.13E-06 | 1.00E+00<br>1.37E-05 | 1.96E-17<br>1.12E-20 | 1.13E-06<br>6.01E-02 |
| 3.40E+03<br>3.40E+03 | 4.40E-05<br>1.53E-09 | 9.31E-06<br>1.95E-06 | 1.00E+00<br>4.00E-05 | 3.70E-16<br>4.88E-19 | 1.95E-06<br>8.01E-02 |
| 3.60E+03<br>3.60E+03 | 4.40E-05<br>4.88E-09 | 7.20E-06<br>3.01E-06 | 1.00E+00<br>1.03E-04 | 5.39E-15<br>1.49E-17 | 3.01E-06<br>9.22E-02 |
| 3.80E+03<br>3.80E+03 | 4.40E-05<br>1.49E-08 | 4.95E-06<br>4.13E-06 | 1.00E+00<br>2.43E-04 | 6.39E-14<br>3.44E-16 | 4.15E-06<br>9.06E-02 |
| 4.00E+03<br>4.00E+03 | 4.40E-05<br>4.37E-08 | 3.02E-06<br>5.10E-06 | 99E-01<br>23E-04 | 6.42E-13<br>6.27E-15 | 5.14E-06<br>7.63E-02 |
| 4.20E+03<br>4.20E+03 | 4.38E-05<br>1.23E-07 | 1.69E-06<br>5.76E-06 | 9.99E-01<br>1.05E-03 | 5.54E-12<br>9.25E-14 | 5.88E-06<br>5.72E-02 |
| 4.40E+03<br>4.40E+03 | 4.34E-05<br>3.25E-07 | 9.25E-07<br>6.15E-06 | 9.98E-01<br>1.97E-03 | 4.07E-11<br>1.11E-12 | 6.47E-06<br>4.07E-02 |
| 4.60E+03<br>4.60E+03 | 4.25E-05<br>7.71E-07 | 5.21E-07<br>6.35E-06 | 9.96E-01<br>3.52E-03 | 2.51E-10<br>1.06E-11 | 7.12E-06<br>2.92E-02 |

# CHEMICAL COMPOSITION OF IMPURE NITROGEN

CONDITION: 5.0000E+02 DYNES CU; 1.5000E+02 DYNES NA
1.1350E+07 TOTAL PRESSURE

| TEMP<br>TEMP<br>(DEG K) | CU ATOM<br>CU ION<br>(FRACTION | NA ATOM<br>NA ION<br>OF TOTAL | N2 MOLEC<br>N ATOM<br>PRESSURE) | N2 MOL-ION<br>N ION | ELECTRONS<br>SPEC INT ?<br>(RELATIVE) |
|---|---|---|---|---|---|
| 4.80E+03 | 4.08E-05 | 3.14E-07 | 9.94E-01 | 1.29E-09 | 8.07E-01 |
| 4.80E+03 | 1.61E-06 | 6.45E-06 | 5.98E-03 | 8.18E-11 | 2.20E-02 |
| 5.00E+03 | 3.81E-05 | 2.05E-07 | 9.90E-01 | 5.55E-09 | 9.47E-01 |
| 5.00E+03 | 2.96E-06 | 6.51E-06 | 9.74E-03 | 5.13E-10 | 1.75E-02 |
| 5.20E+03 | 3.44E-05 | 1.42E-07 | 9.85E-01 | 2.07E-08 | 1.14E-01 |
| 5.20E+03 | 4.81E-06 | 6.54E-06 | 1.53E-02 | 2.71E-09 | 1.47E-02 |
| 5.40E+03 | 2.99E-05 | 1.03E-07 | 9.77E-01 | 6.91E-08 | 1.37E-02 |
| 5.40E+03 | 7.89E-06 | 6.56E-06 | 2.32E-02 | 1.24E-08 | 1.26E-02 |
| 5.60E+03 | 2.48E-05 | 7.63E-08 | 9.66E-01 | 2.10E-07 | 1.64E-01 |
| 5.60E+03 | 9.61E-06 | 6.57E-06 | 3.41E-02 | 5.10E-08 | 1.10E-02 |
| 5.80E+03 | 1.98E-05 | 5.78E-08 | 9.51E-01 | 5.91E-07 | 1.95E-05 |
| 5.80E+03 | 1.21E-05 | 6.58E-06 | 4.87E-02 | 1.98E-07 | 9.72E-03 |
| 6.00E+03 | 1.54E-05 | 4.51E-08 | 9.32E-01 | 1.53E-06 | 2.31E-05 |
| 6.00E+03 | 1.43E-05 | 6.59E-06 | 6.78E-02 | 6.39E-07 | 8.73E-03 |
| 6.20E+03 | 1.21E-05 | 3.71E-08 | 9.08E-01 | 3.58E-06 | 2.81E-05 |
| 6.20E+03 | 1.60E-05 | 6.59E-06 | 9.22E-02 | 1.92E-06 | 8.19E-03 |
| 6.40E+03 | 9.84E-06 | 3.31E-08 | 8.77E-01 | 7.38E-06 | 3.61E-05 |
| 6.40E+03 | 1.71E-05 | 6.59E-06 | 1.23E-01 | 5.01E-06 | 8.25E-03 |
| 6.60E+03 | 8.52E-06 | 3.20E-08 | 8.41E-01 | 1.34E-05 | 4.92E-05 |
| 6.60E+03 | 1.78E-05 | 6.59E-06 | 1.59E-01 | 1.14E-05 | 8.95E-03 |
| 6.80E+03 | 7.76E-06 | 3.29E-08 | 7.97E-01 | 2.19E-05 | 7.00E-05 |
| 6.80E+03 | 1.81E-05 | 6.59E-06 | 2.03E-01 | 2.33E-05 | 1.93E-02 |
| 7.00E+03 | 7.33E-06 | 3.52E-08 | 7.47E-01 | 3.31E-05 | 1.02E-04 |
| 7.00E+03 | 1.84E-05 | 6.59E-06 | 2.53E-01 | 4.37E-05 | 1.22E-02 |
| 7.20E+03 | 7.07E-06 | 3.86E-08 | 6.91E-01 | 4.68E-05 | 1.48E-04 |
| 7.20E+03 | 1.85E-05 | 6.59E-06 | 3.09E-01 | 7.64E-05 | 1.47E-02 |
| 7.40E+03 | 6.90E-06 | 4.28E-08 | 6.29E-01 | 6.31E-05 | 2.15E-04 |
| 7.40E+03 | 1.86E-05 | 6.59E-06 | 3.70E-01 | 1.27E-04 | 1.72E-02 |

# CHEMICAL COMPOSITION OF IMPURE NITROGEN

CONDITIONS: 5.0000E+02 DYNES CU? 1.5000E+02 DYNES NA
1.0050E+07 TOTAL PRESSURE

| TEMP | N ATOM | NA ATOM | N2 MOLEC | N2 MOL-ION | ELECTRONS |
|---|---|---|---|---|---|
| TEMP | N ION | NA ION | N ATOM | N ION | SPEC INTEN |
| (DEG K) | (FRACTION OF TOTAL PRESSURE) | | | | (RELATIVE) |
| 7.?E+03 | ?.78E-06 | 4.77E-08 | 5.64E-01 | 8.14E-05 | 3.09E-34 |
| 7.??E+03 | ?56E-05 | 6.58E-06 | 4.35E-01 | 2.02E-04 | 2.17E-02 |
| 7.?8E+03 | ?.67E-06 | 5.31E-08 | 4.97E-01 | 1.01E-04 | 4.36E-04 |
| 7.?0E+03 | 1.87E-05 | 6.58E-06 | 5.02E-01 | 3.09E-04 | 2.63E-02 |
| ?.80E+03 | ?.57E-06 | 5.89E-08 | 4.30E-01 | 1.22E-04 | 6.06E-04 |
| ?.?0E+03 | 1.87E-05 | 6.58E-06 | 5.69E-01 | 4.59E-04 | 3.16E-02 |
| 8.20E+03 | 6.45E-06 | 6.52E-08 | 3.66E-01 | 1.42E-04 | 8.29E-04 |
| 8.20E+03 | 1.88E-05 | 6.58E-06 | 6.33E-01 | 6.62E-04 | 3.76E-02 |
| 8.40E+03 | 6.32E-06 | 7.18E-08 | 3.06E-01 | 1.61E-04 | 1.11E-03 |
| 8.40E+03 | 1.89E-05 | 6.57E-06 | 6.92E-01 | 9.29E-04 | 4.45E-02 |
| 8.60E+03 | 6.18E-06 | 7.88E-08 | 2.52E-01 | 1.78E-04 | 1.48E-03 |
| 8.60E+03 | 1.89E-05 | 6.57E-06 | 7.45E-01 | 1.27E-03 | 5.22E-02 |
| 8.80E+03 | 6.02E-06 | 8.60E-08 | 2.05E-01 | 1.92E-04 | 1.9?E-03 |
| 8.80E+03 | 1.90E-05 | 6.56E-06 | 7.91E-01 | 1.71E-03 | 6.0?E-02 |
| 9.00E+03 | 5.85E-06 | 9.34E-08 | 1.65E-01 | 2.03E-04 | ?.47E-03 |
| 9.00E+03 | 1.91E-05 | 6.56E-06 | 8.30E-01 | 2.24E-03 | 7.02E-02 |
| 9.20E+03 | 5.68E-06 | 1.01E-07 | 1.31E-01 | 2.12E-04 | 3.14E-03 |
| 9.20E+03 | 1.92E-05 | 6.56E-06 | 8.62E-01 | 2.90E-03 | 8.07E-02 |
| 9.40E+03 | 5.51E-06 | 1.09E-07 | 1.04E-01 | 2.?7E-04 | 3.94E-03 |
| 9.40E+03 | 1.93E-05 | 6.55E-06 | 8.88E-01 | 3.69E-03 | 9.22E-02 |
| 9.60E+03 | 5.33E-06 | 1.18E-07 | 8.26E-02 | 2.21E-04 | 4.88E-03 |
| 9.60E+03 | 1.94E-05 | 6.55E-06 | 9.08E-01 | 4.63E-03 | 1.05E-01 |
| 9.80E+03 | 5.15E-06 | 1.26E-07 | 6.53E-02 | 2.23E-04 | 6.0?E-03 |
| 9.80E+03 | 1.94E-05 | 6.54E-06 | 9.23E-01 | 5.75E-03 | 1.1?E-01 |
| 1.00E+04 | 4.98E-06 | 1.35E-07 | 5.18E-02 | 2.23E-04 | ?.30E-03 |
| 1.00E+04 | 1.95E-05 | 6.54E-06 | 9.34E-01 | 7.05E-03 | 1.33E-01 |

CHEMICAL COMPOSITION OF IMPURE NITROGEN

CONDITION: 5.0000E+02 DYNES CU; 5.0000E+02 DYNES NA
1.1350E+07 TOTAL PRESSURE

| TEMP | CU ATOM | NA ATOM | N2 MOLEC | N2 MOL-ION | ELECTRONS |
|---|---|---|---|---|---|
| TEMP | CU ION | NA ION | N ATOM | N ION | SPEC INTEN |
| (DEG K) | (FRACTION OF TOTAL PRESSURE) | | | | (RELATIVE) |
| 2.00E+03 | 4.41E-05 | 4.40E-05 | 1.00E+00 | 2.73E-30 | 4.48E-09 |
| 2.00E+03 | 1.76E-15 | 4.48E-09 | 2.63E-10 | 2.96E-37 | 2.48E-03 |
| 2.20E+03 | 4.41E-05 | 4.40E-05 | 1.00E+00 | 2.93E-27 | 1.98E-08 |
| 2.20E+03 | 2.98E-14 | 1.98E-08 | 3.64E-09 | 2.53E-33 | 7.51E-03 |
| 2.40E+03 | 4.41E-05 | 4.39E-05 | 1.00E+00 | 9.94E-25 | 6.89E-08 |
| 2.40E+03 | 3.17E-13 | 6.89E-08 | 3.26E-08 | 4.86E-30 | 1.89E-02 |
| 2.60E+03 | 4.41E-05 | 4.37E-05 | 1.00E+00 | 1.39E-22 | 1.99E-07 |
| 2.60E+03 | 2.36E-12 | 1.99E-07 | 2.09E-07 | 2.95E-27 | 4.11E-02 |
| 2.80E+03 | 4.41E-05 | 4.31E-05 | 1.00E+00 | 9.76E-21 | 4.95E-07 |
| 2.80E+03 | 1.33E-11 | 4.95E-07 | 1.03E-06 | 7.26E-25 | 7.94E-02 |
| 3.00E+03 | 4.41E-05 | 4.19E-05 | 1.00E+00 | 3.95E-19 | 1.09E-06 |
| 3.00E+03 | 6.05E-11 | 1.09E-06 | 4.09E-06 | 8.71E-23 | 1.38E-01 |
| 3.20E+03 | 4.41E-05 | 3.98E-05 | 1.00E+00 | 1.03E-17 | 2.15E-06 |
| 3.20E+03 | 2.31E-10 | 2.15E-06 | 1.37E-05 | 5.86E-21 | 2.18E-01 |
| 3.40E+03 | 4.41E-05 | 3.63E-05 | 1.00E+00 | 1.88E-16 | 2.86E-06 |
| 3.40E+03 | 7.73E-10 | 3.85E-06 | 4.00E-05 | 2.47E-19 | 3.12E-01 |
| 3.60E+03 | 4.40E-05 | 3.15E-05 | 1.00E+00 | 2.58E-15 | 6.30E-06 |
| 3.60E+03 | 2.34E-09 | 6.29E-06 | 1.03E-04 | 7.14E-18 | 4.03E-01 |
| 3.80E+03 | 4.40E-05 | 2.53E-05 | 1.00E+00 | 2.83E-14 | 9.37E-06 |
| 3.80E+03 | 6.59E-09 | 9.37E-06 | 2.43E-04 | 1.52E-16 | 4.64E-01 |
| 4.00E+03 | 4.40E-05 | 1.86E-05 | 9.99E-01 | 2.59E-13 | 1.27E-05 |
| 4.00E+03 | 1.77E-08 | 1.27E-05 | 5.23E-04 | 2.53E-15 | 4.71E-01 |
| 4.20E+03 | 4.40E-05 | 1.25E-05 | 9.99E-01 | 2.06E-12 | 1.58E-05 |
| 4.20E+03 | 4.60E-08 | 1.58E-05 | 1.05E-03 | 3.44E-14 | 4.22E-01 |
| 4.40E+03 | 4.38E-05 | 7.73E-06 | 9.98E-01 | 1.44E-11 | 1.83E-05 |
| 4.40E+03 | 1.16E-07 | 1.82E-05 | 1.97E-03 | 3.92E-13 | 3.40E-01 |
| 4.60E+03 | 4.35E-05 | 4.56E-06 | 9.96E-01 | 8.91E-11 | 2.00E-05 |
| 4.60E+03 | 2.80E-07 | 1.97E-05 | 3.52E-03 | 3.78E-12 | 2.56E-01 |

# CHEMICAL COMPOSITION OF IMPURE NITROGEN

CONDITION: 5.0000E+02 DYNES CU; 5.0000E+02 DYNES NA
1.1350E+07 TOTAL PRESSURE

| TEMP<br>TEMP<br>(DEG K) | CU ATOM<br>CU ION<br>(FRACTION | NA ATOM<br>NA ION<br>OF TOTAL | N2 MOLEC<br>N ATOM<br>PRESSURE) | N2 MOL-ION<br>N ION | ELECTRONS<br>SPEC INTEN<br>(RELATIVE) |
|---|---|---|---|---|---|
| 4.80E+03<br>4.80E+03 | 4.28E-05<br>6.32E-07 | 2.67E-06<br>2.07E-05 | 9.94E-01<br>5.98E-03 | 4.86E-10<br>3.09E-11 | 2.13E-05<br>1.86E-01 |
| 5.00E+03<br>5.00E+03 | 4.14E-05<br>1.34E-06 | 1.59E-06<br>2.12E-05 | 9.90E-01<br>9.74E-03 | 2.33E-09<br>2.15E-10 | 2.26E-05<br>1.36E-01 |
| 5.20E+03<br>5.20E+03 | 3.89E-05<br>2.56E-06 | 9.91E-07<br>2.15E-05 | 9.85E-01<br>1.53E-02 | 9.77E-09<br>1.28E-09 | 2.41E-05<br>1.03E-01 |
| 5.40E+03<br>5.40E+03 | 3.53E-05<br>4.39E-06 | 6.47E-07<br>2.17E-05 | 9.77E-01<br>2.32E-02 | 3.63E-08<br>6.53E-09 | 2.61E-05<br>7.96E-02 |
| 5.60E+03<br>5.60E+03 | 3.05E-05<br>6.76E-06 | 4.42E-07<br>2.18E-05 | 9.66E-01<br>3.41E-02 | 1.20E-07<br>2.92E-08 | 2.87E-05<br>6.39E-02 |
| 5.80E+03<br>5.80E+03 | 2.52E-05<br>9.43E-06 | 3.14E-07<br>2.19E-05 | 9.51E-01<br>4.87E-02 | 3.62E-07<br>1.16E-07 | 3.18E-05<br>5.28E-02 |
| 6.00E+03<br>6.00E+03 | 1.99E-05<br>1.21E-05 | 2.30E-07<br>2.19E-05 | 9.32E-01<br>6.78E-02 | 9.98E-07<br>4.16E-07 | 3.54E-05<br>4.46E-02 |
| 6.20E+03<br>6.20E+03 | 1.54E-05<br>1.43E-05 | 1.77E-07<br>2.19E-05 | 9.08E-01<br>9.22E-02 | 2.51E-06<br>1.34E-06 | 4.01E-05<br>3.89E-02 |
| 6.40E+03<br>6.40E+03 | 1.21E-05<br>1.60E-05 | 1.45E-07<br>2.20E-05 | 8.77E-01<br>1.23E-01 | 5.62E-06<br>3.82E-06 | 4.74E-05<br>3.61E-02 |
| 6.60E+03<br>6.60E+03 | 9.91E-06<br>1.71E-05 | 1.29E-07<br>2.20E-05 | 8.41E-01<br>1.59E-01 | 1.11E-05<br>9.45E-06 | 5.96E-05<br>3.61E-02 |
| 6.80E+03<br>6.80E+03 | 8.61E-06<br>1.77E-05 | 1.25E-07<br>2.20E-05 | 7.97E-01<br>2.03E-01 | 1.93E-05<br>2.05E-05 | 7.95E-05<br>3.89E-02 |
| 7.00E+03<br>7.00E+03 | 7.86E-06<br>1.81E-05 | 1.28E-07<br>2.20E-05 | 7.47E-01<br>2.53E-01 | 3.04E-05<br>4.01E-05 | 1.11E-04<br>4.42E-02 |
| 7.20E+03<br>7.20E+03 | 7.41E-06<br>1.83E-05 | 1.36E-07<br>2.20E-05 | 6.91E-01<br>3.09E-01 | 4.43E-05<br>7.23E-05 | 1.57E-04<br>5.19E-02 |
| 7.40E+03<br>7.40E+03 | 7.12E-06<br>1.85E-05 | 1.48E-07<br>2.20E-05 | 6.29E-01<br>3.70E-01 | 6.08E-05<br>1.22E-04 | 2.23E-04<br>6.19E-02 |

# CHEMICAL COMPOSITION OF IMPURE NITROGEN

CONDITION: 5.0000E+02 DYNES CU; 5.0000E+02 DYNES NA
1.1350E+07 TOTAL PRESSURE

| TEMP TEMP (DEG K) | CU ATOM CU ION | NA ATOM NA ION | N2 MOLEC N ATOM | N2 MOL-ION N ION | ELECTRONS SPEC INTEN |
|---|---|---|---|---|---|
| | | (FRACTION OF TOTAL PRESSURE) | | | (RELATIVE) |
| 7.60E+03 | 6.93E-06 | 1.63E-07 | 5.64E-01 | 7.94E-05 | 3.17E-04 |
| 7.60E+03 | 1.86E-05 | 2.19E-05 | 4.35E-01 | 1.97E-04 | 7.43E-02 |
| 7.80E+03 | 6.78E-06 | 1.80E-07 | 4.97E-01 | 9.95E-05 | 4.44E-04 |
| 7.80E+03 | 1.86E-05 | 2.19E-05 | 5.02E-01 | 3.04E-04 | 8.92E-02 |
| 8.00E+03 | 6.64E-06 | 1.99E-07 | 4.30E-01 | 1.20E-04 | 6.14E-04 |
| 8.00E+03 | 1.87E-05 | 2.19E-05 | 5.69E-01 | 4.53E-04 | 1.07E-01 |
| 8.20E+03 | 6.50E-06 | 2.19E-07 | 3.66E-01 | 1.41E-04 | 8.37E-04 |
| 8.20E+03 | 1.88E-05 | 2.19E-05 | 6.33E-01 | 6.55E-04 | 1.27E-01 |
| 8.40E+03 | 6.36E-06 | 2.41E-07 | 3.06E-01 | 1.60E-04 | 1.12E-03 |
| 8.40E+03 | 1.88E-05 | 2.19E-05 | 6.92E-01 | 9.22E-04 | 1.49E-01 |
| 8.60E+03 | 6.20E-06 | 2.64E-07 | 2.52E-01 | 1.77E-04 | 1.48E-03 |
| 8.60E+03 | 1.89E-05 | 2.19E-05 | 7.45E-01 | 1.27E-03 | 1.75E-01 |
| 8.80E+03 | 6.04E-06 | 2.88E-07 | 2.05E-01 | 1.91E-04 | 1.93E-03 |
| 8.80E+03 | 1.90E-05 | 2.19E-05 | 7.91E-01 | 1.70E-03 | 2.03E-01 |
| 9.00E+03 | 5.87E-06 | 3.12E-07 | 1.65E-01 | 2.02E-04 | 2.48E-03 |
| 9.00E+03 | 1.91E-05 | 2.19E-05 | 8.30E-01 | 2.24E-03 | 2.35E-01 |
| 9.20E+03 | 5.70E-06 | 3.38E-07 | 1.31E-01 | 2.11E-04 | 3.15E-03 |
| 9.20E+03 | 1.92E-05 | 2.19E-05 | 8.62E-01 | 2.89E-03 | 2.70E-01 |
| 9.40E+03 | 5.52E-06 | 3.65E-07 | 1.04E-01 | 2.17E-04 | 3.94E-03 |
| 9.40E+03 | 1.93E-05 | 2.18E-05 | 8.88E-01 | 3.68E-03 | 3.08E-01 |
| 9.60E+03 | 5.34E-06 | 3.93E-07 | 8.26E-02 | 2.21E-04 | 4.89E-03 |
| 9.60E+03 | 1.94E-05 | 2.18E-05 | 9.08E-01 | 4.63E-03 | 3.50E-01 |
| 9.80E+03 | 5.16E-06 | 4.21E-07 | 6.53E-02 | 2.23E-04 | 6.00E-03 |
| 9.80E+03 | 1.94E-05 | 2.18E-05 | 9.23E-01 | 5.74E-03 | 3.95E-01 |
| 1.00E+04 | 4.99E-06 | 4.51E-07 | 5.18E-02 | 2.23E-04 | 7.31E-03 |
| 1.00E+04 | 1.95E-05 | 2.18E-05 | 9.34E-01 | 7.04E-03 | 4.45E-01 |

# CHEMICAL COMPOSITION OF IMPURE NITROGEN

CONDITION: 5.0000E+02 DYNES CU; 5.0000E+01 DYNES NA
5.0650E+06 TOTAL PRESSURE

| TEMP<br>TEMP<br>(DEG K) | CU ATOM<br>CU ION | NA ATOM<br>NA ION | N2 MOLEC<br>N ATOM | N2 MOL-ION<br>N ION | ELECTRONS<br>SPEC INTEN<br>(RELATIVE) |
|---|---|---|---|---|---|
| | | | (FRACTION OF TOTAL PRESSURE) | | |
| 2.00E+03<br>2.00E+03 | 9.87E-05<br>1.25E-14 | 9.87E-06<br>3.17E-09 | 1.00E+00<br>3.94E-10 | 8.65E-30<br>1.40E-36 | 3.17E-09<br>2.47E-04 |
| 2.20E+03<br>2.20E+03 | 9.87E-05<br>2.11E-13 | 9.84E-06<br>1.40E-08 | 1.00E+00<br>5.45E-09 | 9.28E-27<br>1.20E-32 | 1.40E-08<br>7.50E-04 |
| 2.40E+03<br>2.40E+03 | 9.87E-05<br>2.25E-12 | 9.77E-06<br>4.86E-08 | 1.00E+00<br>4.88E-08 | 3.16E-24<br>2.31E-29 | 4.86E-08<br>1.88E-03 |
| 2.60E+03<br>2.60E+03 | 9.87E-05<br>1.69E-11 | 9.59E-06<br>1.40E-07 | 1.00E+00<br>3.12E-07 | 4.45E-22<br>1.41E-26 | 1.40E-07<br>4.03E-03 |
| 2.80E+03<br>2.80E+03 | 9.87E-05<br>9.68E-11 | 9.19E-06<br>3.42E-07 | 1.00E+00<br>1.54E-06 | 3.16E-20<br>3.52E-24 | 3.42E-07<br>7.56E-03 |
| 3.00E+03<br>3.00E+03 | 9.87E-05<br>4.53E-10 | 8.41E-06<br>7.30E-07 | 1.00E+00<br>6.12E-06 | 1.32E-18<br>4.36E-22 | 7.31E-07<br>1.24E-02 |
| 3.20E+03<br>3.20E+03 | 9.87E-05<br>1.83E-09 | 7.14E-06<br>1.36E-06 | 1.00E+00<br>2.05E-05 | 3.63E-17<br>3.10E-20 | 1.37E-06<br>1.75E-02 |
| 3.40E+03<br>3.40E+03 | 9.87E-05<br>6.70E-09 | 5.42E-06<br>2.23E-06 | 1.00E+00<br>5.98E-05 | 7.26E-16<br>1.43E-18 | 2.23E-06<br>2.08E-02 |
| 3.60E+03<br>3.60E+03 | 9.87E-05<br>2.32E-08 | 3.56E-06<br>3.16E-06 | 1.00E+00<br>1.55E-04 | 1.14E-14<br>4.75E-17 | 3.18E-06<br>2.03E-02 |
| 3.80E+03<br>3.80E+03 | 9.86E-05<br>7.73E-08 | 2.02E-06<br>3.93E-06 | 1.00E+00<br>3.63E-04 | 1.48E-13<br>1.19E-15 | 4.00E-06<br>1.65E-02 |
| 4.00E+03<br>4.00E+03 | 9.82E-05<br>2.42E-07 | 1.05E-06<br>4.41E-06 | 9.99E-01<br>7.82E-04 | 1.59E-12<br>2.32E-14 | 4.65E-06<br>1.19E-02 |
| 4.20E+03<br>4.20E+03 | 9.74E-05<br>6.77E-07 | 5.54E-07<br>4.66E-06 | 9.98E-01<br>1.57E-03 | 1.37E-11<br>3.42E-13 | 5.34E-06<br>8.35E-03 |
| 4.40E+03<br>4.40E+03 | 9.55E-05<br>1.62E-06 | 3.17E-07<br>4.78E-06 | 9.97E-01<br>2.95E-03 | 9.22E-11<br>3.76E-12 | 6.40E-06<br>6.23E-03 |
| 4.60E+03<br>4.60E+03 | 9.21E-05<br>3.28E-06 | 2.02E-07<br>4.83E-06 | 9.95E-01<br>5.26E-03 | 4.92E-10<br>3.12E-11 | 8.12E-06<br>5.05E-03 |

# CHEMICAL COMPOSITION OF IMPURE NITROGEN

CONDITION: 5.0000E+02 DYNES CU; 5.0000E+01 DYNES NA
5.0650E+06 TOTAL PRESSURE

| TEMP<br>TEMP<br>(DEG K) | CU ATOM<br>CU ION | NA ATOM<br>NA ION<br>(FRACTION OF TOTAL PRESSURE) | N2 MOLEC<br>N ATOM | N2 MOL-ION<br>N ION | ELECTRONS<br>SPEC INTEN<br>(RELATIVE) |
|---|---|---|---|---|---|
| 4.80E+03 | 8.71E-05 | 1.40E-07 | 9.91E-01 | 2.17E-09 | 1.07E-05 |
| 4.80E+03 | 5.82E-06 | 4.87E-06 | 8.94E-03 | 2.07E-10 | 4.37E-03 |
| 5.00E+03 | 8.01E-05 | 1.03E-07 | 9.85E-01 | 8.26E-09 | 1.42E-05 |
| 5.00E+03 | 9.29E-06 | 4.88E-06 | 1.45E-02 | 1.15E-09 | 3.93E-03 |
| 5.20E+03 | 7.14E-05 | 7.76E-08 | 9.77E-01 | 2.82E-08 | 1.86E-05 |
| 5.20E+03 | 1.37E-05 | 4.90E-06 | 2.28E-02 | 5.53E-09 | 3.58E-03 |
| 5.40E+03 | 6.12E-05 | 5.94E-08 | 9.66E-01 | 8.83E-08 | 2.38E-05 |
| 5.40E+03 | 1.88E-05 | 4.91E-06 | 3.45E-02 | 2.39E-08 | 3.26E-03 |
| 5.60E+03 | 5.02E-05 | 4.57E-08 | 9.49E-01 | 2.58E-07 | 2.95E-05 |
| 5.60E+03 | 2.43E-05 | 4.91E-06 | 5.06E-02 | 9.44E-08 | 2.95E-03 |
| 5.80E+03 | 3.95E-05 | 3.53E-08 | 9.28E-01 | 7.07E-07 | 3.56E-05 |
| 5.80E+03 | 2.96E-05 | 4.92E-06 | 7.20E-02 | 3.44E-07 | 2.64E-03 |
| 6.00E+03 | 3.01E-05 | 2.75E-08 | 9.00E-01 | 1.81E-06 | 4.22E-05 |
| 6.00E+03 | 3.43E-05 | 4.92E-06 | 9.98E-02 | 1.15E-06 | 2.38E-03 |
| 6.20E+03 | 2.29E-05 | 2.23E-08 | 8.65E-01 | 4.25E-06 | 5.05E-05 |
| 6.20E+03 | 3.79E-05 | 4.92E-06 | 1.35E-01 | 3.49E-06 | 2.19E-03 |
| 6.40E+03 | 1.81E-05 | 1.94E-08 | 8.22E-01 | 8.83E-06 | 6.33E-05 |
| 6.40E+03 | 4.03E-05 | 4.93E-06 | 1.78E-01 | 9.27E-06 | 2.15E-03 |
| 6.60E+03 | 1.53E-05 | 1.82E-08 | 7.71E-01 | 1.61E-05 | 8.42E-05 |
| 6.60E+03 | 4.17E-05 | 4.93E-06 | 2.28E-01 | 2.15E-05 | 2.28E-03 |
| 6.80E+03 | 1.36E-05 | 1.84E-08 | 7.13E-01 | 2.61E-05 | 1.18E-04 |
| 6.80E+03 | 4.25E-05 | 4.93E-06 | 2.87E-01 | 4.41E-05 | 2.57E-03 |
| 7.00E+03 | 1.27E-05 | 1.95E-08 | 6.47E-01 | 3.87E-05 | 1.69E-04 |
| 7.00E+03 | 4.30E-05 | 4.93E-06 | 3.52E-01 | 8.21E-05 | 3.01E-03 |
| 7.20E+03 | 1.21E-05 | 2.12E-08 | 5.77E-01 | 5.33E-05 | 2.44E-04 |
| 7.20E+03 | 4.33E-05 | 4.93E-06 | 4.23E-01 | 1.42E-04 | 3.61E-03 |
| 7.40E+03 | 1.18E-05 | 2.33E-08 | 5.03E-01 | 6.93E-05 | 3.51E-04 |
| 7.40E+03 | 4.35E-05 | 4.92E-06 | 4.96E-01 | 2.33E-04 | 4.35E-03 |

# CHEMICAL COMPOSITION OF IMPURE NITROGEN

CONDITION: 5.0000E+02 DYNES CU; 5.0000E+01 DYNES NA
5.0650E+06 TOTAL PRESSURE

| TEMP TEMP (DEG K) | CU ATOM CU ION | NA ATOM NA ION | N2 MOLEC N ATOM | N2 MOL-ION N ION | ELECTRONS SPEC INTEN |
|---|---|---|---|---|---|
| | | (FRACTION OF TOTAL PRESSURE) | | | (RELATIVE) |
| 7.60E+03 | 1.15E-05 | 2.58E-08 | 4.30E-01 | 8.59E-05 | 5.00E-04 |
| 7.60E+03 | 4.36E-05 | 4.92E-06 | 5.69E-01 | 3.65E-04 | 5.24E-03 |
| 7.80E+03 | 1.12E-05 | 2.85E-08 | 3.59E-01 | 1.02E-04 | 7.00E-04 |
| 7.80E+03 | 4.38E-05 | 4.92E-06 | 6.39E-01 | 5.49E-04 | 6.29E-03 |
| 8.00E+03 | 1.09E-05 | 3.13E-08 | 2.94E-01 | 1.17E-04 | 9.66E-04 |
| 8.00E+03 | 4.39E-05 | 4.92E-06 | 7.04E-01 | 7.99E-04 | 7.49E-03 |
| 8.20E+03 | 1.06E-05 | 3.44E-08 | 2.37E-01 | 1.30E-04 | 1.31E-03 |
| 8.20E+03 | 4.40E-05 | 4.92E-06 | 7.61E-01 | 1.13E-03 | 8.85E-03 |
| 8.40E+03 | 1.03E-05 | 3.75E-08 | 1.87E-01 | 1.41E-04 | 1.75E-03 |
| 8.40E+03 | 4.42E-05 | 4.92E-06 | 8.09E-01 | 1.56E-03 | 1.04E-02 |
| 8.60E+03 | 1.00E-05 | 4.08E-08 | 1.46E-01 | 1.49E-04 | 2.29E-03 |
| 8.60E+03 | 4.43E-05 | 4.92E-06 | 8.49E-01 | 2.09E-03 | 1.21E-02 |
| 8.80E+03 | 9.69E-06 | 4.43E-08 | 1.13E-01 | 1.55E-04 | 2.96E-03 |
| 8.80E+03 | 4.45E-05 | 4.91E-06 | 8.81E-01 | 2.76E-03 | 1.40E-02 |
| 9.00E+03 | 9.36E-06 | 4.78E-08 | 8.76E-02 | 1.58E-04 | 3.79E-03 |
| 9.00E+03 | 4.47E-05 | 4.91E-06 | 9.05E-01 | 3.58E-03 | 1.60E-02 |
| 9.20E+03 | 9.03E-06 | 5.15E-08 | 6.75E-02 | 1.60E-04 | 4.78E-03 |
| 9.20E+03 | 4.48E-05 | 4.91E-06 | 9.23E-01 | 4.57E-03 | 1.83E-02 |
| 9.40E+03 | 8.70E-06 | 5.53E-08 | 5.20E-02 | 1.60E-04 | 5.96E-03 |
| 9.40E+03 | 4.50E-05 | 4.91E-06 | 9.36E-01 | 5.75E-03 | 2.08E-02 |
| 9.60E+03 | 8.38E-06 | 5.94E-08 | 4.02E-02 | 1.60E-04 | 7.37E-03 |
| 9.60E+03 | 4.52E-05 | 4.91E-06 | 9.45E-01 | 7.16E-03 | 2.36E-02 |
| 9.80E+03 | 8.07E-06 | 6.36E-08 | 3.12E-02 | 1.59E-04 | 9.03E-03 |
| 9.80E+03 | 4.53E-05 | 4.90E-06 | 9.51E-01 | 8.82E-03 | 2.66E-02 |
| 1.00E+04 | 7.77E-06 | 6.79E-08 | 2.44E-02 | 1.57E-04 | 1.10E-02 |
| 1.00E+04 | 4.55E-05 | 4.90E-06 | 9.54E-01 | 1.07E-02 | 2.99E-02 |

# CHEMICAL COMPOSITION OF IMPURE NITROGEN

CONDITION: 5.0000E+02 DYNES CU; 5.0000E+01 DYNES NA
2.0260E+07 TOTAL PRESSURE

| TEMP<br>TEMP<br>(DEG K) | CU ATOM<br>CU ION | NA ATOM<br>NA ION<br>(FRACTION OF | N2 MOLEC<br>N ATOM<br>TOTAL PRESSURE) | N2 MOL-ION<br>N ION | ELECTRONS<br>SPEC INTEN<br>(RELATIVE) |
|---|---|---|---|---|---|
| 2.00E+03 | 2.47E-05 | 2.47E-06 | 1.00E+00 | 8.65E-30 | 7.93E-10 |
| 2.00E+03 | 3.13E-15 | 7.93E-10 | 1.97E-10 | 7.00E-37 | 2.47E-04 |
| 2.20E+03 | 2.47E-05 | 2.46E-06 | 1.00E+00 | 9.28E-27 | 3.50E-09 |
| 2.20E+03 | 5.28E-14 | 3.50E-09 | 2.73E-09 | 6.00E-33 | 7.50E-04 |
| 2.40E+03 | 2.47E-05 | 2.44E-06 | 1.00E+00 | 3.16E-24 | 1.22E-08 |
| 2.40E+03 | 5.63E-13 | 1.22E-08 | 2.44E-08 | 1.15E-29 | 1.88E-03 |
| 2.60E+03 | 2.47E-05 | 2.40E-06 | 1.00E+00 | 4.45E-22 | 3.49E-08 |
| 2.60E+03 | 4.22E-12 | 3.49E-08 | 1.56E-07 | 7.05E-27 | 4.03E-03 |
| 2.80E+03 | 2.47E-05 | 2.30E-06 | 1.00E+00 | 3.16E-20 | 8.56E-08 |
| 2.80E+03 | 2.42E-11 | 8.56E-08 | 7.68E-07 | 1.76E-24 | 7.56E-03 |
| 3.00E+03 | 2.47E-05 | 2.10E-06 | 1.00E+00 | 1.32E-18 | 1.83E-07 |
| 3.00E+03 | 1.13E-10 | 1.83E-07 | 3.06E-06 | 2.18E-22 | 1.24E-02 |
| 3.20E+03 | 2.47E-05 | 1.79E-06 | 1.00E+00 | 3.63E-17 | 3.42E-07 |
| 3.20E+03 | 4.57E-10 | 3.41E-07 | 1.03E-05 | 1.55E-20 | 1.75E-02 |
| 3.40E+03 | 2.47E-05 | 1.36E-06 | 1.00E+00 | 7.26E-16 | 5.58E-07 |
| 3.40E+03 | 1.68E-09 | 5.56E-07 | 2.99E-05 | 7.17E-19 | 2.08E-02 |
| 3.60E+03 | 2.47E-05 | 8.89E-07 | 1.00E+00 | 1.14E-14 | 7.95E-07 |
| 3.60E+03 | 5.81E-09 | 7.89E-07 | 7.74E-05 | 2.37E-17 | 2.03E-02 |
| 3.80E+03 | 2.46E-05 | 5.05E-07 | 1.00E+00 | 1.48E-13 | 1.00E-06 |
| 3.80E+03 | 1.93E-08 | 9.81E-07 | 1.82E-04 | 5.97E-16 | 1.65E-02 |
| 4.00E+03 | 2.46E-05 | 2.64E-07 | 1.00E+00 | 1.59E-12 | 1.16E-06 |
| 4.00E+03 | 6.05E-08 | 1.10E-06 | 3.91E-04 | 1.16E-14 | 1.19E-02 |
| 4.20E+03 | 2.43E-05 | 1.39E-07 | 9.99E-01 | 1.37E-11 | 1.33E-06 |
| 4.20E+03 | 1.69E-07 | 1.16E-06 | 7.84E-04 | 1.71E-13 | 8.35E-03 |
| 4.40E+03 | 2.39E-05 | 7.93E-08 | 9.99E-01 | 9.23E-11 | 1.60E-06 |
| 4.40E+03 | 4.05E-07 | 1.19E-06 | 1.48E-03 | 1.88E-12 | 6.23E-03 |
| 4.60E+03 | 2.30E-05 | 5.05E-08 | 9.97E-01 | 4.93E-10 | 2.03E-06 |
| 4.60E+03 | 8.21E-07 | 1.21E-06 | 2.63E-03 | 1.56E-11 | 5.05E-03 |

# CHEMICAL COMPOSITION OF IMPURE NITROGEN

CONDITION: 5.0000E+02 DYNES CU; 5.0000E+01 DYNES NA
2.0260E+07 TOTAL PRESSURE

| TEMP TEMP (DEG K) | CU ATOM CU ION | NA ATOM NA ION | N2 MOLEC N ATOM | N2 MOL-ION N ION | ELECTRONS SPEC INTEN |
|---|---|---|---|---|---|
| | | (FRACTION OF TOTAL PRESSURE) | | | (RELATIVE) |
| 4.80E+03 | 2.18E-05 | 3.51E-08 | 9.96E-01 | 2.17E-09 | 2.67E-06 |
| 4.80E+03 | 1.45E-06 | 1.22E-06 | 4.48E-03 | 1.04E-10 | 4.38E-03 |
| 5.00E+03 | 2.00E-05 | 2.57E-08 | 9.93E-01 | 8.31E-09 | 3.55E-06 |
| 5.00E+03 | 2.32E-06 | 1.22E-06 | 7.30E-03 | 5.75E-10 | 3.93E-03 |
| 5.20E+03 | 1.79E-05 | 1.95E-08 | 9.89E-01 | 2.84E-08 | 4.66E-06 |
| 5.20E+03 | 3.41E-06 | 1.22E-06 | 1.15E-02 | 2.77E-09 | 3.59E-03 |
| 5.40E+03 | 1.53E-05 | 1.50E-08 | 9.83E-01 | 8.90E-08 | 5.99E-06 |
| 5.40E+03 | 4.67E-06 | 1.23E-06 | 1.74E-02 | 1.20E-08 | 3.29E-03 |
| 5.60E+03 | 1.27E-05 | 1.17E-08 | 9.74E-01 | 2.59E-07 | 7.53E-06 |
| 5.60E+03 | 6.00E-06 | 1.23E-06 | 2.56E-02 | 4.68E-08 | 3.01E-03 |
| 5.80E+03 | 1.02E-05 | 9.26E-09 | 9.63E-01 | 6.98E-07 | 9.35E-06 |
| 5.80E+03 | 7.25E-06 | 1.23E-06 | 3.67E-02 | 1.67E-07 | 2.78E-03 |
| 6.00E+03 | 8.11E-06 | 7.66E-09 | 9.49E-01 | 1.71E-06 | 1.18E-05 |
| 6.00E+03 | 8.28E-06 | 1.23E-06 | 5.12E-02 | 5.31E-07 | 2.65E-03 |
| 6.20E+03 | 6.67E-06 | 6.81E-09 | 9.30E-01 | 3.73E-06 | 1.54E-05 |
| 6.20E+03 | 9.01E-06 | 1.23E-06 | 6.99E-02 | 1.48E-06 | 2.68E-03 |
| 6.40E+03 | 5.77E-06 | 6.55E-09 | 9.07E-01 | 7.18E-06 | 2.15E-05 |
| 6.40E+03 | 9.45E-06 | 1.23E-06 | 9.32E-02 | 3.59E-06 | 2.92E-03 |
| 6.60E+03 | 5.25E-06 | 6.73E-09 | 8.78E-01 | 1.24E-05 | 3.11E-05 |
| 6.60E+03 | 9.71E-06 | 1.23E-06 | 1.22E-01 | 7.76E-06 | 3.37E-03 |
| 6.80E+03 | 4.96E-06 | 7.22E-09 | 8.44E-01 | 1.97E-05 | 4.61E-05 |
| 6.80E+03 | 9.86E-06 | 1.23E-06 | 1.56E-01 | 1.53E-05 | 4.02E-03 |
| 7.00E+03 | 4.79E-06 | 7.93E-09 | 8.04E-01 | 2.95E-05 | 6.87E-05 |
| 7.00E+03 | 9.95E-06 | 1.23E-06 | 1.96E-01 | 2.81E-05 | 4.90E-03 |
| 7.20E+03 | 4.69E-06 | 8.84E-09 | 7.58E-01 | 4.19E-05 | 1.02E-04 |
| 7.20E+03 | 1.00E-05 | 1.23E-06 | 2.42E-01 | 4.88E-05 | 6.02E-03 |
| 7.40E+03 | 4.62E-06 | 9.91E-09 | 7.06E-01 | 5.71E-05 | 1.49E-04 |
| 7.40E+03 | 1.00E-05 | 1.23E-06 | 2.94E-01 | 8.11E-05 | 7.39E-03 |

# CHEMICAL COMPOSITION OF IMPURE NITROGEN

CONDITION: 5.0000E+02 DYNES CU; 5.0000E+01 DYNES NA
2.0260E+07 TOTAL PRESSURE

| TEMP<br>TEMP<br>(DEG K) | CU ATOM<br>CU ION | NA ATOM<br>NA ION<br>(FRACTION OF | N2 MOLEC<br>N ATOM<br>TOTAL PRESSURE) | N2 MOL-ION<br>N ION | ELECTRONS<br>SPEC INTEN<br>(RELATIVE) |
|---|---|---|---|---|---|
| 7.60E+03 | 4.57E-06 | 1.11E-08 | 6.50E-01 | 7.51E-05 | 2.16E-04 |
| 7.60E+03 | 1.01E-05 | 1.23E-06 | 3.50E-01 | 1.30E-04 | 9.05E-03 |
| 7.80E+03 | 4.53E-06 | 1.25E-08 | 5.90E-01 | 9.55E-05 | 3.07E-04 |
| 7.80E+03 | 1.01E-05 | 1.23E-06 | 4.10E-01 | 2.01E-04 | 1.10E-02 |
| 8.00E+03 | 4.48E-06 | 1.39E-08 | 5.28E-01 | 1.18E-04 | 4.30E-04 |
| 8.00E+03 | 1.01E-05 | 1.23E-06 | 4.72E-01 | 3.01E-04 | 1.33E-02 |
| 8.20E+03 | 4.42E-06 | 1.55E-08 | 4.65E-01 | 1.42E-04 | 5.92E-04 |
| 8.20E+03 | 1.01E-05 | 1.23E-06 | 5.34E-01 | 4.39E-04 | 1.59E-02 |
| 8.40E+03 | 4.36E-06 | 1.72E-08 | 4.03E-01 | 1.66E-04 | 8.00E-04 |
| 8.40E+03 | 1.02E-05 | 1.23E-06 | 5.95E-01 | 6.23E-04 | 1.90E-02 |
| 8.60E+03 | 4.29E-06 | 1.89E-08 | 3.45E-01 | 1.89E-04 | 1.07E-03 |
| 8.60E+03 | 1.02E-05 | 1.22E-06 | 6.53E-01 | 8.65E-04 | 2.24E-02 |
| 8.80E+03 | 4.20E-06 | 2.08E-08 | 2.91E-01 | 2.10E-04 | 1.40E-03 |
| 8.80E+03 | 1.02E-05 | 1.22E-06 | 7.06E-01 | 1.18E-03 | 2.62E-02 |
| 9.00E+03 | 4.11E-06 | 2.27E-08 | 2.42E-01 | 2.29E-04 | 1.81E-03 |
| 9.00E+03 | 1.03E-05 | 1.22E-06 | 7.54E-01 | 1.56E-03 | 3.04E-02 |
| 9.20E+03 | 4.01E-06 | 2.47E-08 | 1.99E-01 | 2.45E-04 | 2.30E-03 |
| 9.20E+03 | 1.03E-05 | 1.22E-06 | 7.96E-01 | 2.05E-03 | 3.51E-02 |
| 9.40E+03 | 3.90E-06 | 2.68E-08 | 1.63E-01 | 2.58E-04 | 2.90E-03 |
| 9.40E+03 | 1.04E-05 | 1.22E-06 | 8.31E-01 | 2.63E-03 | 4.03E-02 |
| 9.60E+03 | 3.79E-06 | 2.89E-08 | 1.32E-01 | 2.68E-04 | 3.61E-03 |
| 9.60E+03 | 1.04E-05 | 1.22E-06 | 8.61E-01 | 3.33E-03 | 4.60E-02 |
| 9.80E+03 | 3.68E-06 | 3.11E-08 | 1.07E-01 | 2.75E-04 | 4.45E-03 |
| 9.80E+03 | 1.05E-05 | 1.22E-06 | 8.84E-01 | 4.16E-03 | 5.21E-02 |
| 1.00E+04 | 3.57E-06 | 3.34E-08 | 8.60E-02 | 2.80E-04 | 5.43E-03 |
| 1.00E+04 | 1.06E-05 | 1.22E-06 | 9.03E-01 | 5.14E-03 | 5.88E-02 |

## DOCUMENT CONTROL DATA - R & D

*(Security classification of title, body of abstract and indexing annotation must be entered when the overall report is classified)*

| 1. ORIGINATING ACTIVITY (Corporate author) | 2a. REPORT SECURITY CLASSIFICATION |
|---|---|
| General Electric Company <br> 7500 Lindbergh Blvd <br> Philadelphia, Pa 19153 | Unclassified |
| | 2b. GROUP |

**3. REPORT TITLE**

Electric Arcs in Turbulent Flows, IV

**4. DESCRIPTIVE NOTES** *(Type of report and inclusive dates)*

Scientific.    Final.

**5. AUTHOR(S)** *(First name, middle initial, last name)*

Gerhard Frind and Ben Lee Damsky

| 6. REPORT DATE | 7a. TOTAL NO. OF PAGES | 7b. NO. OF REFS |
|---|---|---|
| January 1970 | 87 | 18 |

| 8a. CONTRACT OR GRANT NO. <br> F33615-67-C-1374 <br> b. PROJECT NO. 7063-00 12 <br> c. DoD Element 61102F <br> d. DoD Sub-element 681307 | 9a. ORIGINATOR'S REPORT NUMBER(S) |
|---|---|
| | 9b. OTHER REPORT NO(S) *(Any other numbers that may be assigned this report)* <br> ARL 70-0001 |

**10. DISTRIBUTION STATEMENT**

This document has been approved for public release and sale; its distribution is unlimited.

| 11. SUPPLEMENTARY NOTES <br><br> TECH OTHER | 12. SPONSORING MILITARY ACTIVITY <br> Aerospace Research Laboratories (ARN) <br> Wright Patterson AFB, Ohio 45433 |
|---|---|

**13. ABSTRACT**

Heat, mass, and momentum transfer were investigated experimentally in very long cylindrical axial flow arcs in laminar and turbulent flow conditions. Special attention was given to assure that the end of the arc tube had a section of fully developed flow. In this section the number of significant terms in the energy balance equation is reduced and interpretation of experimental results is implified. Strong evidence is presented for the existence of turbulence by the fact that all three transfer mechanisms are considerably accelerated in what we condier the "turbulent mode" and also by direct optical study of the arc by a light probe. The onset of turbulence was found with all our methods to occur around 1.5 gram/sec gas flow rate. A considerable number of measurements of heat and momentum transfer are presented in the following operating ranges: Gases-argon and nitrogen; tube diameters-0.5 and 0.7 cm; tube length-50 cm; mass flow rates-0.1 to 15 gram/sec; ambient pressure - 1 to 20 atmosphere; currents 25 to 200 amperes (some higher).

**DD** FORM 1 NOV 65 **1473**

| 14. KEY WORDS | LINK A | | LINK B | | LINK C | |
|---|---|---|---|---|---|---|
| | ROLE | WT | ROLE | WT | ROLE | WT |
| Arc Plasma | | | | | | |
| Heat Transfer | | | | | | |
| Heat, Mass, Momentum Transfer | | | | | | |
| Laminar | | | | | | |
| Turbulent | | | | | | |
| Arc Plasmas | | | | | | |